Department of Electronic Systems
Aalborg University

Sensing the Orientation of Passive UHF Tags Using a Commercial RFID System

*Master***Thesis**

Mobile Communications / Group 990 / 2010-2011

General Report Information

TITLE:
Sensing The Orientation of Passive UHF Tags Using a Commercial RFID System

PROJECT PERIOD:
September 2010 – May 2011

PROJECT GROUP:
Mobile Communications – group 990

GROUP MEMBERS:
Germán Corrales Madueño
Laura Luque Sánchez
Lucas Chavarría Giménez

SUPERVISOR:
Rasmus Krigslund

Number of pages in report: 104

Number of copies printed: 2

ABSTRACT

The purpose of this project is to estimate the object orientation using passive UHF tags in a commercial RFID system. Two algorithms are proposed: A bayesian estimator called Probabilistic Orientation Algorithm, and a nonparametric procedure called KNN Orientation Algorithm.

The algorithms consist on two stages: Calibration and Estimation phases. The former is used by the system to learn the expected received power values.

The developed methods are evaluated in an experimental setup using a commercial RFID system. The results shows high accuracy estimating the inclination of the objects.

Afterwards, several improvements to the system are presented and analyzed in order to reduce the costs in economical terms. In addition to this, the system shows great potential to work under dynamic environments.

Preface

This report has been written by group 990 in 2011 at Aalborg University.

Each chapter is preceded by an introduction showing its content. Furthermore, a conclusion is written at the end of each one summarizing the important aspects of the chapter. Finally, the last chapter includes a summary of the whole report followed by the general conclusions and some proposed ideas for future work.

Literature references follow IEEE recommendations. Texts, figures, formulas and tables are referenced using number in brackets which indicates the position on the reference list:

Text [Reference Number]
Figure (number): Figure Description [Reference Number]
Table (number): Table Description [Reference Number]
[Reference Number]: Formula [units]

A CD containing the report in digital format and some references used in this project is attached to the report.

Mobile Communications - Group 990
Aalborg University, 23^{rd}May 2011

Germán Corrales Madueño	
Laura Luque Sánchez	
Lucas Chavarría Giménez	

Contents

Chapter 1

Introduction

This project is focused on detecting the objects orientation, which it is a new area of research in Radio Frequency Identification (RFID). RFID is commonly used to wirelessly identify objects. In a supply chain the major challenge is to transport huge quantities of products from the manufacturer to the client in the fastest and most efficient possible way. In such scenario, RFID system plays a very important role as it can provide a complete overview of the supply chain, which then helps to manage all the logistic procedures. For instance, it will allow to keep an updated database with all the articles in the warehouse in an automatic way. Detecting the object orientation can be really important in applications where the object has to be in a fixed orientation (vertical, horizontal, etc.). A simple example is the widely used “This side up” marker in the box. In this way by operating with a common RFID system, if a change in the orientation is detected, a potential problem with the product integrity could exist and therefore, it could be checked before it arrives to the final client, saving costs and improving the delivery process.

The key aspect in this project is to work with common commercial UHF passive tags, which are intensively used due to their low cost. It can be argued that accelerometers sensors could be added to the tag, providing very precise data about the orientation. However, the cost of the tags will considerably raise up, specially in the case of applications where a large number of tags are used. On the other hand, the proposed line of research will allow to use the already deployed tags in the supply chains.

As mentioned above, there is no reference work to consider, and therefore a project flow where each step is a goal itself is carefully defined. This project will follow the structure represented in the Figure 1.1. For a better understanding, each project stage is defined in the following list:

1. Estimate the Orientation

   This block is carried out in two different ways: using a probabilist method and with a proximity technique. The objective is to estimate the orientation of the tag attached to the object. Those algorithms are developed and validated later with an experiment where an artificial tag is used. The motivation for employing an artificial tag is that, in this way, it is possible to use a spectrum analyzer to measure the received power.

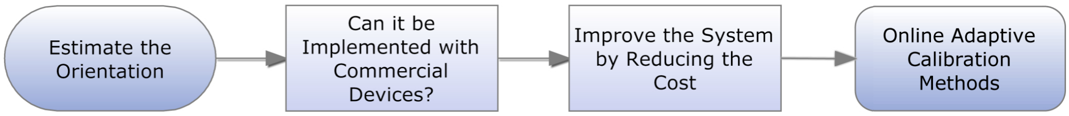

Figure 1.1: Diagram flow of the project

On the other hand, a commercial device will require an important extra work in order to achieve the data needed. In other words, before investing time in using commercial devices, a simple test is run to validate the methods. This procedure is deeper analyzed and explained in Chapters 3 and 4.

2. Can It be Implemented with Commercial Devices?

   In the previous block the algorithms are validated with the data obtained from an experiment. As mentioned above, this experiment has been done with a dipole which is not a real tag. This block focuses on modeling the system with commercial devices. Lastly, the orientation methods are evaluated in a more realistic scenario, in order to prove that the algorithms are working properly with commercial RFID passive tags (Chapter 5).

3. Improve The System by Reducing the Cost

   The main concern of this block will be to improve the system. For that aim several improvements are proposed: to reduce the number of antennas used and to decrease the time needed for the measurements. This corresponds to Chapter 6.

4. Online Adaptive Calibration Method

   The system will be tested in different scenarios such as static and dynamic environments where reference tags will be used in order to facilitate the orientation estimation process. In addition to this the calibration phase required by the algorithms before estimating the orientation will be removed.

Before proceeding with the development of an orientation algorithm, it is necessary to properly define the targeted problem. The reader can find a brief introduction to RFID technology in the Appendix A. In addition to this, a technical view of the RFID protocol is available in Appendix B. The scenario is described in the next section.

1.1 Scenario

The proposed scenario is a supply chain where the orientation of the box is an important parameter, for example due to the fragility of the item. In this scenario the object is placed inside a cardboard box with an UHF passive tag attached.

One of the part of this supply chain consists in a conveyor belt to enter the arriving boxes to a warehouse, where the items are stored before they are sent to the final client. Owing to the fact that the object is easy breakable, several workers are visually checking that the arriving boxes have not been tilted before they are digitally added to the warehouse database with an RFID reader. In other words, when a new box arrives to be stored, it is visually checked before it is accepted.

1.2 Problem Definition

From the presented scenario, it is clear that having workers to check if the boxes have been tilted is a waste of resources. Thus the main aim is to detect the orientation of the boxes using the currently deployed tags and reader. In this way, the RFID reader installed in the supply chain will not only catalogue the arriving items, but it will also check the orientation is the desired one. The results will be evaluated in terms of error Cumulative Density Function (CDF), where the main references are the outcome error for the 90% and 0% of the time.

1.2.1 Delimitations

RFID orientation is a complex problem where many situations can be studied such as: different frequencies, passive and active tags, etc.. In order to simplify the problem the following limitations are taken into consideration:

- Ultra High Frequency (UHF): the working frequency is 865.7 MHz.
- Commercial Passive Tags: This system will use commercial UHF passive tags.
- Collisions between tags will not be taken into account. It is supposed that the protocol will avoid the collisions.
- Only a single interrogator will be used: not multiple or dense interrogator.
- A short tag population in the interrogating area will be assumed.
- The distance between the object and the antennas of the reader is fixed to a constant value.
- The sizes of the object will be fixed.
- In the scenario proposed, there is no strict time requirements to estimate the orientation, any interval below 30 seconds will be accepted.
- The boxes are made with cardboard. The effect of different materials to which the tag is attached will not be considered.
- Only one box orientation is estimated at the same time.

Once the problem to solve has been defined, and the initial parameters have been chosen, it is possible to proceed with the following step: To determine a suitable channel model for the defined problem because RFID is sending the information wirelessly.

Chapter 2

Channel Propagation Models

Previously, it was shown that the main goal is to be able to detect the orientation of the objects using an RFID system. As it will be explained in following chapters, the orientation will be estimated by using one parameter which is the received power from the tag response. In any communication system the power that reaches the receiver side is different that the transmitted one due to effects of the noise, reflections, shadowing caused by objects and other effects introduced by the transmission channel. Thus, it is really important to have an overview of how the power is changing through the path from the transmitted to the receiver, which is modeled by deterministic equations and random variables that constitute the propagation models. As in other technologies based on radio waves propagation, there are many propagation models that can be used in order to study the channel behavior in an UHF RFID communication. This chapter will explain some of them, either deterministic models or probabilistic models.

2.1 Deterministic Propagation Models

In order to achieve a successful read, the received power in the tag must be higher than the tag sensitivity or power-up threshold. On the other hand, the backscattered power from the tag to the reader must be high enough to make the reader able to receive the information with an adequate Signal to Noise Ratio (SNR) and a reasonable Bit Error Rate (BER).

As a first model, using Friis equation, the received power in the tag can be written as follows [1]:

$$P_{RxTag}(dBm) = P_{TxReader}(dBm) + G_{Reader}(dBi) + G_{Tag}(dBi) - L_{Path}(dB) \text{ [dBm]} \quad (2.1)$$

Where:

- P_{RxTag} is the received power in the tag [dBm].
- $P_{TxReader}$ is the transmitted power by the reader [dBm].
- G_{Reader} is the reader antenna gain [dBi].
- $G_{Tag}(dBi)$ is the tag antenna gain [dB].

- L_{Path} is the path loss term [dB].

On the other hand, the received power in the reader is shown in the following equation [1]:

$$P_{RxReader}(dBm) = P_{RxTag}(dBm) - T_b(dB) + G_{Reader}(dBi) + G_{Tag}(dBi) - L_{Path}(dB) \text{ [dBm]} \tag{2.2}$$

Where:

- $P_{RxReader}$ is the received power in the reader [dBm].
- T_b is the tag backscattering coefficient [dB].

This model is a very simple one where it is only taken into account the transmitted and received powers, the antenna gains and the path losses. More terms can be added to these equations in order to model different effects. For example, the effect of the material where the tag is placed, cable losses or polarization losses can be considered. Due to the fact that this project is not focused on working with deterministic models, no more complicated model will be taken into account.
The previous equations consider a static channel without any kind of random terms. In the next section it will be seen that in order to model the channel properly, it is necessary to take into account some probabilistic methods.

2.2 Probabilistic Propagation Models

In indoor environments the received signal is not only direct line of sight radio wave. A large number of reflected radio waves should be considered as well. These reflected waves interfere with the direct wave, which cause significant variation of received signal. The reflected waves arrive from different directions with different time delays. Due to these different time delays, different phase shifts between reflected waves will be introduced. The combination of different waves, causes either constructive or destructive addition, which relies on relative phase shift. Also, moving the receiver by a short distance the received signal strength can be changed because, small movements change the phase relationship between the incoming waves. All these signal fluctuations cause multipath components (small scale fading). Since RFID is a combination of Line of Sight (LOS) and Non Line of Sight (NLOS) communication, it is very important to take into account these reflections effects. In this kind of propagation channels a deterministic description is not efficient any more. In order to model those components, it is needed to use a stochastic description model.

Table 2.1 shows the models that are often used in indoor radio propagation which can be applied to an RFID communication [2].

In an RFID environment it can be found three important situations [3]:

- **Multipath propagation with a direct path:** A dominant LOS component between the reader and the tag exists.

Distribution	PDF	Use
Lognormal	$\frac{1}{\sqrt{2\pi\sigma^2 r^2}} e^{\frac{-ln(r^2)}{2\sigma^2}}$	Shadowing or Slow Fading effect
Rayleigh	$\frac{r}{\sigma^2} e^{\frac{-r^2}{2\sigma^2}}$	Fast Fading effect. NLOS
Rice or Rician	$\frac{r}{\sigma^2} e^{-\frac{(r^2+A^2)}{2\sigma^2}} I_0\left(\frac{r \cdot A}{\sigma^2}\right)$	Fast Fading effect with LOS

Table 2.1: Most common fading channel models distributions. r is the envelope of the received signal [2].

- **Multipath propagation due to objects close to the tag without direct path:** There is no LOS component as the tag receives the signal from reflections or diffractions on ground and objects close to the tag (fast fading effect).
- **Multipath propagation due to objects far from the tag:** In this case, the multiple paths suffer different delays. Also, obstacles between the reader and the tag cause shadowing effect.

2.2.1 Lognormal Channel Model

The Lognormal channel is used to model the effect of the shadowing produced by objects placed in the way of the signal. The Probability Density Function (PDF) of the received power that models this effect is [2]:

$$pdf_P(p) = \frac{1}{2p\sigma\sqrt{2\pi}} e^{\frac{-(ln\sqrt{p}-\overline{P_{rx}})^2}{2\sigma^2}} \tag{2.3}$$

Where:

- pdf() is the Probability Density Function.
- p is the received power [W].
- $\overline{P_{rx}}$ is the mean received power [W].
- σ^2 is the variance of the received signal.
- σ is the standard deviation of the received signal.

2.2.2 Rician Channel Model

When a significant part of the signal envelope is due to a dominant component, such as LOS components, the signal envelop follows a Rician distribution which is given by [4]:

$$pdf_r(r) = \frac{r}{\sigma^2} \cdot e^{\left[-\frac{r^2+A^2}{2\sigma^2}\right]} \cdot I_0\left(\frac{rA}{\sigma^2}\right) \tag{2.4}$$

Where:

- r is the envelop of the signal [V].

- A is the peak of the LOS component [V].
- σ^2 is the variance of the diffuse component.
- $I_0()$ is the modified Bessel function of the first kind and zero order.

To determine the PDF of the power at the receiver in watts, we need to find the Cumulative Density Function (CDF) of the received power and then get the Probability Density Function (PDF) [5]:

$$\begin{aligned} F_p(p) &= P(P \leq p) \\ &= P(r^2 \leq p) \\ &= P(r \leq \sqrt{p}) \\ &= F_r(\sqrt{p}) \end{aligned} \tag{2.5}$$

Where:

- $F()$ is the Cumulative Densitity Function (CDF).
- $P(P \leq p)$ is the probability of the received power at the receiver, P, is lower or equal than p.

In order to get the PDF, it is needed to differentiate the previous expressions to obtain:

$$\begin{aligned} pdf_p(p) &= \frac{d}{dp} F_r(\sqrt{p}) \\ &= f_r(\sqrt{p}) \frac{d}{dp}\sqrt{p} \\ &= pdf_r(\sqrt{p}) \frac{1}{2}\sqrt{\frac{1}{p}} \end{aligned} \tag{2.6}$$

By operating Equation 2.4 and Equation 2.6, the PDF can be written in terms of power at the receiver as:

$$pdf_p(p) = \frac{1}{2\sigma^2} \cdot e^{-\frac{p+A^2}{2\sigma^2}} \cdot I_0\left(\frac{A\sqrt{p}}{\sigma^2}\right) \tag{2.7}$$

$$= \frac{1}{2\sigma^2} \cdot e^{-K} \cdot e^{-\frac{p}{2\sigma^2}} \cdot I_0\left(\frac{\sqrt{2K \cdot p}}{\sigma}\right) \tag{2.8}$$

Where K is the ratio of the power of the LOS components to the power of the diffuse components ($K = \frac{A^2}{2\sigma^2}$).
Taking into consideration that the average power is $\overline{P_{rx}} = 2\sigma^2 + A^2$, the pdf of the squared envelope follows a non-central chi-square distribution with two degrees of freedom [6]:

$$pdf_p(p) = \frac{1+K}{\overline{P_{rx}}} \cdot e^{-K} \cdot e^{-(1+k)\cdot\frac{p}{\overline{P_{rx}}}} \cdot I_0\left(2\sqrt{\frac{K(1+K)}{\overline{P_{rx}}} \cdot p}\right) \tag{2.9}$$

Where:

- $\overline{P_{rx}}$ is the averaged power [W].
- K is the Rician Factor ($K = \frac{A^2}{2\sigma^2}$).

2.2.3 Rayleigh Channel Model

When the signal consists of a large number of planes waves at the receiver side, the received signal is the sum of the in-phase and the quadrature-phase components which are modeled as a zero mean Gaussian random variable (X), or Normal Distribution $N(0, \sigma)$ as it is shown in Equation 2.10 [7]:

$$pdf_X(x) = \frac{1}{\sqrt{2\pi\sigma^2}} \mathrm{e}^{\frac{-X^2}{2\sigma^2}} \tag{2.10}$$

Where:

- X is either the in phase or quadrature received component of the signal [V].
- σ^2 is the variance.

Thus, the received signal is a sum of two independent zero mean Gaussian distributions with the same variance. Then, the received envelop is a Rayleigh distribution variable, R, which Probability Density Function is [7]:

$$pdf_R(r) = \frac{r}{\sigma^2} \mathrm{e}^{\frac{-r^2}{2\sigma^2}} \tag{2.11}$$

Where:

- r is the envelop of the signal [V].
- σ^2 is the variance.

The procedure is to find the CDF and then the PDF as in the Rician case. Then, the Probability Density Function of the received power is [7]:

$$pdf_P(p) = \frac{1}{2\sigma^2} \mathrm{e}^{\frac{-p}{2\sigma^2}} \tag{2.12}$$

Where:

- p is the received power [W].

It means that while the signal envelope is modeled as a Rayleigh distribution, the received power is modeled by an exponential distributed signal, where the average power is $\overline{P_{rx}} = 2\sigma^2$. Rewriting the equation:

$$pdf_P(p) = \frac{1}{\overline{P_{rx}}} \mathrm{e}^{\frac{-p}{\overline{P_{rx}}}} \tag{2.13}$$

Notice that from Equation 2.13 it can be seen that Rayleigh is an especial case of Rician distribution with the K factor equals to zero, which means no Line of Sight components.

2.3 Channel Propagation Models Conclusions

In order to get a good model of the channel and the environment it will be used probabilistic propagation models. Lognormal provides a simple model based on a Gaussian random variable where the main effect modeled is the shadowing, while Rayleigh can model the fading when there is no LOS situation and MultiPath Components (MPCs) are reaching the freceiver antenna. On the other hand, Ricean can model a situation where there is a dominant component such as LOS path. With these models presented most of the situations that can exists in an RFID environment are covered. However, in this case, due to the scenario that will be analyze is not affected by shadowing, Lognormal channel will not be considered. Thus, only Rician and Raileygh channel models should be applied.

In the following chapter two algorithms will be developed to estimate the orientation based on the received power. Later, in other chapters, they will be validated and evaluated in real situations where both algorithms will try to detect the orientation of the tag.

Chapter 3

Orientation Estimation Methods

In Chapter 1 the problem was defined: To estimate the orientation of an object. This chapter focuses on the development of two different methods, which use the received power, for that purpose. In order to estimate the orientation it is needed to analyze the main parameters that are affecting to the received power. An alteration in the orientation will produce a modification in the polarization of the signal, changing the received power. Thus, before proceeding to develop the algorithms, the effects of the tag orientations will be study, above all how the polarization of the electric waves varies with the orientation.

Firstly, some basis about polarization will be explained in order to, afterwards, analyze the best polarization of the RFID commercial reader that will be used. Then, a probabilistic method is explained and finally, as the orientation estimation is a new area of research and there is no references, a second algorithm based on proximity techniques is also developed. In this way, the robustness of the former one can be analyzed by comparing with the latter one.

3.1 Effect of Tag Orientation

The methods to estimate the orientation will be based on the power that is received from the target. In order to see how the polarization affects to the accuracy of those methods, it is necessary some knowledge about polarization.

3.1.1 Polarization

The polarization of an antenna is the orientation of the electric field of the radiated radio wave with respect to the Earth's surface and it is determined by the physical structure of the antenna and by its orientation [8].
An electromagnetic wave moves electrons in the plane perpendicular to the direction of propagation. The direction in which the electric field is pointing determines the polarization of the radiated wave [1]. Depending on the variation of this direction in time, the polarization will be:

- Linear polarization: The electric field can point any direction in the plane perpendicular to the direction of propagation, but this direction is constant in time. The most usual linear polarization are vertical and horizontal.

- Circular polarization: The electric field rotates around the propagation as time goes by. However, the magnitude does not change. It can be split into vertical and horizontal components with the same magnitude and out of phase by 90°. Depending on the sense of rotation it can be right-handed or left-handed.

- Elliptical polarization: The tip of the electric field describes an ellipse [9]. It is a general case of circular polarization and it can be derived from that by adjusting the ratio of horizontal and vertical components and their phase relationship. As well as the circular one, there are two types of elliptical polarized waves: right or left handed.

The antenna of the UHF tag is usually a simple dipole, so it is linear polarized. Regarding the commercial reader, in Section 3.1.4 different possible polarizations are defined and one of them is chosen.

3.1.2 How Does the Polarization Affect?

The orientation of the tag affects directly to the power that the reader receives from the tag due to the polarization mismatch.

A simple dipole has current flowing only in one direction, hence it creates a linearly polarized radiated wave with the polarization direction being the long axis of the dipole [1]. In this way, a second similar dipole oriented along the axis of the first one will receive the maximum signal while another dipole placed perpendicular to the field will receive not signal at all. This can be seen in Figure 3.1 where the first case shows a completely matched receiver antenna which receives the maximum possible signal. The two other diagrams are dipoles perpendicular to the field and, therefore, not signal is received.
The extreme situations have been referred but there are some intermediate orientations where, although a polarization mismatch exists, the signal is still received. Those losses in the received signal can be calculated and used to improve the orientation methods as will be explained later.

3.1.3 Polarization Mismatch

To calculate the losses due to polarization mismatch, it is necessary to explain the concept of Polarization Loss Factor (PLF).
When the tag is activated, the response wave travels from the tag to the antenna reader, but only a portion of the incident power is coupled into the receiver antenna. That portion of power is given by the Polarization Loss Factor in the Equation 3.1 [10]:

$$P_r = F \cdot P_i \tag{3.1}$$

Where:

- Pr is the received power or power coupled into the receiver antenna
- Pi is the incident power
- F is the Polarization Loss Factor

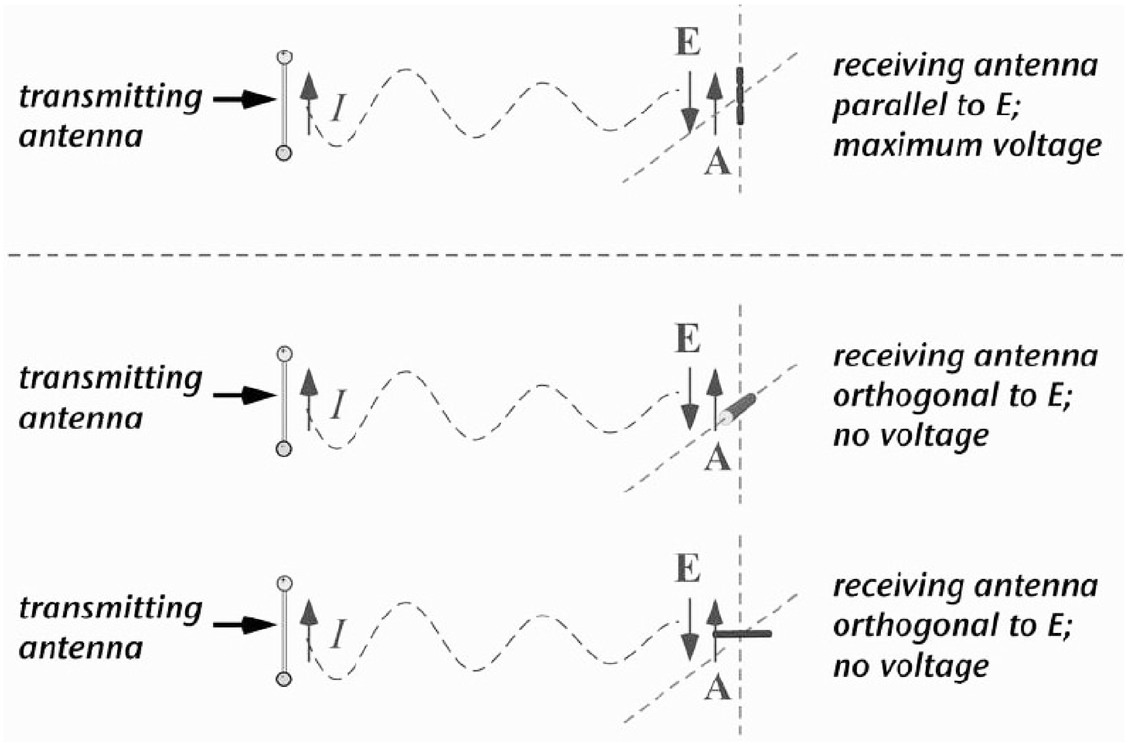

Figure 3.1: Dependency of the received signal with the polarization [1]

This factor (PLF) has a different expression for each kind of polarization. As it was said, in this system all the antennas are going to be processed as linear polarized, so only the losses for linear polarized antennas will be studied. In this case the PLF can be considered as a degenerate case of elliptical polarization and it follows the next equation [10]:

$$F = \cos^2(\alpha) \tag{3.2}$$

Where:

- α is the angle between the incident wave polarization and the receiver antenna.

3.1.4 Reader Antenna Polarization

As it was explained in Section 3.1.1 there are different polarizations that can be used for the reader antenna: linear, circular and elliptical. In this project, due to the fact that many linearly polarized multipath signals with different orientation exist at the receive site, the circular polarized antenna is a better choice than the other two. This is because the circular polarized antenna is always able to receive the signal, no matter the orientation. There is another possibility that comes out from the combination of two linearly polarized antennas: dual linear polarization.

To make the choice of the reader antenna polarization different characteristics are presented [11]:

- Circular polarization: The main advantage is that it does not care about the orientation of the tag since it will always receive its response (keep in mind this is referred to polarization mismatch, and not to the radiation pattern which can also cause that the reader does not read the tag). On the other hand, when a circular polarized antenna receives a linear polarized signal the polarization loss factor is 3dB.

- Dual linear polarization: It is the combination of two linearly polarized antennas where each component has its own output connector. These two components may be vertically and horizontally polarized or they may be slant-linear polarized where each one is oriented 45°off of the horizontal and the vertical [11]. This dual polarization always receives the signal as well as the circular one. Furthermore, when the received signal matches with the orientation of one of the linearly polarized antennas, the total power of the signal is received. It is also possible to combine the signal received in the vertical and horizontal antennas in order to get full power in all the orientations. Thus, the losses due to the polarization mismatch are removed by combining the signals from the vertical and horizontal antennas. In this way, as the power is higher, the range where the tags can be read is increased.

As one of the goals of this project is to estimate the orientation, it is not important to have a system orientation independent. Therefore the chosen antenna polarization is the dual linearly polarized antenna because of its advantages such as a longer read range (this is critical when working with passive tags) and the possibility to get the vertical and horizontal components separately.

The reader consists in two linear polarized antennas (one vertical and one horizontal), so the polarization of the incident wave is known. In this way it is possible to know the losses due to polarization mismatch for a certain orientation of the tag by calculating the PLF.

In the following sections the methods to find the orientation of the objects are explained. The main idea is to estimate the orientation expressed in terms of the spherical coordinates, θ and ϕ. For that, the received signal will be split into the two orthogonal components (vertical and horizontal) at the reader antennas.

3.2 Probabilistic Orientation Algorithm

A method for estimating the orientation (inclination and azimuth) of passive UHF RFID tags based on Bayes theorem is presented in this section.

3.2.1 Method Definition

This section focuses on estimating the orientation which makes maximum the following probability:

$$\max_{\theta,\phi}\{p(\theta,\phi|y_1,y_2,y_3)\} \tag{3.3}$$

Where:

- y_i is the received power in antenna i.
- θ,ϕ are the components of the tag orientation.

To obtain this probability in an easier way, the previous expression is developed. Assuming θ and ϕ independent, the expression can be written as the multiplication of two probabilities:

$$\begin{aligned}\max_{\theta,\phi}\{p(\theta,\phi|y_1,y_2,y_3)\} &= \max_{\theta,\phi}\{p(\theta|y_1,y_2,y_3)\cdot p(\phi|y_1,y_2,y_3)\}\\ &= \max_{\theta,\phi}\{p(\theta|y_1,y_2,y_3)\}\cdot \max_{\theta,\phi}\{p(\phi|y_1,y_2,y_3)\}\end{aligned} \tag{3.4}$$

In order to simplify the problem, the next assumption is taken into account:

$$p(\theta|y_1,y_2,y_3) = p(\theta|y_{1\theta},y_{2\theta},y_{3\theta}) \tag{3.5}$$

$$p(\phi|y_1,y_2,y_3) = p(\phi|y_{1\phi},y_{2\phi},y_{3\phi}) \tag{3.6}$$

In this way, it is assumed that the elevation angle (θ) and the azimuth angle (ϕ) only depend on the received signal in the vertical axis (y_θ) and in the horizontal axis (y_ϕ) respectively [12].

Focusing only in one term of the Equation 3.4, the probability of θ given the received signal in the different vertical antennas can be written as a function of the probability of receiving a certain signal given a value of θ by applying Bayes theorem:

$$\max_{\theta}\{p(\theta|y_{1\theta},y_{2\theta},y_{3\theta})\} \propto \max_{\theta}\{\frac{p(y_{1\theta},y_{2\theta},y_{3\theta}|\theta)\cdot p(\theta)}{p(y_{1\theta},y_{2\theta},y_{3\theta})}\} \tag{3.7}$$

As it is needed to find the θ value that maximize this expression, and due to the relationship of proportionality, it can be simplified [12]:

$$\max_{\theta}\{p(\theta|y_{1\theta},y_{2\theta},y_{3\theta})\} \propto \max_{\theta}\{p(y_{1\theta},y_{2\theta},y_{3\theta}|\theta)\cdot p(\theta)\} \tag{3.8}$$

It can be assumed that the three used antennas (y_1, y_2, y_3) are independent because each one is affected by a different environment:

$$p(y_{1\theta},y_{2\theta},y_{3\theta}|\theta) = p(y_{1\theta}|\theta)\cdot p(y_{2\theta}|\theta)\cdot p(y_{3\theta}|\theta) \tag{3.9}$$

Now the Equation 3.8 for the first time instant is analyzed. There is not information about the tag orientation so far. That is why it is assumed that θ is uniformly distributed from 0 to π.

In this time instant:

$$p(\theta|y_\theta(1)) = p(y_\theta(1)|\theta)\cdot p(\theta) \tag{3.10}$$

Where:

- $y_\theta(1)$ is the received signal in the three antennas in time instant 1 $(y_{1\theta}(1), y_{2\theta}(1), y_{3\theta}(1))$
- $p(\theta|y_\theta(1))$ is the posterior probability for time instant 1
- $p(y_\theta(1)|\theta)$ is the likelihood for time instant 1
- $p(\theta)$ is the prior probability for time instant 1

In the next time instant, the probability of θ given the received signal in the three antennas will be:

$$p(\theta|y_\theta(2)) = p(y_\theta(2)|\theta) \cdot p(y_\theta(1)|\theta) \cdot p(\theta) \tag{3.11}$$

Where:

- $p(\theta|y_\theta(2))$ is the updated posterior probability for time instant 2
- $p(y_\theta(2)|\theta)$ is the updated likelihood for time instant 2
- $p(y_\theta(1)|\theta) \cdot p(\theta)$ is the updated prior probability for time instant 2

In this way, assuming that in the first time instant the $p(\theta)$ has uniform distribution, it is possible to calculate the posterior probability for any time instant by updating the prior probability. The higher the number of samples, the more accurate the algorithm will be because the posterior probability is continuously updated and should converge to the right value.

Regarding the likelihood and as it was said before, the likelihood can be divided into three terms, each one corresponding to one antenna:

$$p(y_{1\theta}, y_{2\theta}, y_{3\theta}|\theta) = p(y_{1\theta}|\theta) \cdot p(y_{2\theta}|\theta) \cdot p(y_{3\theta}|\theta) \tag{3.12}$$

The probability of receiving a certain signal given θ (likelihood) can be defined as a the channel distribution.
In order to calculate the mean of the channel distribution, it is used some available experimental data where several samples of the received power in the two components (vertical and horizontal) of each antenna are measured. The mean for the vertical component is obtained as the summation of the received power in the vertical component of one antenna for all the time instants:

$$\mu_i = \frac{\sum_{j=0}^{N} y_{i\theta}(j)}{N} \tag{3.13}$$

Where:

- $y_{i\theta}(j)$ is the received power in the vertical axis for the antenna i in the time instant j
- N is the number of samples

Once the Probability Density Function given by the selected channel model is created, it is needed to find the received power Probability Density Function for all the possible orientations and look for the maximum value. For that, these steps for the vertical component are followed:

1. Obtain all the channel distributions which mean is the one previously calculated for all the values of θ.
2. Evaluate the real received power in the vertical antenna (y_θ) for each different channel distribution, getting in this way the probability of receiving that power.

3. Find the θ that gives the maximum for all the probabilities calculated in the second step.

The same procedure should be follow to find the optimum ϕ.

3.3 K-Nearest Neighbor Orientation Algorithm

To estimate the objects orientation in an RFID system is a novel area of research, where no reference results can be found. Consequently, a second method will allow to properly analyze the robustness and performance of the Probabilistic Orientation Algorithm.

The shape of the underlying density functions for this case can be unknown, and therefore a non parametric procedure is needed. Several algorithms can be classified into the non parametric techniques, but it should be noted that this algorithm is introduced to serve as a results reference and to be compared with the Probabilistic method. K-Nearest Neighbor Algorithm is chosen because it is a simple technique which fits with the requested features.

3.3.1 KNN as Estimator

The logical step is to determine the overall outcome that can be expected from this algorithm, or in other words, how good is this procedure to classify the data. It can be proved that within a large sample case, the simplest rule in KNN, 1-NN ($K = 1$), presents a probability of error which is lower than twice the Bayes probability [13] [14]. Clearly, this technique is not the optimal one, however will be valid in order to analyze the Probabilistic Orientation Algorithm.

Because of only the nearest neighbor is considered, it could be argued the possibility of using more than one neighbor to estimate the orientation. However, it is shown that the error probability of 1-NN rule is less than twice the probability of error of any other nonparametric decision rule (based on the infinity sample set) [13]. This behavior could be extended for any number of samples for a certain classes of distributions, meaning that while it is a suboptimal estimator it is an admissible one. This KNN method will skip the probability estimation and it will directly jump to the decision functions, or in other words, it will determine the orientation of the object by using decision functions as defined in the following section.

3.3.2 Method Definition

Let the set x_i denote the resulting set of measurements within a certain category, β. The training set T is given by $T = \{(x_1, \beta_1), (x_2, \beta_2), \cdots, (x_n, \beta_n)\}$, which is needed to determine the class of a new input pair (x, β). This new pair will consider [13]:

$$x'_n \in \{x_1, x_2, \cdots, x_n\} \tag{3.14}$$

as a nearest neighbor if Equation 3.15 is satisfied:

$$min\ \{d(x_i, x)\} = d(x'_n, x) \qquad i = 1, 2, \cdots, n. \tag{3.15}$$

Where:

- x_i is the set of measurements within a certain category.
- x'_n is the nearest neighbor.
- x is the measurement to be classified.

In simple terms, this algorithm is based on finding the minimum distance across all the training data set. Once the minimum distance (nearest neighbor) is obtained, the measured sample is classified into the same category than the nearest neighbor belongs to. It is computationally efficient and simple.
In this case, the element x is a set of received power values and β is a category for each combination of the orientation angles (θ and ϕ) respectively. As an example, if $\theta = \{0, 90\}$ and $\phi = \{0, 90\}$, it will result in 4 categories $\{(\theta = 0, \phi = 0), \cdots, (\theta = 90, \phi = 90)\}$, where each of these resulting categories will have a set of received power values associated.
To compute the distance between the new input and the training data, several functions could be used, such as absolute distance and euclidean distance, which are shown in Equations 3.16 and 3.17 respectively. Because the received power are given in dBm, absolute distance is chosen. In this way, the function will return the difference in dB values.

$$d_A(x, x_i) = \sum_{i=1}^{n} |x - x_i| \tag{3.16}$$

$$d_E(x, x_i) = \sum_{i=1}^{n} \sqrt{x^2 - x_i^2} \tag{3.17}$$

In Figure 3.2 is shown an example of a computed matrix distance, with θ within the set (0,45,90) and ϕ going from 0° to 330° with steps of 30°. Note that, in this case, i index is from 1 to 3 and j index is moving from 1 to 12. By selecting the minimum difference (right corner in the same figure), the nearest neighbor is found.
Once all the distances are calculated, the minimum value is chosen and the new input is classified into the same category as the nearest neighbor. From Figure 3.2 it can be seen that the nearest neighbor is into the category ($\theta = 0, \phi = 0$).

3.4 Orientation Estimation Methods Conclusions

To summarize, the main ideas of this chapter are: To use dual linear polarized antennas to be able to split the received signal in two orthogonal components (vertical and horizontal) and to develop two algorithms, Probabilistic Orientation Algorithm and KNN Orientation Algorithm to estimate the orientation of an object.

The Probabilistic Algorithm is a Bayesian estimator where it is assumed that the vertical and horizontal components of the received signal are independent. Because of the algorithm is based on Bayes theory, it is expected to be the optimal estimator and therefore, it will provide the lowest error probability. On the other hand, KNN Algorithm is a

Figure 3.2: Difference in dB between the new sample and the training data for each category.

suboptimal non parametric procedure which will be used to compare the results with the Probabilistic method.

In the next chapter the orientation methods will be validated with data from an artificial RFID sytem in order to verify that they are working properly. Afterwards, the system will be evaluated with commercial tags and reader.

Chapter 4

Algorithms Validation

In this chapter the algorithms defined in the previous chapter to estimate the orientation will be validated. It means that with a simple test, the potential of sensing the orientation will be studied. Firstly, an artificial RFID system will be used to check that the algorithm (the code and way that it is working) is correctly developed. This will be carried out with an experiment that will be named as Experiment I. In order to validate the algorithms accuracy, the PDF and CDF functions of the error when estimating the orientation will be obtained.

Once the algorithms have been validated, they will be ready to use a commercial RFID system (with commercial RFID devices) to prove that the algorithms work with real devices as well. This will be explained in Chapter 5.

4.1 Calculating PDF and CDF Error Functions

The obtained error in the estimation of the tag orientation using the algorithms is calculated as:

$$e_\theta = \text{real } \theta \text{ orientation} - \text{estimated } \theta \text{ orientation} \tag{4.1}$$

$$e_\phi = \text{real } \phi \text{ orientation} - \text{estimated } \phi \text{ orientation} \tag{4.2}$$

Where e is the error in estimating the orientation, "real orientation" is the real orientation of the tag and "estimated orientation" is the estimation of the orientation of the tag.
Due to the fact that the measurements were taken using discrete values of θ and ϕ, the error will also consist of discrete values so, the error should be treated as a discrete random variable in order to obtain the PDF and CDF functions.

The PDF function is calculated obtaining the relative frequency of each possible error value. This is done by counting the number of times one error value appears within the whole set of obtained error values and normalizing it by the number of realizations of the experiment. In this case, the measurements were taken for each spherical coordinate set $[\theta, \phi]$ so the total number of realizations is (number of values of θ) $\cdot$ (number of values of ϕ).

Since θ and ϕ are treated as independent angles, two different PDF functions will be obtained: one for θ angle and another one for ϕ angle. The discrete PDF functions are calculated as follows [15]:

$$f_\theta(\theta) = \sum_i \frac{\text{Number of times that error } \theta_i \text{ appears}}{\text{Number of Experiment Realizations}} \delta[\theta - \theta_i] \tag{4.3}$$

Where:

- $f_\theta(\theta)$ is the Probability Density Function of the obtained error estimating θ.
- $\theta_i \in \{0°, 45°, 90°\}$.
- $\delta[\theta - \theta_i]$ is the δ function centered in θ_i.

Analogously, for ϕ orientation:

$$f_\phi(\phi) = \sum_i \frac{\text{Number of times that error } \phi_j \text{ appears}}{\text{Number of Experiment's Realizations}} \delta[\phi - \phi_j] \tag{4.4}$$

Where:

- $f_\phi(\phi)$ is the Probability Density Function of the obtained error estimating ϕ.
- $\phi_j \in \{0°, 30°, 60°, \ldots, 330°\}$.
- $\delta[\phi - \phi_j]$ is the δ function centered in ϕ_j.

Once the PDF functions are obtained, then the CDF functions are calculated as [15]:

$$F_\theta(\theta) = \sum_{\theta_i \leq \theta} f_\theta(\theta_i) = \sum_i f_\theta(\theta_i) u(\theta - \theta_i) \tag{4.5}$$

Where:

- $F_\theta(\theta)$ is the Cumulative Density Function of the obtained error estimating θ.
- $i = 1 \ldots$ Number of θ values.
- $\theta_i \in \{0°, 45°, 90°\}$.
- u is the unit step function.

$$F_\phi(\phi) = \sum_{\phi_j \leq \phi} f_\phi(\phi_j) = \sum_j f_\phi(\phi_j) u(\phi - \phi_j) \tag{4.6}$$

Where:

- $F_\phi(\phi)$ is the Cumulative Density Function of the obtained error estimating ϕ.
- $j = 1 \ldots$ Number of ϕ Values.
- $\phi_j \in \{0°, 30, 60, \ldots, 330°\}$.
- u is the unit step function.

After the previous description, it is possible to go beyond theoretical concepts towards a more empirical work using Experiment I as a starting point.

4.2 Experiment I Definition

To check that the algorithms were well implemented, they will be validated by using an artificial RFID system. This experiment was carried out by Aalborg University [12] before starting to work on this project but, it is completely valid to use their power values to validate that the algorithms were well developed (the code and the way that it is working). After this process, a new experiment will be carried out with new power values measured using a commercial RFID system (see Chapter 5).

For Experiment I a tag was modeled using a folded meandered dipole antenna printed on a Printed Circuit Board (PCB) and connected to an optical diode and to a signal generator using fiber optics instead of copper cables which can modify the radiation pattern of the antenna [12]. In this sense, there was not any reader to activate the tag since the dipole was directly radiating the signal coming from the generator. The signal radiated by the dipole was measured using 3 horn linear dual polarized (vertical and horizontal) antennas designed by Aalborg University. To sample the received signal it was used a spectrum analyzer. The dipole was rotated for each value of θ and for each value of ϕ to take 12 samples on each orientation. These 12 samples will be used to create the channel model distribution (see Chapter 2). In this way, a virtual calibration table which contains the mean received power for all possible orientations is created. The algorithms will predict which one is the most probably orientation of the tag based on this calibration table and the instantaneous received power from the target. This way of taking some measurements from the environment and then to create the calibration table will be called "Offline Calibration". Notice that this calibration table is only needed to be created once. In following chapters it will be attempted to be removed as much as possible this calibration stage.
More details about the experiment setup are shown in Table 4.1.

Parameter	**Value**
θ Values	0°, 45°, 90°
ϕ Values	0°, 30°, 60°, 90°, 120°, 150°, 180°, 210°, 240° , 270°, 300°, 330°
Samples per Orientation	12
Distance Tag - Antennas	1.5 m
Tag height	1 m above ground
Antennas height	1.85 m above ground
Difference in height Tag - Antennas	0.85 m
Object where the Tag was placed	No object

Table 4.1: Experiment I Parameters [12].

4.3 Experiment I Results

Before having a look to the results, it is needed to define the possible situations where it will be difficult for the algorithms to estimate the orientation. Due to the radiation pattern of the tag, the received power in the antennas will be similar (ideally, the same) in a rotation of 180 degrees in the plane of the tag. Calling to the ends of the tag end A and end B, the received power is similar if the positions of end A and end B are interchanged. Thus, it will be more difficult for the algorithms to predict the correct orientation when this kind of rotation is applied. On the other hand, the algorithms will make a mistake as well if any rotation of 180 degrees in the ϕ component is applied. This errors are due to the physical characteristics and the radiation pattern of the tag so, consider errors greater than 180 degrees will not be considered from now on. For example, if the algorithm makes a mistake of 200 degrees, it will virtually translated it into a 180 degrees scale considering, in this case, a 20 degrees error. In order to have a clear understanding of these situations, they are shown on Figure 4.1.

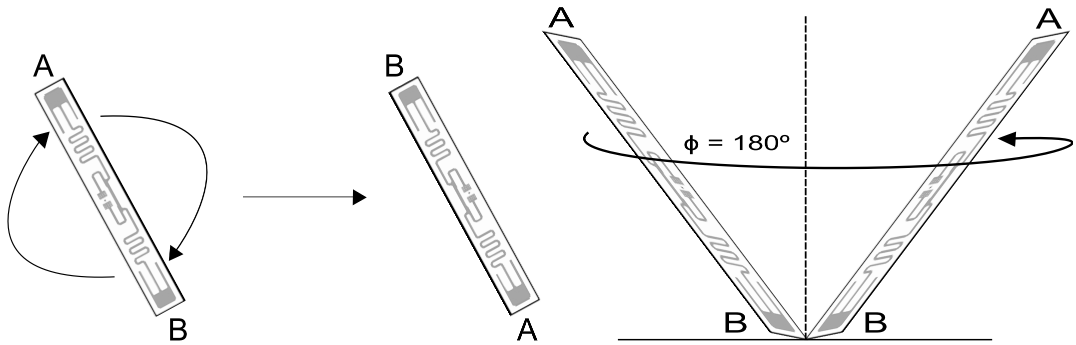

(a) Rotation of 180 degrees within tag plane (b) Any rotation of 180 degrees in ϕ angle

Figure 4.1: Situations where it is difficult for the algorithms to predict the orientation, because the received power will be the same.

Once it has been defined why the algorithms can fail, everything is ready to check the results. The algorithms have been made to estimate the tag orientation for all the θ and ϕ values where the measurements were taken and Rayleigh and Rician distributions were used in order to model the channel. Figure 4.2 and Figure 4.3 show the obtained PDF and CDF functions for θ and ϕ using a Rayleigh channel. Figure 4.4 and Figure 4.5 show the obtained PDF and CDF functions using a Rician channel.

The figures show that the algorithms are not making any mistake in estimating the θ angle. For a good interpretation of this result, it has to be taken into account that the PDF and CDF are not defined for angles between 0 and 45 degrees. The graphics show an error of 0 degrees but actually it is not known what it is happening around 0 degrees. Maybe the algorithms are making mistakes of i.e. 20 degrees and it is not shown in the figure due to the discrete nature of this random variable. This is because the algorithms are only as precise as the granularity we have in the set of measurements. As an example, 20 degrees is not defined so the PDF is gathered around 0 degrees. It is only possible to assure that the error in the estimation of θ is lower than 45 degrees.

The same argumentation can be used for ϕ figure. According to the Figure 4.3, the obtained error is always equal or lower than 30 degrees. But once again it is not known what

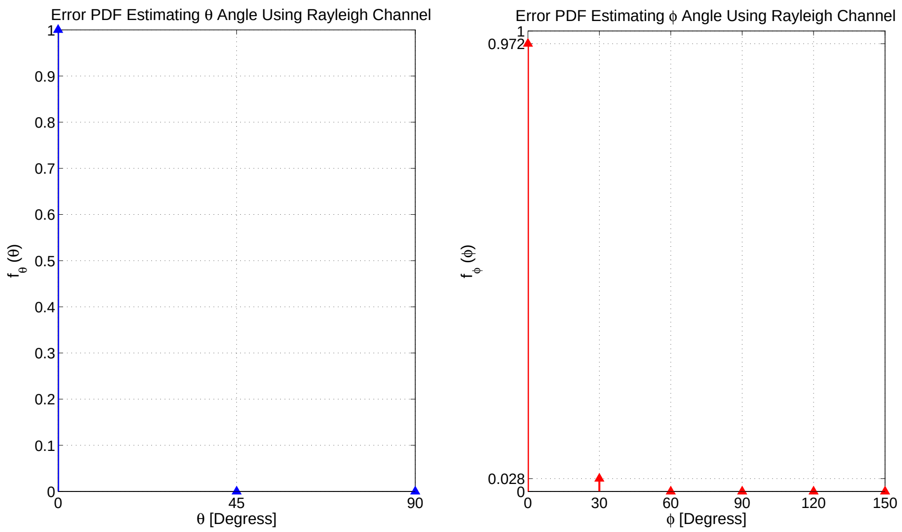

Figure 4.2: Probabilistic Algorithm: Error PDF Function for θ and ϕ Angles Using Rayleigh Channel

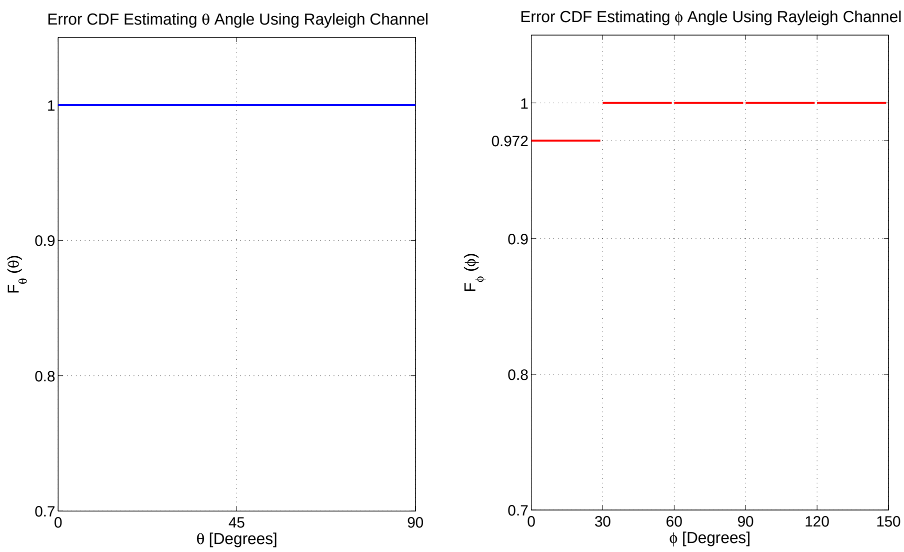

Figure 4.3: Probabilistic Algorithm: Error CDF Function for θ and ϕ Angles Using Rayleigh Channel

is happening for values between 0 and 30 degrees because ϕ is not defined between those values. Anyway, it is possible to assure that the error in estimating ϕ is lower than 30 degrees.

From the Figures (4.3 and 4.5) it can be seen that Rayleigh or Rician distribution gives the same error values. But it does not mean that nothing is changing when they are applied.

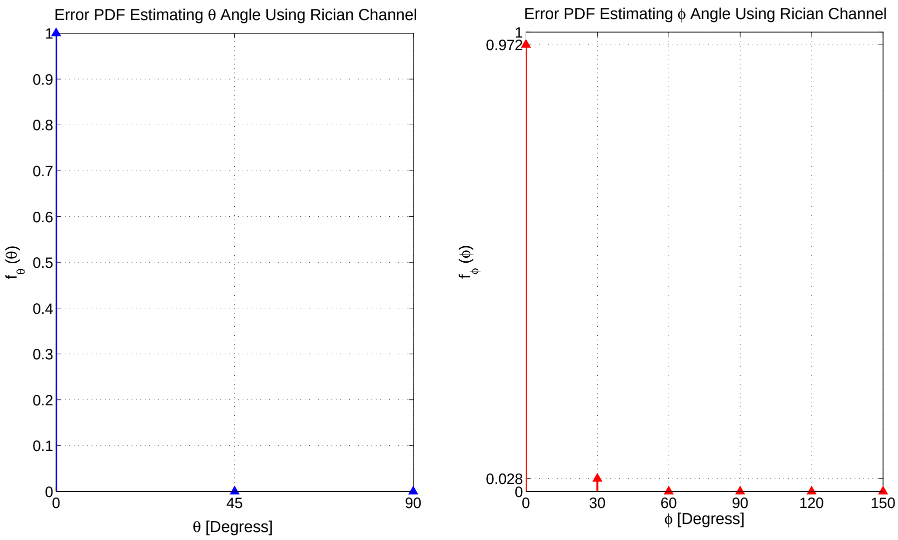

Figure 4.4: Probabilistic Algorithm: Error PDF Function for θ and ϕ Angles Using Rician Channel

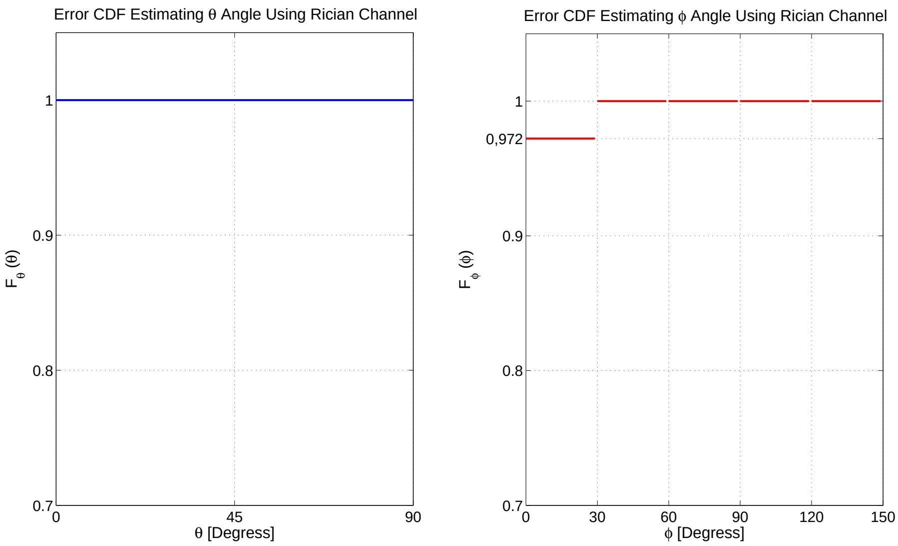

Figure 4.5: Probabilistic Algorithm: Error CDF Function for θ and ϕ Angles Using Rician Channel

Having a look to the core of the algorithm and plotting in Figure 4.6 and in Figure 4.7 the intermediate posterior PDF, it can be seen that the PDF using a Rayleigh distribution has one peak over the real orientation and another one around another possible orientation, whereas Rician distribution has only one peak where the real orientation is. This is because when the Rician distribution is used, it is considered that there is LOS component. This means that there is a component which dominates the rest of the components. Thus, only one peak appears in the figure making easier for the algorithm to take the decision. Nevertheless, there is no LOS dominant component using Rayleigh distribution. Because of this, more peaks appear in the plot making more difficult to take the decision. Despite this, in both cases the most probable estimated orientation is the same.

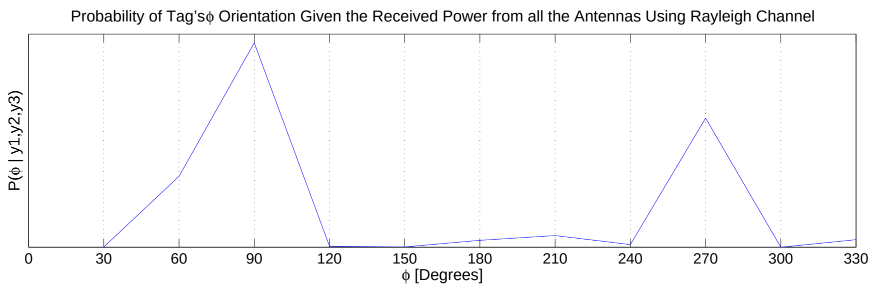

Figure 4.6: A Posteriori Probability Using Rayleigh Channel.Estimation $\phi = 90°$

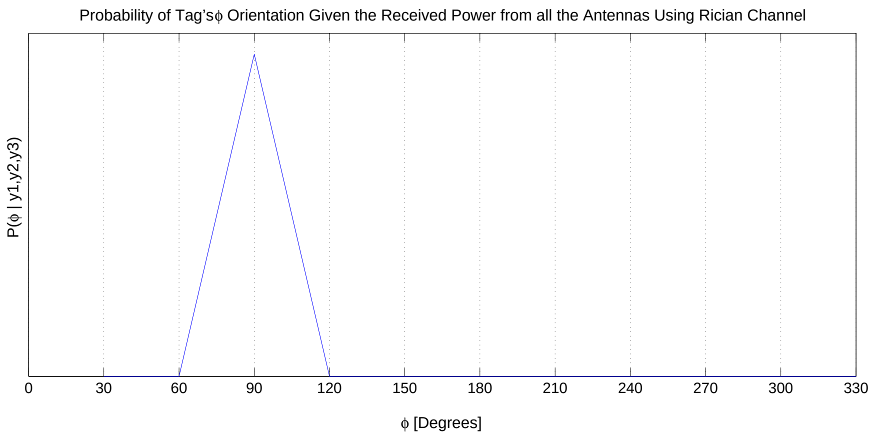

Figure 4.7: A Posteriori Probability Using Rician Channel. Estimation $\phi = 90°$

From the Probabilistic Orientation Algorithm outcome error it can be seen the capability of detecting the tag orientation with high accuracy. In addition to this, KNN Orientation Algorithm results prove that it is able to detect the possible orientations with no error all the time. Even though it was not expected a high accuracy in the KNN method, a possible explanation could be the low received signal variance. In the remaining chapters, it will be studied the robustness of the bayesian estimator contrasted with the suboptimal KNN procedure.

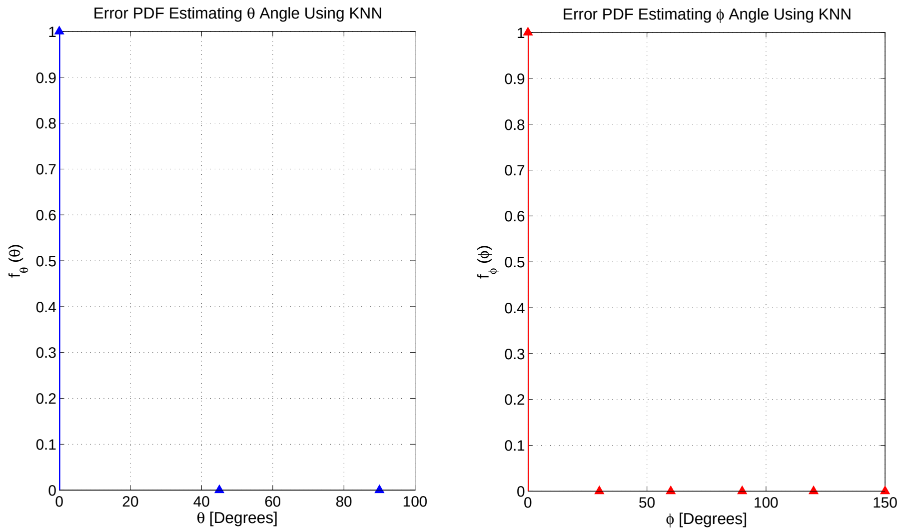

Figure 4.8: KNN Algorithm: Error CDF Function for θ and ϕ Angles Using KNN

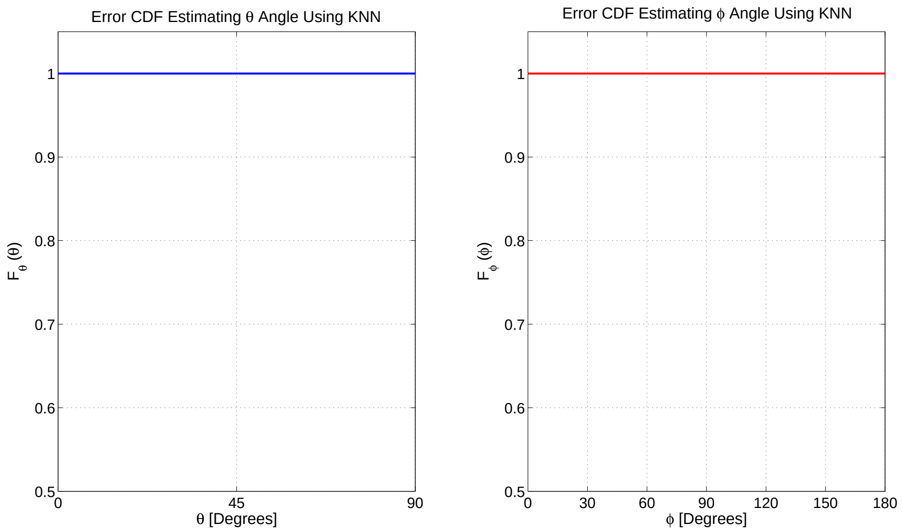

Figure 4.9: KNN Algorithm: Error CDF Function for θ and ϕ Angles Using KNN

4.4 Experiment I Conclusions

The main goal of this chapter was to validate the developed algorithms to estimate the orientations. Due to the symmetrical nature of the radiation pattern of the tag, the errors in the orientation estimation are limited to the interval $[0°, 180°]$. For example, if an error of $210°$ is committed, it will be shifted to $mod(210, 180) = 30°$. The obtained errors will depend on the granularity of the values of $[\theta, \phi]$ used to take the measurements.

From this validation it can be seen that it is possible to detect both orientations with no errors the 97% of the time in the worst case. The same result is obtained for both channel models, Rayleigh and Rician. Because of the this result, it is not necessary to work with Rayleigh and Rician channels. Consequently, only one propagation model is selected. Rayleigh channel is the best option because it can not be assumed LOS situations for all the possible orientations, i.e when a tag is facing one antenna the rest of the antennas will not have a LOS path.
After the results of Experiment I it can be stated that the algorithms are working properly and are ready for the next step: To use a commercial RFID system with commercial UHF RFID Tags and a commercial RFID reader.

Chapter 5

Algorithms Evaluation with Commercial Devices

The previous chapter proved the capability of the system to detect the orientation, but it is needed to test the algorithms in realistic scenarios like using commercial tags and reader. In this evaluation the tag is attached to a cardboard box, which is filled with several materials such as polystyrene, porcelain and metal. First of all the experiment setup with commercial devices, called Experiment II, is explained. Afterwards, the results of the orientation algorithms are presented.

5.1 Experiment II Using Commercial Tags and Reader

The experiment carried out by Aalborg University is recreated, but this time the antennas are connected to a commercial reader. The artificial tag - a folded meandered dipole antenna printed on PCB - is replaced with a commercial UHF RFID passive tag. Moreover, as it is explained in Section 4.2 (page 23), a set of 12 azimuth orientations ($\phi = 0°$, 30°, $\cdots$, 330°) values and 3 values for inclination angles ($\theta = 0°, 45°, 90°$) is examined.

Since the reader has 4 ports, only four antennas can be connected at the same time. Because of dual linear polarized antennas are used, 2 ports will be required by each antenna. Therefore, in order to connect three antennas (6 ports), the experiment is split in two parts: Antenna 1+Antenna 2 and Antenna 3+Antenna 4 (notice that the last antenna is not truly necessary to compare with Experiment I). In other words, the experiment is performed for the first set of antennas, repeated for the remaining set and finally the datasets are combined into one complete dataset. Figure 5.1 represents where the antennas and the target were placed. In next chapter it is analyzed how many of these antennas are sufficient to properly estimate the orientation.

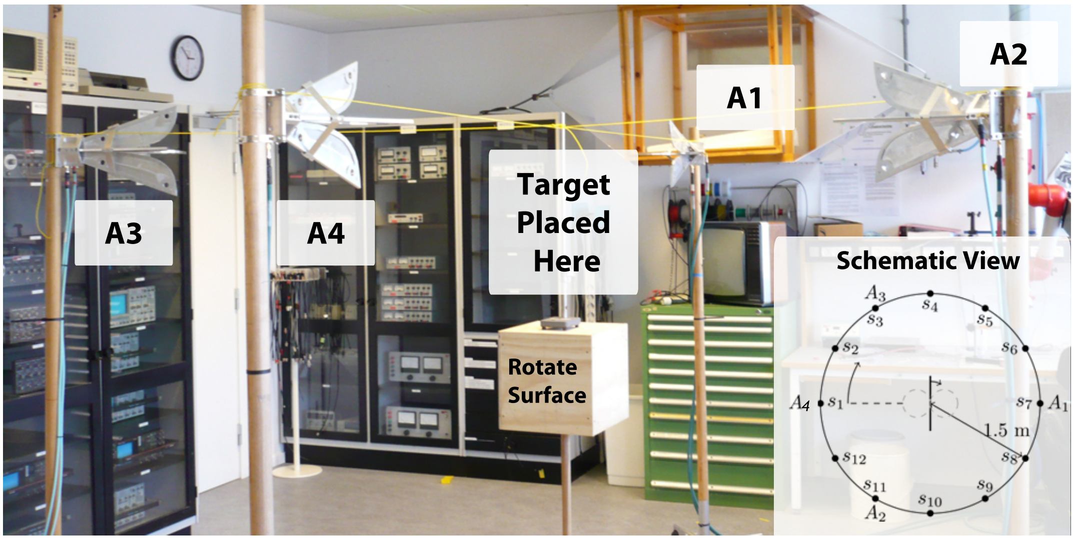

Figure 5.1: Experiment setup with four antennas placed equidistant to the tag, which is in the center of the circumference.

The hardware used and the experiment setup is summarized in Table 5.1.

Parameter	Value
Reader Model	Impinj Speedway Revolution [16]
Reader transmit Power	27.5 dBm
Tag Model	ALN-9640 Squiggle Inlay [17]
θ Values	0°, 45°, 90°
ϕ Values	0°, 30°, 60°, 90°, 120°, 150°, 180°, 210°, 240°, 270°, 300°, 330°
Samples per Rotation	250 samples in average
Distance Tag - Antennas	1.5 m
Tag height	1.65 m above ground
Antennas height	1.85 m above ground
Difference in height tag - Antennas	0.2 m
Object where the tag was placed	Polystyrene, polystyrene with metal plate, polystyrene with porcelain plate

Table 5.1: Experiment II Parameters.

The experiment will be done in several scenarios and for two subsets of antennas. Thus, it is needed to design a setup where the measurements take the minimum possible time. That is why, an automatic system is designed, which is able to rotate the box and to collect the data from the commercial reader. Everything is controlled from a computer, in which human interaction is only needed to modify the θ angle (vertical plane) of the tag.

The basic idea is to collect all the tag responses from all the antennas during a specific time interval. This time interval will depend on the tag reading rate (about 100 times per second): as a result, 100 Radio Signal Strength Indicator (RSSI) values are captured each second. Clearly, some of the tag orientations will significantly increase the gain mismatch, and therefore the reading rate will drop.

As shown in Figure 5.2, most of the samples fall in the same interval and, therefore, the variance of the signal is low (less than 1 dB). Thus, a high number of samples is not needed. Consequently, the time interval will be large sufficient to allow enough time for the reader to collect RSSI values from all the angles in each antenna. In practice, an interval of 4 seconds will fit these requirements.
While testing the experiment setup, the tag was undetected in several angles due to the gain mismatch. In order to focus in the evaluation of the algorithm, not in the technology itself, the box was placed at similar height to the the antennas one (0.75 m closer than the previous experiment).

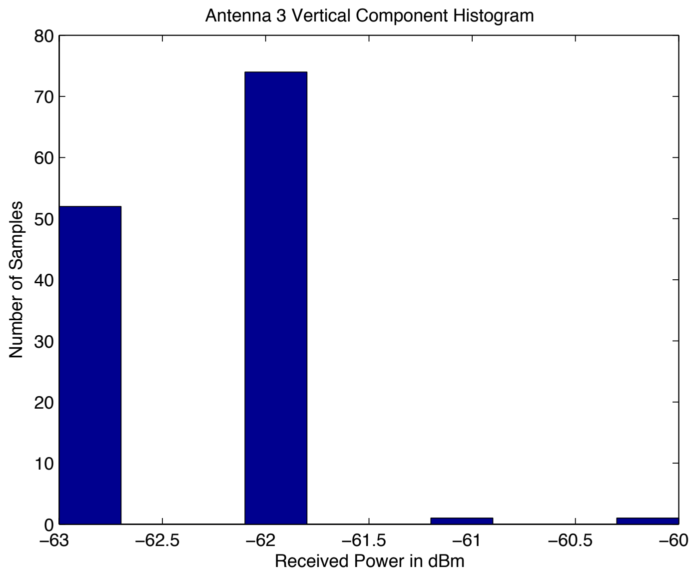

Figure 5.2: Histogram of the signal power received from one of the antennas -128 samples-

The following sections provide a better understanding of the system: each block of the setup is briefly explained.

5.1.1 Control Station

A computer is running a Java program, which is in charge of synchronizing all the different blocks and collect the tag responses from all the antennas by using the reader. The process is the following (see also Figure 5.3):

1. It configures the reader by using the Low Level Reader Protocol (LLRP). This protocol will be introduced in Section 5.1.2.

2. It tells the reader to start the query round and it stores the tag responses into the proper file.

3. It communicates with the Arduino board by USB port to send a trigger signal that will rotate the box 30°.

4. It waits 7 seconds until the box is stabilized and it goes to step 1. This process finishes when the azimuth orientation reaches 330°.

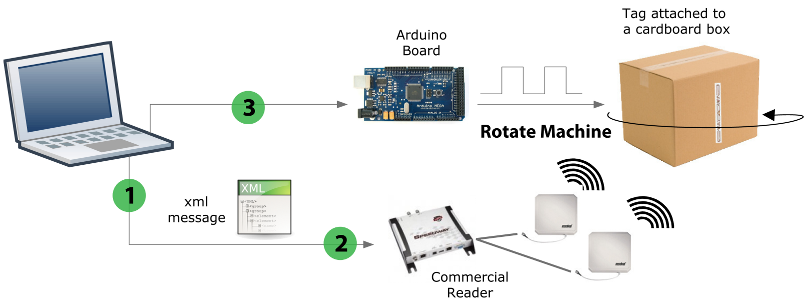

Figure 5.3: Schematic representation of the system setup used in the experiment with commercial devices.

Finally, all the stored data is loaded in Matlab and the orientation algorithms are applied.

5.1.2 Commercial Reader and LLRP Protocol

The commercial reader used in the experiment follows two protocols: EPC Global Class 1 Generation 2 UHF Air Interface Protocol Standard, so called “Gen 2” [18] (see also Appendix B) and Low Level Reader Protocol, known as “LLRP”. The first one defines the physical and logical requirements for passive tags in RFID while LLRP defines the interface between the reader and its controller software and hardware [19]. The advantage of this LLRP Protocol is the possibility to design systems where readers from different manufactures can work together.

The main idea is to use XML messages (Extensible Markup Language) for the communication between the controller software and the Reader. For example, in order to configure the reader a Reader Operation Specifications file is used (from now on ROSPEC), in which several parameters are configured, such as:

- Which antennas should be used by the reader. (4 Antennas)
- Transmitted power in dBm. (27.5 dBm)
- Number of tags to read, before it sends the report to the computer. (1 tag)
- Duration: this parameter sets the maximum time to generate the XML response (report) that the computer is waiting. (4 s)

When a XML file with the ROSPEC is sent to the reader, it will start querying the tags in the area following the parameters given in the configuration. The reader will generate a report for each tag read or when the 4 seconds time interval is finished. Lastly, the report is forwarded to the computer that will store the data.

5.1.3 Arduino Board

Arduino board is a tool with a complete development kit that allows to generate a trigger signal needed to rotate the box with the electric motor. A program is made to read the characters via COM port (USB in this case): if this character is “1”, it will generate a 10 ms pulse in the pin 47 of the board. This pin is connected to the rotor that changes the box orientation in 30°.

(a) The Arduino board used in the experiment to control the electric motor [20].

(b) Commercial reader used in the experiment. Impinj Speedway Revolution [16]

Figure 5.4: Commercial reader and the Arduino board used in the experiment.

Once all the blocks are defined, the algorithms evaluation results are presented in Section 5.2.

5.2 Experiment II Results in Terms of Error CDF

The main difference of this section compared with Chapter 4 (page 21) is that the algorithms are evaluated with commercial RFID devices. As it was mentioned at the beginning of this chapter, three different situations are considered: cardboard box filled with polystyrene, metal and porcelain.

First of all, the Probabilistic Orientation Algorithm is evaluated followed by the KNN Orientation Algorithm. The examination begins with the simplest case (cardboard box filled with polystyrene), in which the radiation pattern of the tag is expected to be as a dipole due to the relative permittivity (ε_r) of the polystyrene with respect to the air (2.4 and 1 respectively [21]). Through this section it will be also studied the case of porcelain inside the box ($\varepsilon_r = 7$), which is an intermediate situation because the radiation pattern will be affected but it will not have a strong impact as other materials like metal. Lastly, the algorithms are tested with an object that will severely modify the response of the tag.

The procedure is as follows: In the first place, the power values from all the antennas are collected in all θ and ϕ orientation angles to build the Offline Calibration table. As second step, new data will be collected to evaluate the accuracy of the orientation algorithms. In other words, the Offline Calibration table or phase could be understood as the process to store data before estimating the orientation of the target. This calibration requires to be done each time the contents of the box is changed. That is why, it will be also studied the possibility of using the simplest case (only polystyrene) as calibration data for the other two cases. In this way, the Offline Calibration phase does not require to be performed for each new material.

5.2.1 Probabilistic Orientation Algorithm

The probabilistic Orientation Algorithm is defined in Chapter 3 (see page 11). The results are represented using discrete CDF. In addition to this, a result summary is presented in Figures 5.12 and 5.13 (see pages 43 and 44).

Probabilistic Algorithm: Cardboard Box Filled with Polystyrene

This is the simplest case (the radiation pattern of the tag is expected to be as a dipole). Figure 5.5 presents how the received power in one of the antennas is changing due to ϕ variations (note that 12 ϕ positions means 360° or a full loop in the azimuth plane). It can be seen that in certain positions the received power drop to a -90 dBm. This value is artificially set when the reader is not able to activate the tag, and therefore, there is no response.

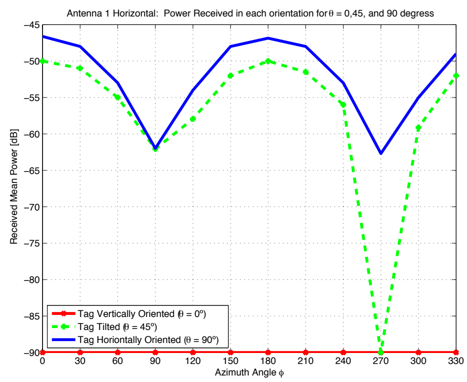

(a) Received power values for horizontal Antenna 1 component for different tag orientations.

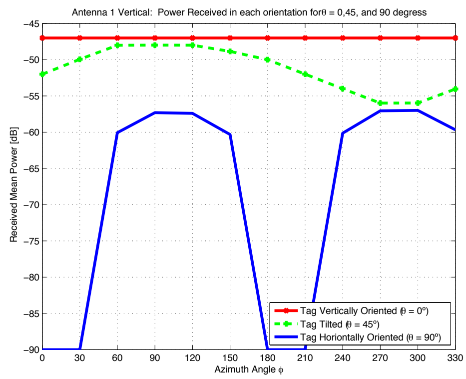

(b) Received power values for vertical Antenna 1 component for different tag orientations.

Figure 5.5: RSSI values for vertical and horizontal Antenna 1 components. (In dBm)

The top angular sensitivity of the tag used is represented in Figure 5.6, where it is placed horizontally (the rotations are made in the plane XZ). It can be seen how the values drops significantly for 90° and 270°. Since the sensitivity is low for 90° and 270°, a low received power in the reader is expected (as in Figure 5.5a). It is important to mention that the tag needs a certain level of power from the reader to be able to backscatter the signal. In practice this threshold seems to be around -65 dBm.

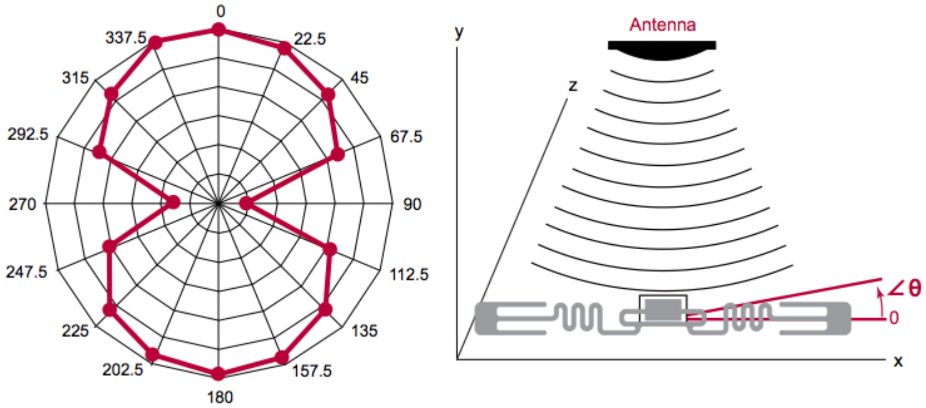

Figure 5.6: Tag Top Angular Sensitivity and Relative Orientation [17]

Theoretically, no response should be present in the vertical antennas when the tag is horizontally oriented (Figure 5.5b), because a total polarization mismatch should exist, but in practice, reflections could occur and the polarization could be shifted. In this way, the tag is activated. Despite the fluctuations due to the artificial -90 dBm values, the power collected in the vertical component varies in a short range (less than 2 dB) as expected, because the sensitivity is maximum all over the tag (like a dipole).

The evaluation of the Probabilistic Orientation Algorithm throws an error lower than 90° the 90% of the time for ϕ and no error is made to estimate θ. By taking into consideration the results from the previous chapter (no error was made the 97% of the time), it is an important worsening in the outcome. (See Figure 5.7).

However, the error was expected to increase due to the variations introduced by the commercial tag compared with the artificial tag. The artificial tag does not require to be powered from the reader, because it is always sending a signal. For commercial devices, the signal needs to change the polarization before reaching the tag if a PLF mismatch exists, but with enough power to activate it.

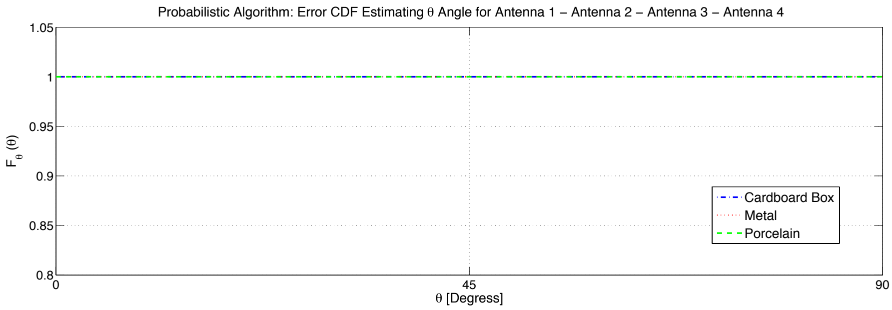

(a) Error CDF Estimating θ Angle Using Rayleigh Channel with commercial RFID system.

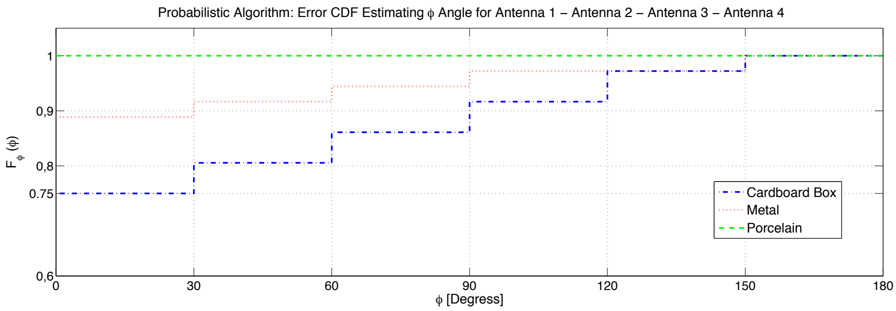

(b) Error CDF Estimating ϕ Angle Using Rayleigh Channel with commercial RFID system.

Figure 5.7: Probabilistic Orientation Algorithm: Error CDF Estimating θ and ϕ using Rayleigh Channel with commercial RFID System.

Although a degradation in the results was expected, the source of errors greater than 90° is analyzed: the received power in the horizontal antennas when the tag is vertically oriented ($\theta = 0$) should be taken into account (see Figure 5.8a). In this figure (recall that when the tag is not read, an artificial -90 dBm is added), there is no tag response for antennas 1,2 and 3; besides antenna 4 receives the same amount of power for 10 out of the 12 ϕ steps. Thus the algorithm is unable to detect the ϕ angle (all the angles have the same probability). On the other hand, the inclination of the tag (θ) is detected with no error. (See Figure 5.7a)

As a conclusion, the estimation fails because the tag is not activated from three of the antennas in any angle and the fourth one detects the same amount of power for almost all the orientations, thus there is no information to process and the algorithm fails. By subtracting the error caused by this situation, the error decreases. In this case the performance is similar to the previous chapter.

Probabilistic Algorithm: Cardboard Box Filled with Porcelain and Metal plates

In this scenario the cardboard box contains a porcelain plate or a metal piece and the remaining space is filled with polystyrene. It can be seen in Figure 5.7 that it is possible to detect without error θ and ϕ in all the orientations for the porcelain case.

It is worthy to mention the differences in the results compared to the cardboard box

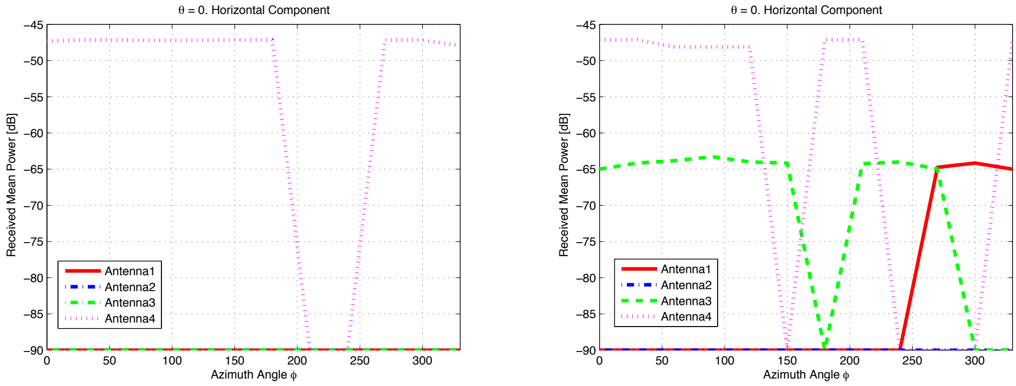

(a) Cardboard box only with Polystyrene received power from all the antennas in the Horizontal component for $\theta = 0$.

(b) Cardboard box with Porcelain received power from all the antennas in the Horizontal component for $\theta = 0$.

Figure 5.8: Received Power From All the Antennas for Only Polystyrene and Porcelain Cases. [dBm]

filled only with polystyrene: This time the tag was activated from at least one horizontal antenna (when the tag is vertically oriented ($\theta = 0°$), as Figure 5.8b shows. Even though the power levels are almost constant, which could case the algorithm to fail, it is compensated with the information from other antennas. For example, if $\phi = 150°$ is taken as a reference, there is no difference for antenna 3 with respect to $\phi = 0°$; but the remaining antennas provide different information depending on the angle. Although it is not presented in this report, a similar argument could be drawn for the cardboard box with metal inside.

With respect to the metal object, the overall performance is also better than the cardboard box filled only with polystyrene. The error CDF is lower than 30° for the 90% of the time for ϕ, while θ is estimated with no error (see Figure 5.7).

Probabilistic Algorithm: Using the Cardboard Box with Polystyrene as Calibration for Porcelain and Metal Scenarios

The three considered scenarios require an Offline Calibration Phase, but to calibrate the system for each different material inside is costly from a practical point of view. According to this, the possibility of using the calibration data from the simple scenario (cardboard box filled with polystyrene) for the remaining situations is analyzed in Figure 5.9.
Although it is possible to use the calibration data from a different scenario, it has an impact in the results. The box inclinations are detected with no error the 86% of the time and the error is always lower than 45°. Analogously, ϕ estimations are worsening, going from 30° to 120° the 90% of the time. Nonetheless, it should be taken into account that the error is lower or equal to 30° the 82% of the time.

It is also possible to use porcelain or metal objects as calibration data, but the obtained results are similar to the presented in this report, therefore the conclusion remains the same.

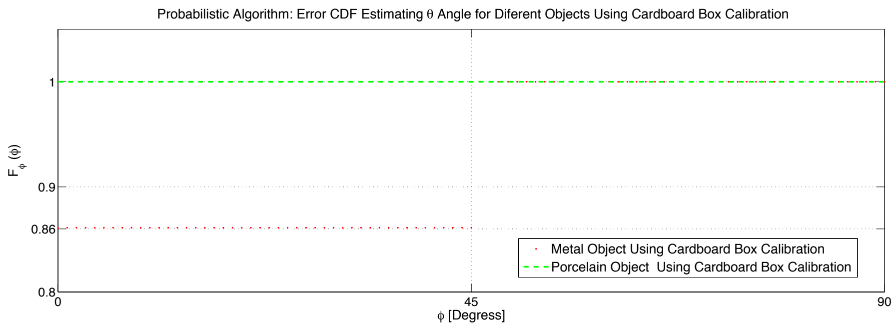

(a) Probabilistic Algorithm: Error CDF estimating θ angle using cardboard box with polystyrene as calibration data.

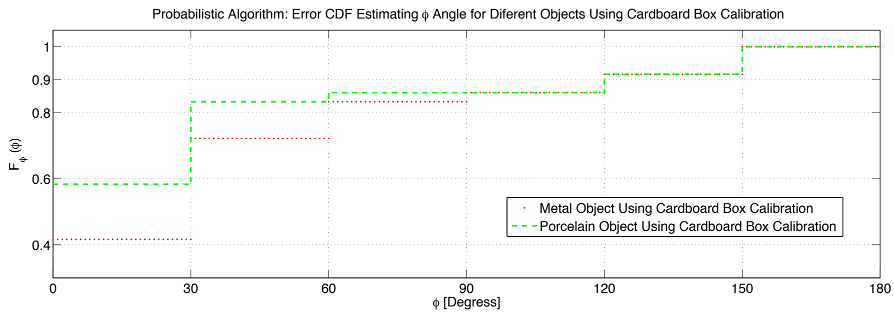

(b) Probabilistic Algorithm: Error CDF estimating ϕ angle using cardboard box with polystyrene as calibration data.

Figure 5.9: Probabilistic Algorithm: Error CDF for θ and ϕ for metal and porcelain objects using cardboard box with polystyrene as calibration data.

5.2.2 KNN Orientation Algorithm

This section deals with the same analysis than the Probabilistic Orientation Algorithm. All the experiment parameters are the same; the only difference is the estimator used (KNN).A results summary is presented in Figures 5.12 and 5.13 (see pages 43 and 44).

KNN Algorithm: Cardboard Box Filled with Polystyrene

The KNN Orientation Algorithm shows impressive results as can be seen in Figure 5.10: it is able to detect θ and ϕ angles with no error. The performance of this algorithm in this scenario is expected to be highly precise due to the low variance of the signal over time as shown in Figure 5.2. It should be noted that the method is not able to overcome the described problem of no response for the horizontal antennas when the tag is vertically oriented, but it decreases such uncertainty due to the information provided from the vertical antennas.

KNN Algorithm: Cardboard Box Filled with Porcelain and Metal plates

In the same way that the cardboard box filled only with polystyrene, the 100% of the time the error is 0 for both objects, as can be seen in Figure 5.10. Even though this algorithm is not the optimal one, it presents a high precision when the calibration data used is similar to the estimation phase data, due to the low variance in the signal.

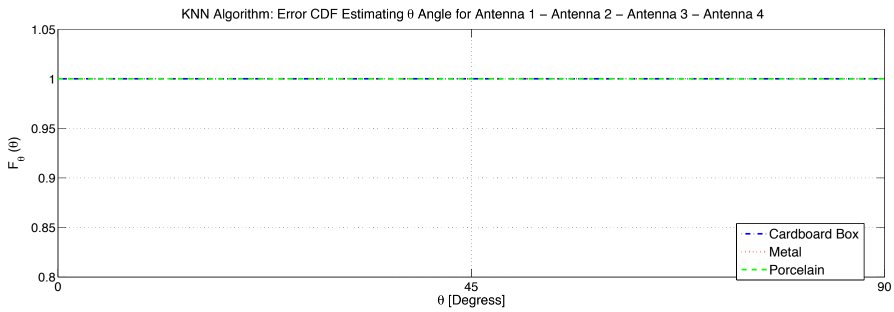

(a) Error CDF Estimating θ Angle Using KNN Orientation Algorithm.

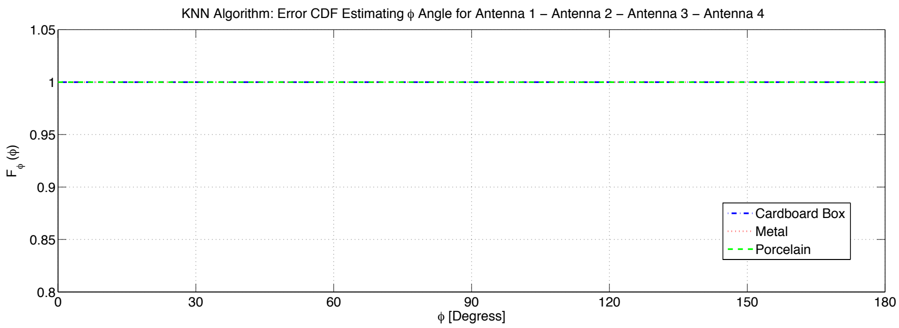

(b) Error CDF Estimating ϕ Angle Using KNN Orientation Algorithm.

Figure 5.10: CDF for θ and ϕ for KNN Orientation Algorithm.

KNN Algorithm: Using the Cardboard Box with Polystyrene as Calibration for Porcelain and Metal Scenarios

This section allows to analyze in a deeper view the global performance of the KNN Algorithm because previous tests are highly influenced by the variance of the signal. In this case, by using the cardboard box with polystyrene as calibration data to estimate the orientations for porcelain and metal scenarios, it will be possible to evaluate the KNN method in harder conditions.

A worsening in the result for θ and ϕ can be seen in Figure 5.11, where the errors changed from 0° to 90° with respect to ϕ the 90% of the time, and from 0° the 100% of the time to 0° the 97% of the time of θ. From this data, it is clear the impact in the result for the azimuth orientations when object used to calibrate the algorithm is not the same than the target. Even though the error made the 90% of the time is lower than the Probabilistic Algorithm, their performance, in general terms is quite similar.

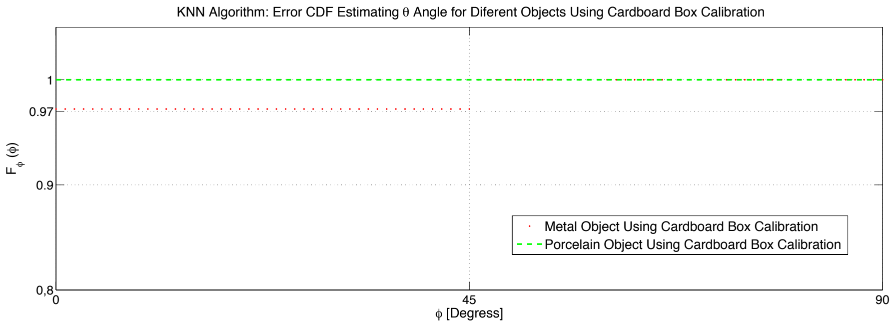

(a) KNN Algorithm: Error CDF for θ angle using a cardboard box with polystyrene as calibration data.

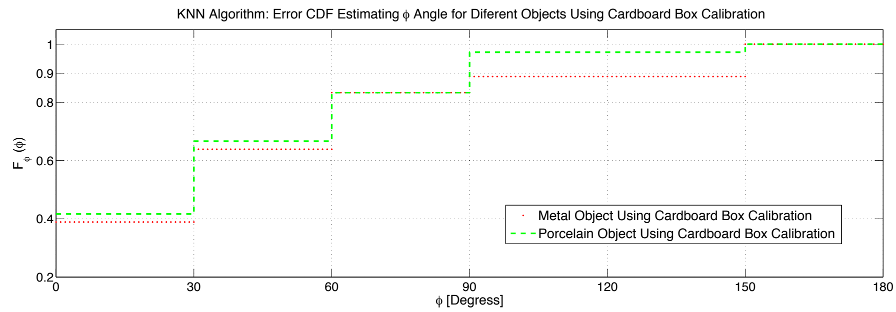

(b) KNN Algorithm: Error CDF for ϕ angle Using with cardboard box with polystyrene as calibration data.

Figure 5.11: KNN Algorithm: Error CDF for θ and ϕ angles using a cardboard box with polystyrene as calibration data.

5.3 Algorithm Evaluation Conclusions

To conclude this chapter, an overview of the orientation algorithms is presented. In addition to this, two new figures are introduced: Figures 5.12 and 5.13. The first one presents the maximum error made by the orientation algorithms for ϕ the 90% of the time. The second one is focused on another point of view: the percentage of time in which the algorithms can estimate the orientations with no error.

By taking into account the worst case for ϕ, where the cardboard box with metal is calibrated with polystyrene (Figure 5.12), it presents an error lower than 120° the 90% of the time for the Probabilistic Algorithm. On the other hand, KNN Orientation Algorithm has an error lower than 90°. It can be conclude that using calibration data from a different material has a strong impact in the results for both algorithms while estimating ϕ.

KNN Orientation Algorithm shows perfect results when the calibration data is used from the same material. This behavior is expected due to the low variance of the received signal as can be seen in Figure 5.2 (see page 33).

It is worthy to mention that most of the errors in the estimation of ϕ are inherent to the method and technology themselves in the Probabilistic Orientation Algorithm. It means that the horizontal antennas do not receive any signal when the tag is vertically oriented ($\theta = 0°$) due to the polarization mismatch. Thus, the algorithm is not able to estimate

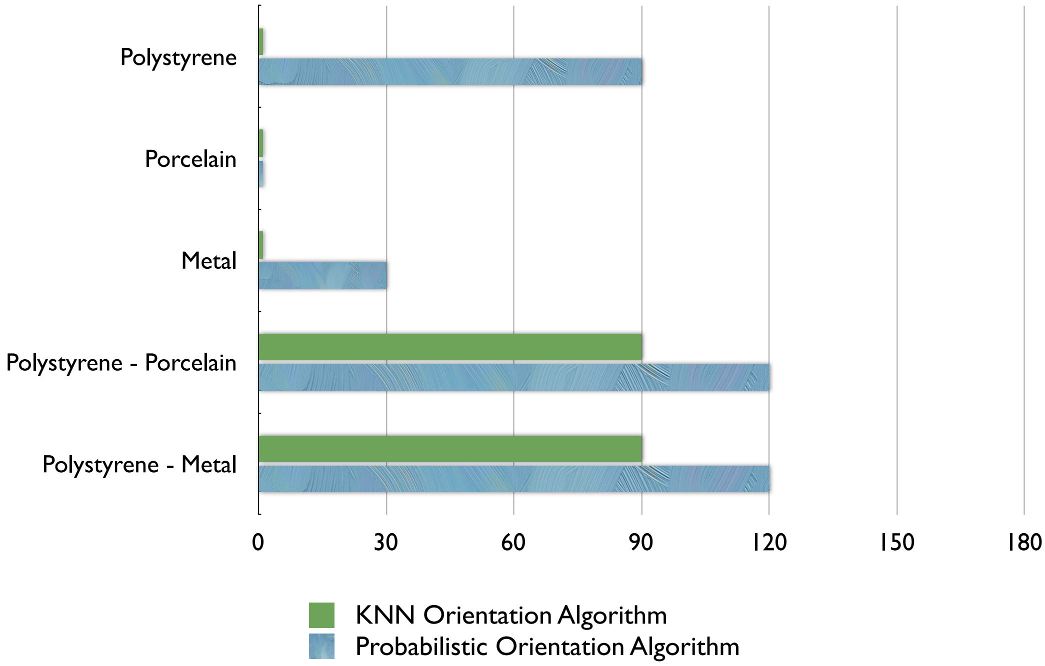

Figure 5.12: ϕ Maximum Error in degrees around tge 90% of the time for Probabilistic and KNN Orientation Algorithms -CDF at 90%-

the ϕ angle. In the case of KNN Orientation Algorithm, this situation is partially fixed by using the information from the vertical antennas as well.

It was expected a degradation in the results compared with the artificial tag experiment. The error was shifted from detecting both angles with no error the 97% of the time, to 90-120° the 90% of the time, in the worst case. The artificial tag used in the previous chapter does not need to be activated and therefore if the signal changes its polarization, due to the reflections, it will be received. On the other hand, commercial tags do not only require a change in the polarization, but a certain amount of power to supply energy to the circuit and to backscatter the signal to the reader as well.

In addition to the presented results, Figure 5.13 puts on view the percentage in which the estimations made by the orientation algorithms have no error; in other words, how much time the orientation is calculated with error equal to zero.
It can be said that the revealed error was too high for the Probabilistic Orientation Method to be used in real applications, however this argument is made by taking into account the behavior the 90% of the time. On the other hand, the method is able to estimate with no error the 40% of the time all the ϕ orientations and with an error lower than 90° the 83% of the time. This means that the Algorithm is able to work but with a precision lower

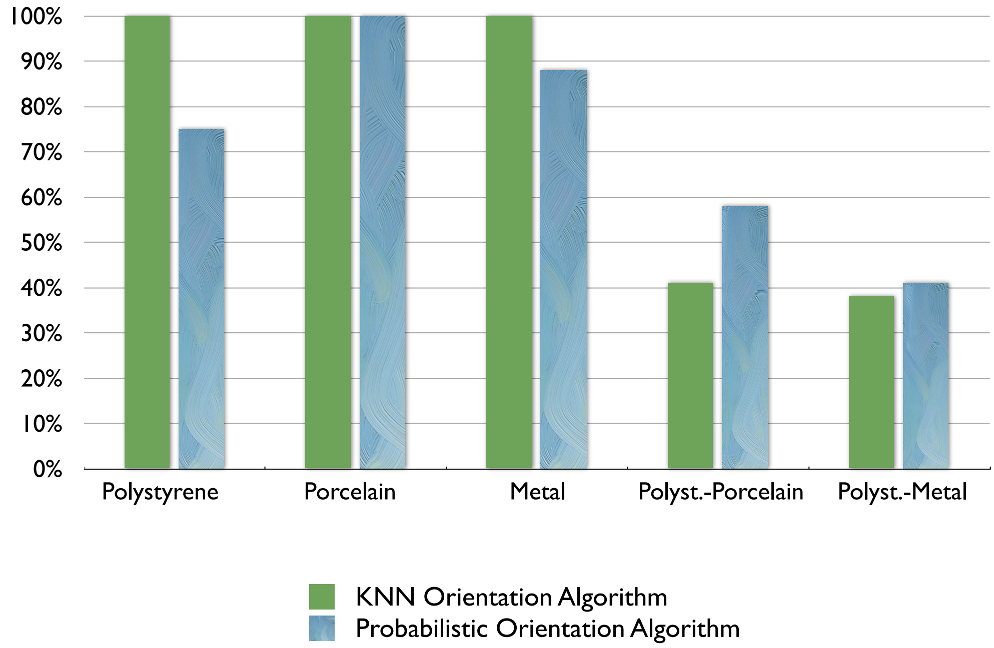

Figure 5.13: Percentage of Time in which the Probabilistic and KNN Orientation Algorithms Detect Orientations with No Error

than the 90%.

Regarding θ, the Probabilistic method proved that is able to detect if the box is tilted $90°$ or $45°$ with no error, in all the scenarios proposed. In contrast, the KNN Orientation Algorithm distinguishes variations of $90°$ with no error and the error is equal or lower than $45°$ the 97% of the time.

The following chapter will be focused on reducing the expenses of the system. In this point, the algorithms need to be calibrated measuring the received power at all possible orientations and it was shown how the orientation estimation is carried out using four antennas. The next step will be to decrease the elapsed time calibrating the system by reducing the number of the calibration points and the number of the antennas that contribute to the orientation estimation. With this, it will be check if it is possible to decrease the costs of the implementation of the system.

Chapter 6

Improving the System by Reducing the Costs

In Chapter 3 it was explained how to find the orientation of a passive RFID tag by using a probabilistic method and a proximity technique. However, these methods are carried out with the obtained data in a previous calibration phase. Concerning the proposed scenario in Section 1.1, it will be required to calibrate the algorithms for each object in the warehouse every time the environment changes. Clearly, this is a time consuming task that makes difficult the adaptability of this system.

Reducing the process of calibrating the system, the cost and time needed will be decreased as well. This will allow to easily make a new calibration in case of the objects, materials, boxes or environment are modified because the calibration phase will be faster.

This chapter focuses on improving the previous phase to the orientation estimation. In addition to this, the system will be enhanced to work only with one commercial RFID reader by decreasing the number of antennas [1]. This allows the cost of the system lessen. For that purpose, a reduction in the number of points for the calibration and the number of antennas will be studied.

6.1 How to Reduce the Calibration Phase?

In the experiments carried out (see chapters 4 and 5) the received power in the receiver antennas from the tag is measured in many different orientations: several values of θ and different ϕ values. Moreover, if the angle resolution rises up, the number of possible orientations increases considerably.

If the received power in some of these orientations is calculated analytically, the number of measurements and, therefore, the time needed is significantly reduced. For that purpose, concepts like Polarization Loss Factor (explained in Section 3.1.3) and antenna radiation pattern are essential.
An antenna radiation pattern is a mathematical function or a graphical representation

[1] Common commercial reader allows to work with a maximum of two dual linear polarized antennas.

of the properties of an antenna as a function of space coordinates. In other words, the radiation property represents the spatial distribution of the radiated energy as a function of the observer's position [22]. An example of radiation pattern of a dipole is shown in Figure 6.3.

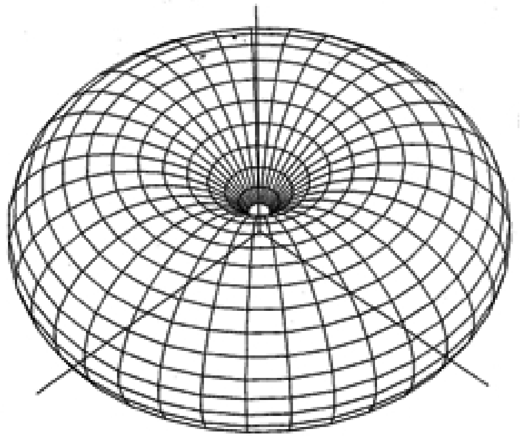

Figure 6.1: Radiation pattern of a dipole antenna
[23]

The goal is to determine the losses due to the orientation of the tag. A common erroneous thought is that the PLF is affecting to both orientations, azimuth and elevation angle. Actually, only the elevation angle is causing polarization mismatch and the losses due to azimuth angle are given by the radiation pattern of the tag. This can be better explained by classifying the losses into two types regarding its cause:

- Losses due to polarization mismatch: these losses are caused because of the polarization mismatch between the receiver antenna and the tag. It is possible to calculate them as was explained in Section 3.1.3:

$$PLF = cos^2(\alpha) \tag{6.1}$$

  Applying this formula it is equivalent to make the projection of the tag antenna over the plane that contains the receiver antenna. For instance, to calculate the polarization mismatch between an antenna placed with θ equal to 45° and an horizontal antenna, it is needed to project the first antenna into the horizontal plane in order to get the part of power that will be coupled into the second antenna. See Figure 6.2.

- Losses due to the antenna radiation pattern: once the polarization mismatch has been calculated, the problem is reduced to two different antennas lied down in the same plane (keep in mind that taking into account the PLF is like make the projection of the antenna in the plane of interest). Although both have the same polarization (vertical or horizontal), there could still be a gain mismatch between them due to the ϕ angle. This means that depending on the observation angle the antenna will receive higher or lower power. This power is given by the radiation pattern of the

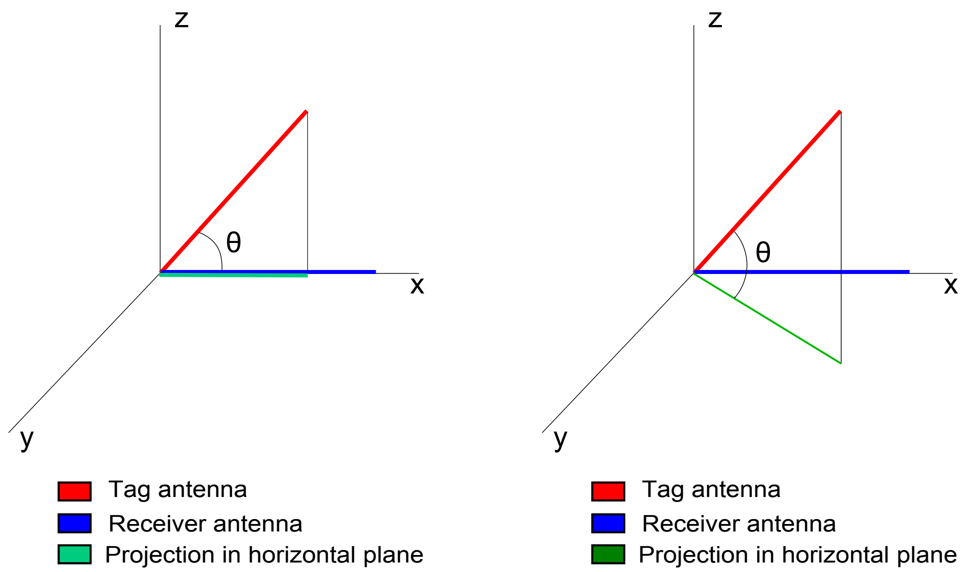

(a) Equal azimuth angle for Rx and tag (b) Different azimuth angle for Rx and tag

Figure 6.2: Projection of an antenna in the horizontal plane in order to calculate the polarization mismatch

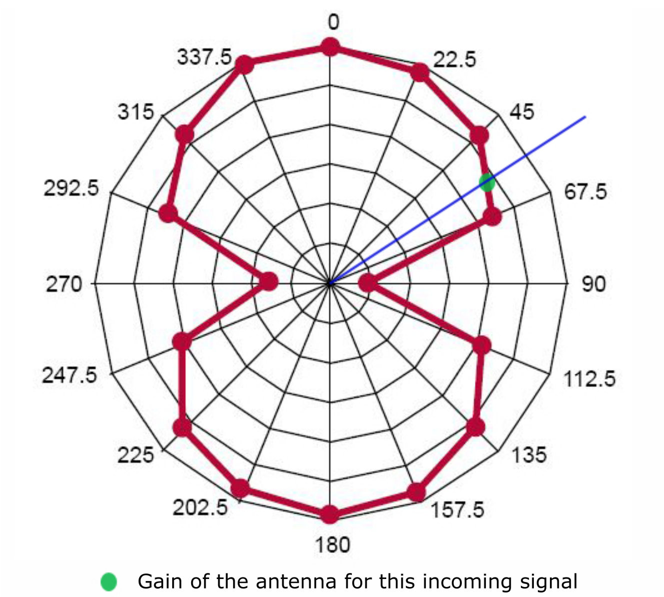

Figure 6.3: Radiation pattern of Alien 9640 tag [17]

antenna which characterize its gain for the waves coming from each location around it (see Figure 6.3 for a better understanding).

Applying these concepts of PLF and radiation pattern the calibration phase will attempt to be reduced in the next section.

6.2 Reducing the Calibration Phase

The theory explained in the previous section shows that it is possible to reduce the calibration phase by calculating the received power from some orientations but, due to the dynamic nature of the environment, reflections and other non-ideal conditions, those calculations will not fit perfectly real situations. In this section it will be analyzed the effect of estimating the received power values and its impact on the results of the orientation estimation.

The results will be analyzed using an iterative approach in order to identify which situation gives the best calculated power values and the best results in the estimation of the orientation.

6.2.1 Estimating the Received Power Values for $\theta = 45°$

From the calibration phase all the received power values for all possible orientations (θ, ϕ) were obtained. As a starting point, the received power values for $\theta = 45°$ will be estimated using all the already measured received power values at $\theta = 0°$ and $\theta = 90°$.

To estimate the received power at vertical antennas for $\theta = 45°$, the samples already measured for $\theta = 0°$ from the vertical antennas will be used. To estimate the received power at the horizontal antennas it will be used the samples obtained for $\theta = 90°$ from the horizontal antennas. Then, the Polarization Loss Factor will be applied to those values already measured in order to calculate all the values for $\theta = 45°$. This consists in a correction of -3 dB in the power.

To simplify the representation of the results, only the estimated power values for Antenna 1 will be presented. The results for the other antennas are more or less similar to the one presented. Figures 6.4a and 6.4b show real and estimated power values for $\theta = 45°$, for the vertical and horizontal polarized antennas, using a cardboard box filled with polystyrene, porcelain and metal. As it can be seen, the estimated received power for the vertical antenna when the box is filled with polystyrene does not fit well the real value. This is because, for $\theta = 0°$, the antenna is receiving almost a constant received power for all ϕ orientations, as it is expected if the radiation pattern of the tag is taken into account. Then, if the correction of -3dB is applied to estimate the received power for $\theta = 45°$, a constant received power for all ϕ orientations will be again obtained but 3dB lower. In a real situation, a change in the orientation modifies also the reflections and the received power fluctuates. This effect is not considered using the 3dB correction.

On the other hand, it can be seen how the estimation of the received power at the horizontal antenna fits well the real received power. In this case, the same fluctuations for θ

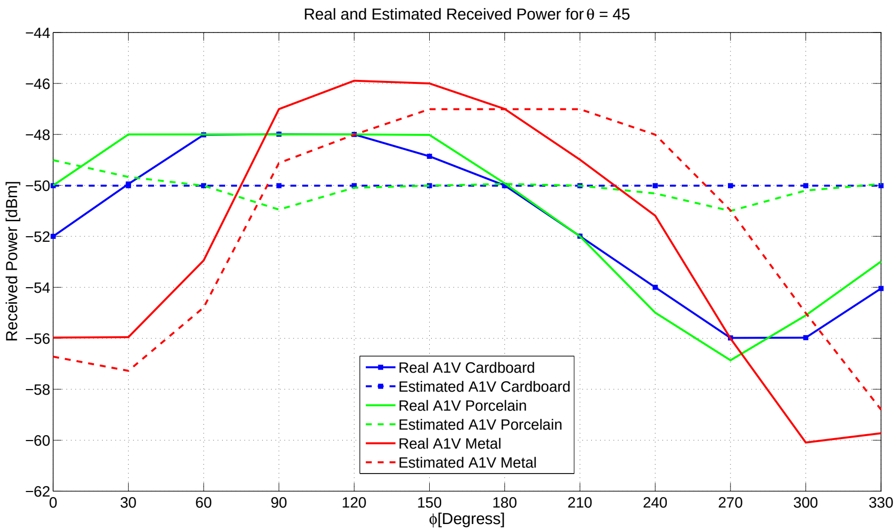

(a) Estimation of the Received Power at Antenna 1 Vertical for $\theta = 45°$.

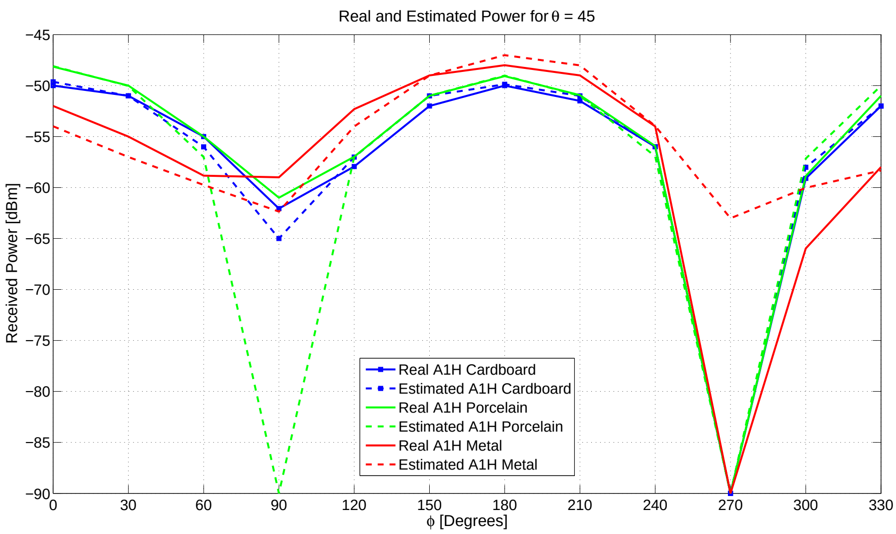

(b) Estimation of the Received Power at Antenna 1 Vertical for $\theta = 45°$.

Figure 6.4: Estimated Received Power for $\theta = 45°$ for Antenna 1 Vertical and Horizontal.

equal to 90° are reflected in the calculations for θ equal to 45° when the 3dB PLF is applied.

From these pictures, it can be said that it seems a good idea to estimate the received power for θ equal to 45° in this way. To confirm it, it is needed to have a look to the obtained results on estimating the orientation of the tag.

Figures 6.5a and 6.5b show the results for ϕ angle for both algorithms. It can be seen how, as it was expected, due to the power values are calculated instead of using real data, the results are not as good as before. In the graphics both cases can be compared: the

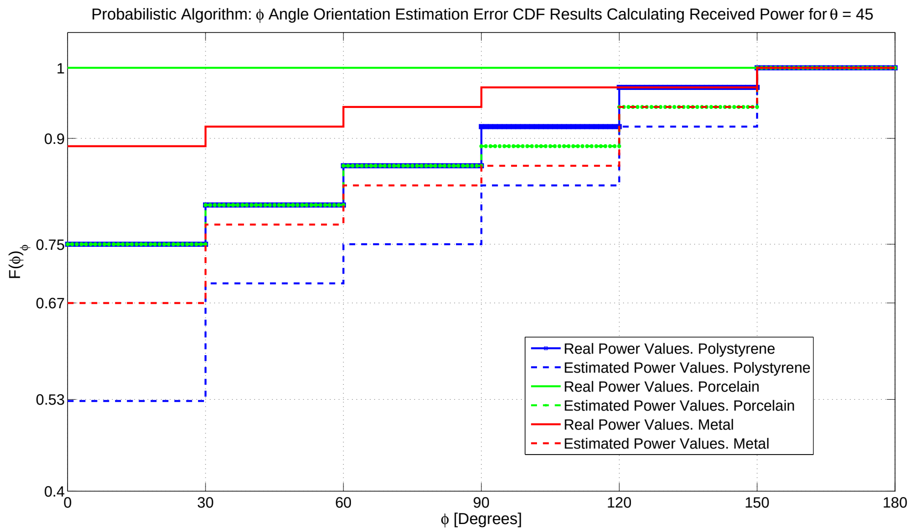

(a) Orientation Estimation Error CDF Results for Probabilistic Algortihm.

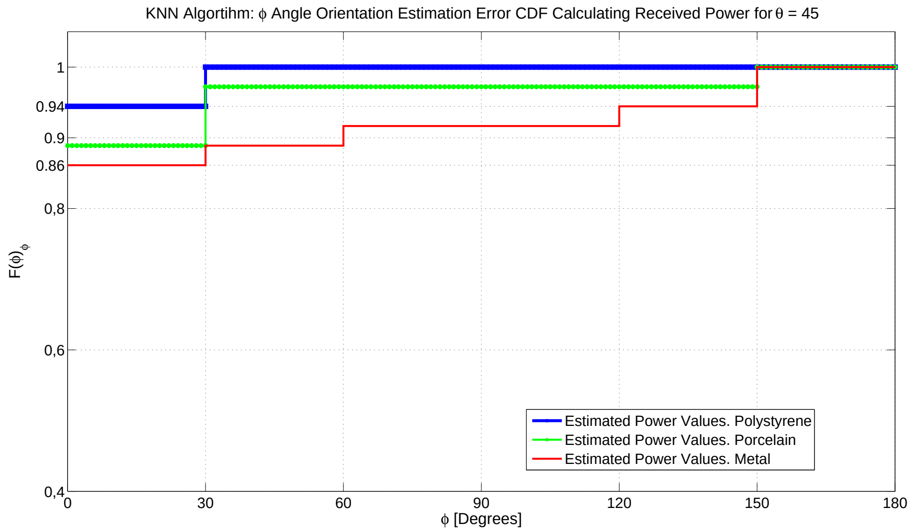

(b) Orientation Estimation Error CDF Results for KNN Algortihm.

Figure 6.5: Orientation Estimation Error CDF Results when the Received Power for $\theta = 45°$ is Estimated. Probabilistic and KNN Algorithm Results

previous one when real power values were used and the new one, when the power values are calculated for all the materials. Comparing with previous results, the error increases. For Probabilistic Algorithm, the error is lower or equal than 120° the 94% percent of the time for metal and porcelain and the 92% of the time for polystyrene. On the other hand, the algorithm is not making any errors the 53%, 67% and 75% of the time for polystyrene, metal and porcelain respectively.

Respect to KNN it is shown that it is still better than Probabilistic Algorithm. Despite it, the committed error is increased compared to the previous situation where the CDF was 1 for all the orientations.

In order to reduce the number of figures, the plots for the estimation of θ angle will not be shown. From the obtained results, it can be drawn that it is possible to estimate the orientation for θ angle almost without errors. The error CDF function for θ angle is almost always 1. KNN algorithm has some problems in estimating the θ orientation only when the box is filled with porcelain. In this case, the 97% of the time the error is 0° and the 3% of the time the error is equal to 45°. On the other hand, Probabilistic Algorithm is always estimating this angle without errors.

It was shown that the estimated power values for the vertical antennas were constant for all ϕ orientations. This situation will introduce an error in the orientation estimation due to the fact that, for $\theta = 45°$, the received power should not be a constant. A possible way to fix it is to use the radiation pattern of the tag so, the received power will change with the orientation of the tag and it will not be a constant value for all ϕ anymore. Figure 6.3 shows the radiation pattern of Alien 9640 tag, the one is being used. Unfortunately, the information provided by the manufacturer is not enough since the graphic does not have any data about the gain values. Thus, another radiation pattern will be used. Figure 6.6 shows an empirically measured radiation pattern of Alien 9640 tag and it contains information of the gain of the tag measured exactly for the orientations that are being studied in this project [24].

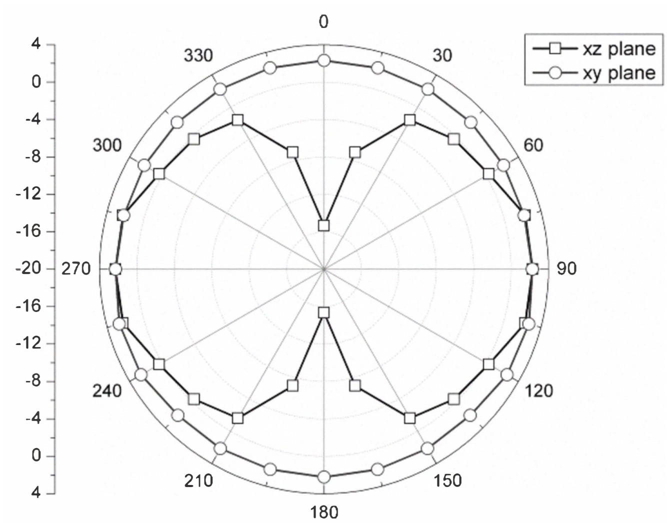

Figure 6.6: Measured Radiation Pattern of Alien 9640 Tag [24]

Now, the received power at the vertical antennas is calculated using the received power at the same polarized antenna for $\theta = 0°$, for all ϕ orientations, and corrected by the Polarization Loss Factor and by the gain of the tag. It must be considered the fact that the tag is tilted 45° and the radiation pattern has been measured with the tag 0° oriented so, the values of the radiation pattern should be modified in order to have the correct data.

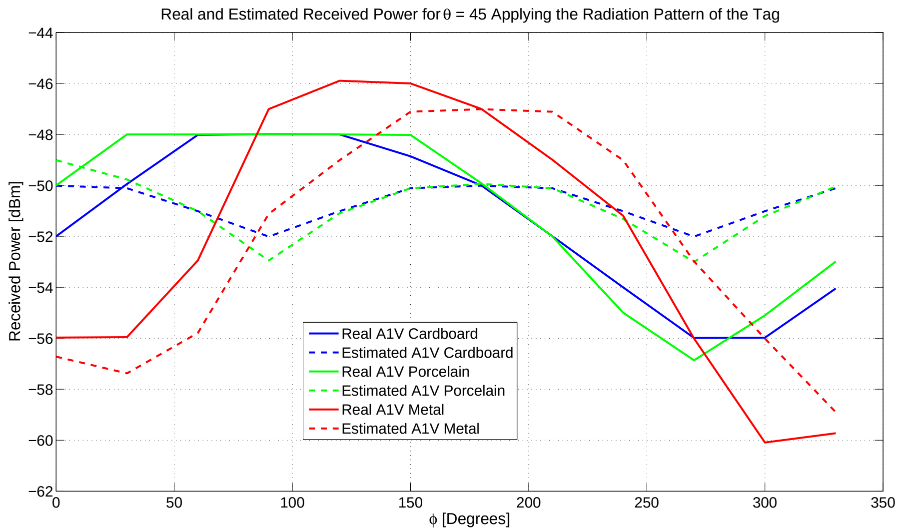

Figure 6.7: Estimated Received Power for $\theta = 45°$ at Antenna 1 Vertical for Different Materials Using PLF and Radiation Pattern of the Tag

Figure 6.7 shows the predicted received power for $\theta = 45°$ at the vertical Antenna 1 for different materials. As it can be seen, besides of the fact that the power is not a constant anymore, the estimated power does not fit so much the real received power plot. This is happening because of several factors, such us the radiation pattern of the tag shows the gain in an ideal environment where the reflections are absent.
On the other hand, it can be seen as well that the real and estimated power are not in phase. In some cases, when the theory predicts that the received power should be maximum, the real received power is minimum. Once again, the reflections and the effects of the environment are modifying the power values.

Now, it is time to have a look to the orientation estimation using these power values. The figures for the error CDF estimating θ will not be plotted due to the big amount of figures that this chapter will have, being cumbersome for the reader to follow the reading flow. Concerning the estimation of θ, the Probabilistic Algorithm makes an error of 45° the 11% of the time when the box is filled with metal and the KNN Algorithm makes the same error the 3% of the time but for porcelain. The rest of the cases, both algorithm predict the θ orientation with no errors.

Figure 6.8 shows the results in the estimation of the orientation for ϕ angle. By comparing it with Figure 6.5 it can be seen that the improvement in the calculation of the received power does not make the results getting better on the orientation estimation. Actually, the results are the same. Once again, it is evidenced that KNN gives better results on the estimation due to this algorithm is able to estimate the orientation with no errors at least the 86% of the time.

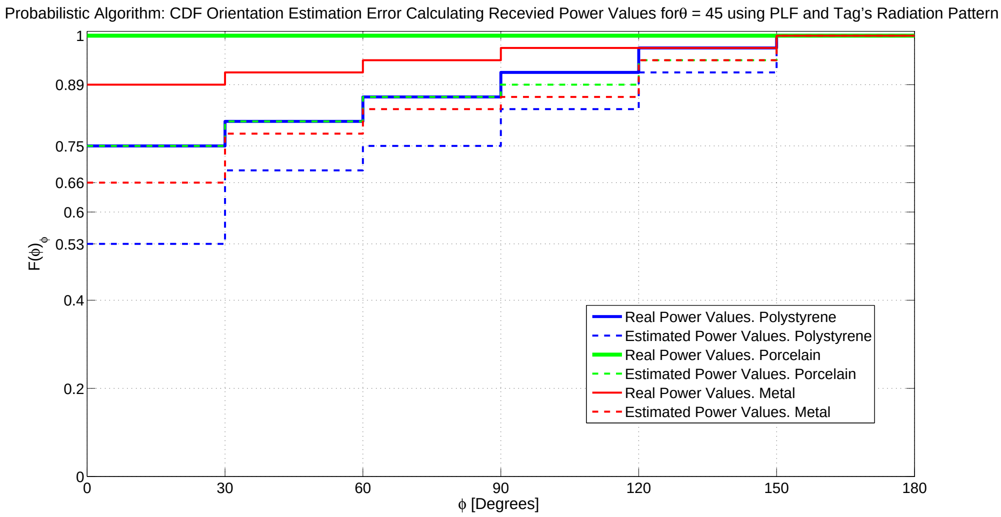

(a) Orientation Estimation Error CDF Results for Probabilistic Algorithm.

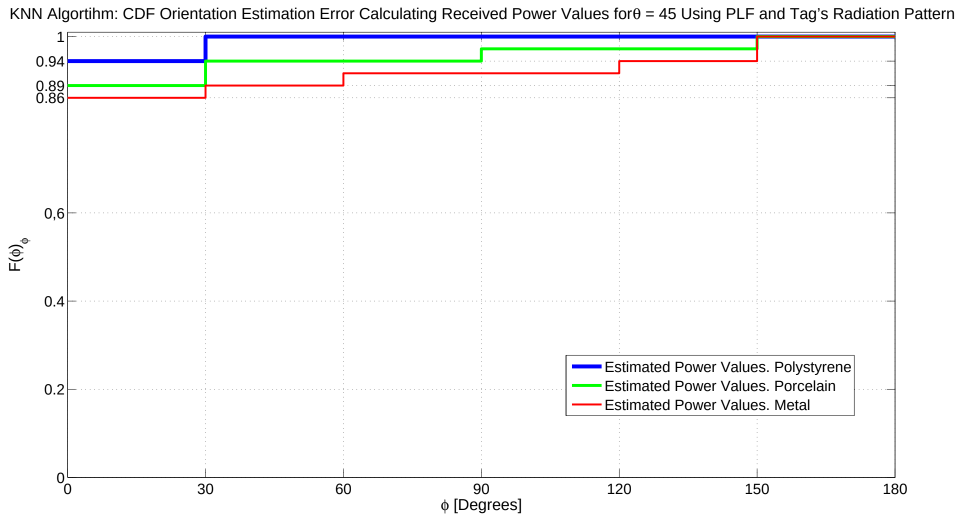

(b) Orientation Estimation Error CDF Results for KNN Algortihm.

Figure 6.8: Orientation Estimation Error CDF Results when the Received Power for $\theta = 45°$ is Estimated Using PLF and Tag Radiation Pattern. Probabilistic and KNN Algorithm Results.

6.2.2 Estimating the Received Power Values for $\theta = 0°$ and $\theta = 90°$

Previously, the orientation was estimated with the received power values calculated for $\theta = 45°$ using the measured values for $\theta = 0°$ and $\theta = 90°$. Now, the next step is to check if it is possible to estimate the power values for $\theta = 0°$ and $90°$. A good estimation of these values will allow to avoid the calibration stage for all orientations.

Using the radiation pattern of the tag it is possible to estimate the received power for all

ϕ orientations. Because of this, only one measurement in $\phi = 0°$ is needed. Then, starting from this value, just by applying the gain of the tag it is possible to get the rest of the values for all ϕ orientations. The only requirement is that, for this starting point, the power should be measured for both orientations, vertical and horizontal, in order to get a correct initial value for vertical and horizontal polarized antennas.

As it was shown before, the predicted received power using the radiation pattern will not fit so well the reality. Thus, it is needed to use a few reference tags to measure the received power for some discrete ϕ orientations.

Reference tags are just normal passive tags placed around the target, in known positions or orientations, when the measurements are taken.

Once the received power values are calculated for all the orientations, the power values from the reference tags will be used to correct the received power previously calculated taking into account the effects of the environment. Then, the most important thing is to know where to place the reference tags to get a good estimation of the received power.

Some tests were done to know where is the best place to put the reference tags. In the beginning, the reference tags were placed in the positions where the antennas receive the maximum power value. In this situation, the predicted minimum received power values were not correct and the estimated received power did not fit the real one. The next step was to measure the minimum received power. In this case three references tags were placed in all the points where the antennas are receiving the minimum power and one extra tag was placed in one point where one antenna is receiving the maximum power. In this case, information about the minimum and maximum received power values were obtained. This makes a total amount of eight tags, four for the vertical antennas and four for the horizontal antennas. Notice that the experiments were carried out using four dual linear polarized antennas. In case of the number of antennas is decreased, the number of needed tags will be reduced as well.

In order to not to present too many figures, the estimated received power will not be presented. However, it can be said that the results do not fit so much the reality. Due to the ideal radiation pattern of the tag used, some mistakes on the calculations are made.

Figures 6.9a and 6.9b show the results on the estimation of ϕ orientation calculating the received power for $\theta = 0°$ and $\theta = 90°$ for Probabilistic and KNN algorithms. This time, the Probabilistic Algorithm is not making any mistake the 61%, 69% and 75% of the time for metal, porcelain and polystyrene objects respectively. On the other hand, the error is lower than 30° the 90% of the time for porcelain, the 89% percent of the time for polystyrene and lower than 120° the 94% of the time for metal. KNN Algorithm has decreased its accuracy. Now, KNN is not making any mistake on the estimation the 58%, 66% and 72% of the time for metal, polystyrene and porcelain objects respectively. Besides that, the error is lower or equal than 90° the 94% of the time for polystyrene and lower or equal than 90° the 89% of the time for porcelain and metal.

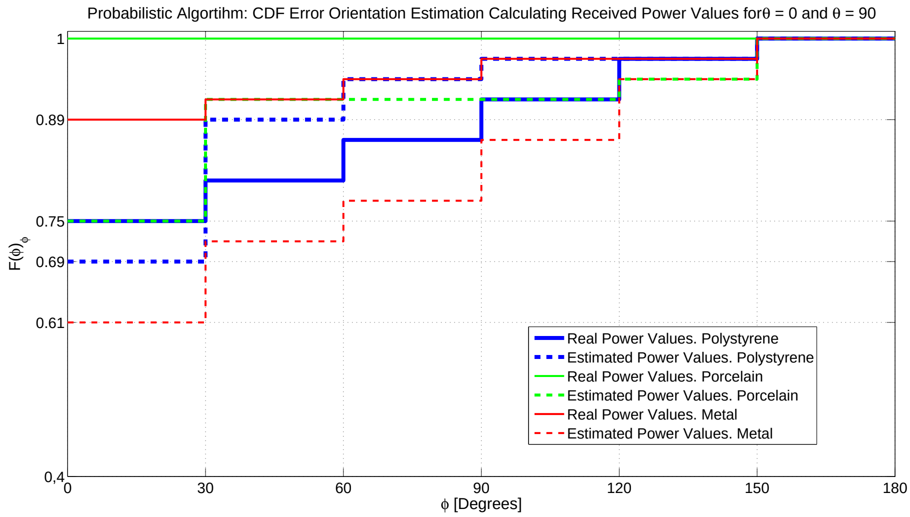

(a) Orientation Estimation Error CDF Results for Probabilistic Algorithm.

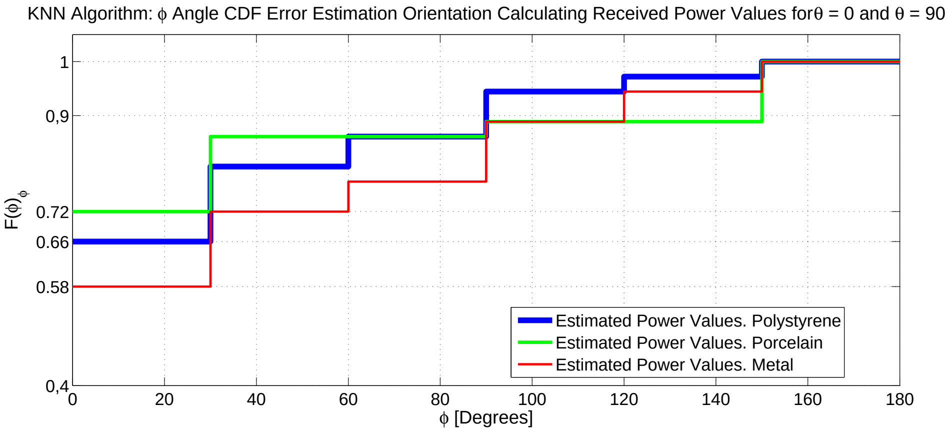

(b) Orientation Estimation Error CDF Results for KNN Algortihm.

Figure 6.9: ϕ Orientation Estimation Error CDF Results when the Received Power for $\theta = 0°$ and $\theta = 90°$ are Estimated. Probabilistic and KNN Algortihm Results.

For θ orientation, the Probabilistic Algorithm gets no errors the 94%, 97% and 78% of the time for polystyrene, porcelain and metal respectively whereas KNN gets no errors the 100%, 100% and 92% of the time for the same kind of materials.

6.2.3 Estimating the Received Power Values for $\theta = 0°$, $45°$ and $90°$

Once the contribution on the orientation estimation for each case has been analyzed, it is necessary to see what happen if all of them are put together at the same time. Now, the received power values for $\theta = 0°$ and $\theta = 90°$ are estimated as was shown in the previous section and, after that, using the PLF and the radiation pattern of the tag, the power values for $\theta = 45°$ are calculated.

Figures 6.10 and 6.11 show the results estimating θ and ϕ orientations when the received

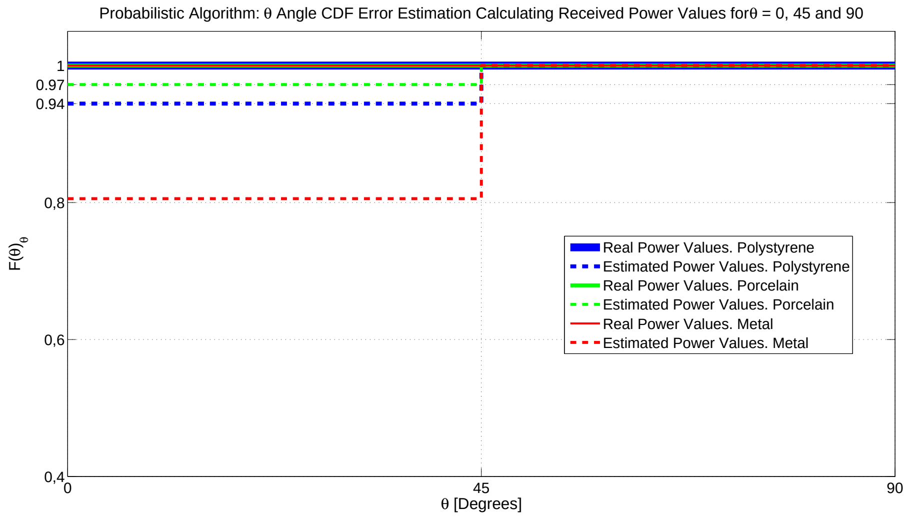

(a) θ Orientation Estimation Error CDF Results for Probabilistic Algorithm.

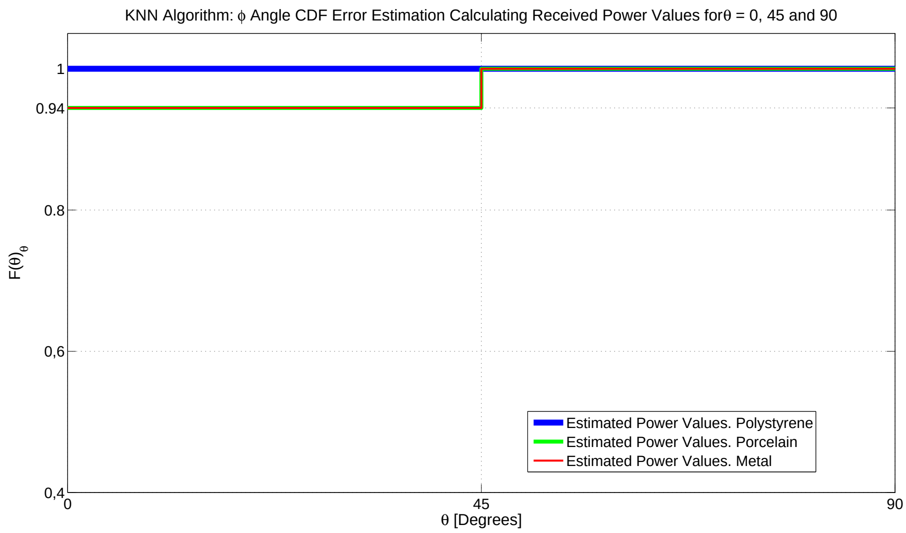

(b) θ Orientation Estimation Error CDF Results for KNN Algortihm.

Figure 6.10: θ Orientation Estimation Error CDF Results when the Received Power for $\theta = 0°$, $45°$ and $90°$ are Estimated. Probabilistic and KNN Algortihm Results.

power for $\theta = 0°$, $45°$ and $90°$ are calculated. From the results, it can be seen that for θ, the Probabilistic Algorithm is not making a mistake the 80%, 94% and 97% of the time for metal, polystyrene and porcelain objects. On the other hand, KNN is not committing any errors the 94% of the time for metal and porcelain and the 100% of the time for cardboard.

For ϕ orientation, the Probabilistic Algorithm is not making a mistake the 47%, 50% and 53% of the time for metal, porcelain and polystyrene respectively whereas the 86% of the time the error is lower or equal than $90°$ for polystyrene and metal and lower or equal

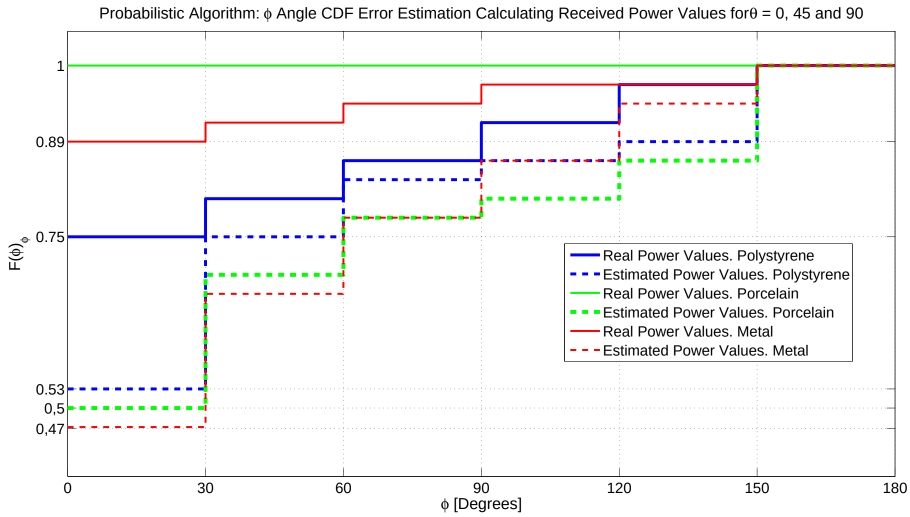

(a) ϕ Orientation Estimation Error CDF Results for Probabilistic Algorithm.

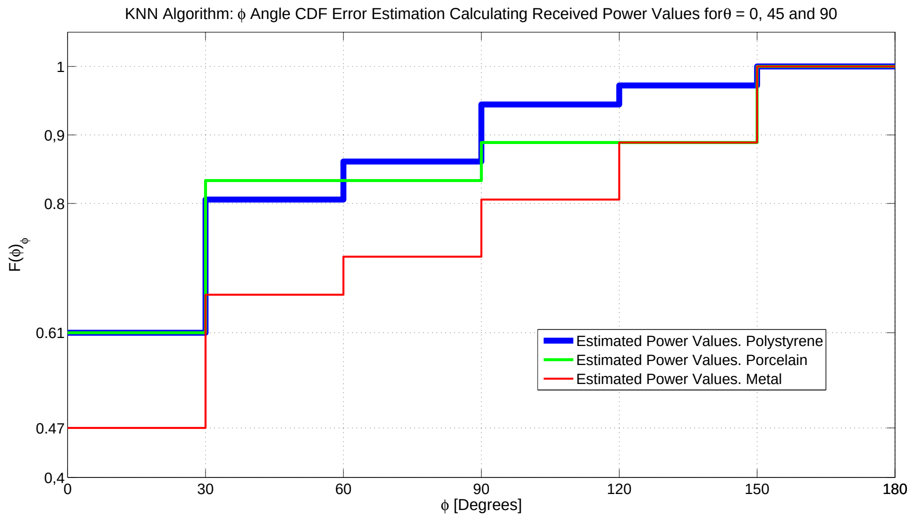

(b) ϕ Orientation Estimation Error CDF Results for KNN Algortihm.

Figure 6.11: ϕ Orientation Estimation Error CDF Results when the Received Power for $\theta = 0°$, $45°$ and $90°$ are Estimated. Probabilistic and KNN Algortihm Results.

than 120° for porcelain.

KNN does not make a mistake the 47% of the time for metal and the 61% of the time for polystyrene and porcelain. The error is lower or equal, the 88% of the time, than 90° and 120° for porcelain and metal and lower or equal than 90° the 94% of the time. The KNN results are a bit better than the ones obtained using probabilistic.

As a conclusion, it has been shown that it is possible to estimate the θ orientation of the tag by reducing the calibration phase. The degree of how this phase can be reduced depends on the application and on its error specifications. If the previous results are acceptable for a concrete application, then it is only needed to measure the received power in eight points which reduces considerably the calibration phase since, before, it was needed to calibrate the power in thirty-six different orientations.

6.3 Subset of Antennas

Chapters 4 and 5 focused on validating the algorithm using artificial RFID system and commercial RFID devices respectively. In the last case four antennas were used as it was explained in Section 5.1.

In this section the goal is to study the possibility of using a subset of antennas. This subset of antennas can be seen as an improvement of the system in the sense that it makes it cheaper, more scalable and easier to implement. The usage of more antennas is an extra cost and it is needed to evaluate if it provides large improvements. In other words, it is interesting to check if two dual polarized antennas provide satisfactory precision and, otherwise, three or four antennas must be utilized which makes the setup more expensive. On the other hand, the accuracy of the algorithm can decrease when less antennas are used to estimate the tag orientation. In order to analyze how this affects to the algorithm and its viability, the error made using different number of antennas (2, 3 and 4) are shown to check if the results are also valid with a smaller number of antennas.

Some considerations about the results that are going to be shown are presented here:

- The tag is placed equidistant to the antennas.
- As was explained in Chapter 3, the higher the number of samples of the received power is, the better the results are. For this study 100 samples were used in the algorithm.
- The results shown correspond to the Probabilistic Algorithm.

The first step is the selection of the antennas. All the possible combinations of two and three antennas are studied in order to make the right decision about which groups of three and two antennas will be used. Afterwards, the results with four, three and two antennas are going to be presented. The cases of polystyrene, porcelain and metal inside the box are analized.

Possible Combinations of Three Antennas

In Figure 6.12, it can be seen the error CDF for θ and ϕ in the experiment carried out using all the possible combinations of three antennas for the case of the cardboard box filled with polystyrene. The results are quite similar for the different groups of antennas: θ is always perfectly estimated and, regarding ϕ, around 90% of the time the error is lower than 90°. The small differences are due to the surrounded environment in the room where the measurements were taken. For example, there is a wall behind antenna 1 while antenna 2 is located in front of a window. The signal is not reflected or attenuated in the same way for both situations and this causes fluctuations in the received power. As a result, the conclusion is that it does not matter which group of three antennas is selected.

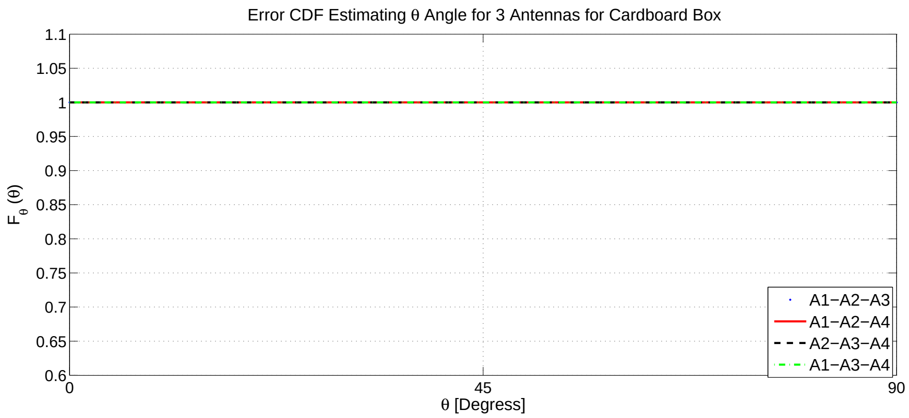

(a) Error CDF for θ using 3 antennas in the case of the cardboard box.

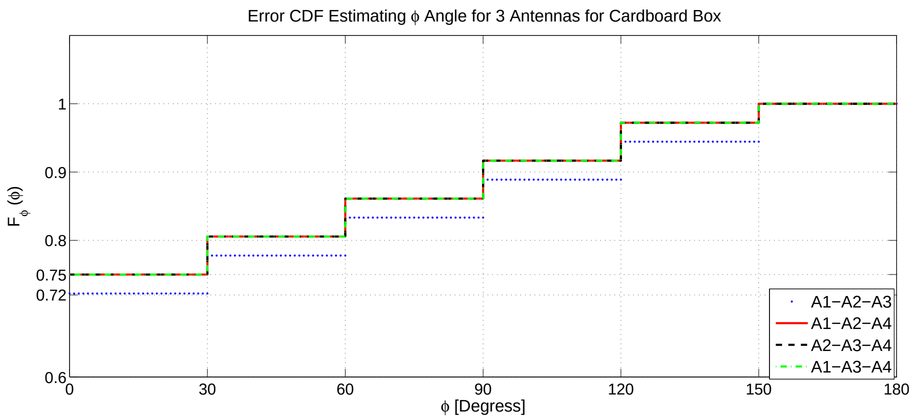

(b) Error CDF for ϕ using 3 antennas in the case of the cardboard box.

Figure 6.12: Error CDF for θ and ϕ using 3 antennas in the case of cardboard box.

Concerning the ϕ orientation estimated without error, most of the cases show that the 75% of the time the error is 0°.

Possible Combinations of Two Antennas

Decreasing the number of antennas makes the system cheaper and easier to implement. With only two antennas the process can be carried out with a four ports reader while with three or four antennas the system become more complex and expensive (it would be needed a commercial reader with eight ports or to replace the antennas in the four ports reader and repeat the process). In order to decrease the number of antennas, it is necessary to check how the accuracy of the system is affected when only two antennas to estimate the tag orientation are used. In figure 6.13 the error CDF for ϕ when using two antennas is shown. Regarding θ, the results are the same than for three antennas: the 100% of the time the inclination is perfectly estimated for any combination of antennas (the graphic of the error CDF is not presented because it is not giving so much information). Due to the similarity of the results when different groups of two antennas are chosen, it can be stated again that it is not very important which one are used.

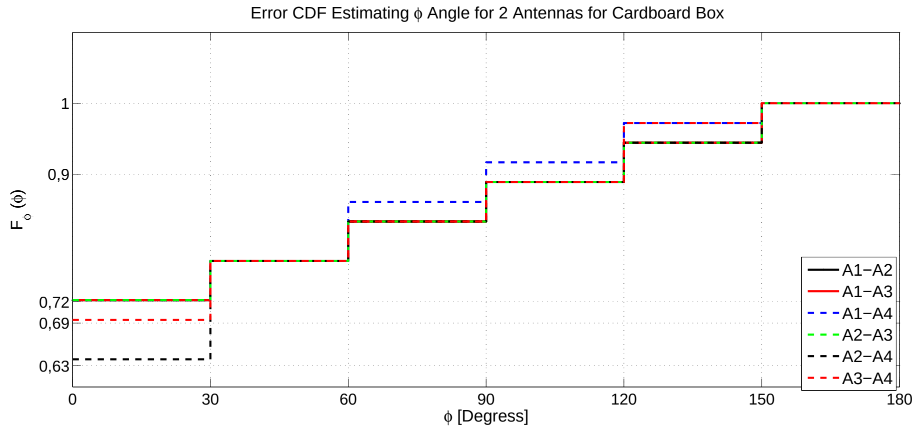

Figure 6.13: Error CDF for ϕ using 2 antennas in the case of cardboard box.

6.3.1 Comparison Between Different Number of Antennas

In order to compare the CDF for 2, 3 and 4 antennas, all the cases are shown together. For a clearer and more understandable figure, only one of the combinations of two and three antennas are drawn. As it was mentioned, there is not a big difference between them, so one of the cases was chosen: A1-A3 (2 antennas) and A1-A3-A4 (3 antennas). The Figure 6.14 represents the error CDF for θ and ϕ in the cardboard box case.
It is noticeable that the results are identical for the cases with three and four antennas: the system is able to estimate θ without error and the 75% of the time the error in the estimation of ϕ is 0° as well. Besides, the 90% of the time the error is lower than 90°. When two antennas are used, the error for ϕ estimation increases slightly, being 0 the 72% of the time and 90° approximately the 90%.
As it was mentioned before, the previous analysis refers to the situation where the tag attached to the cardboard box with polystyrene is estimated. The next step is to analyze the data from another experiments to see what happens when the tag is attached to an object. In this case, the object used is a porcelain plate (see Figure 6.15).
Despite the number of antennas is decreased from four to three, the estimation of the azimuth and elevation angles is perfect (the results for θ are not visually presented because it does not differ from the case with cardboard). Even with two antennas the results are very good: almost the 95% of the time the error is 0.
The same conclusion can be extracted from the Figure 6.16 which represents the error CDF for ϕ when the tag is attached to the cardboard box with a metal plate inside. In this case, using four antennas more accuracy is got than with three or two for the case of ϕ. However, the improvement in the orientation estimation is not significantly. The main cause of this could be that the radiation pattern of the tag is quite affected by the metal plate and the data from different positions respect to the tag becomes more important. Concerning θ, the 100% of the time there is no error for any number of antennas used.

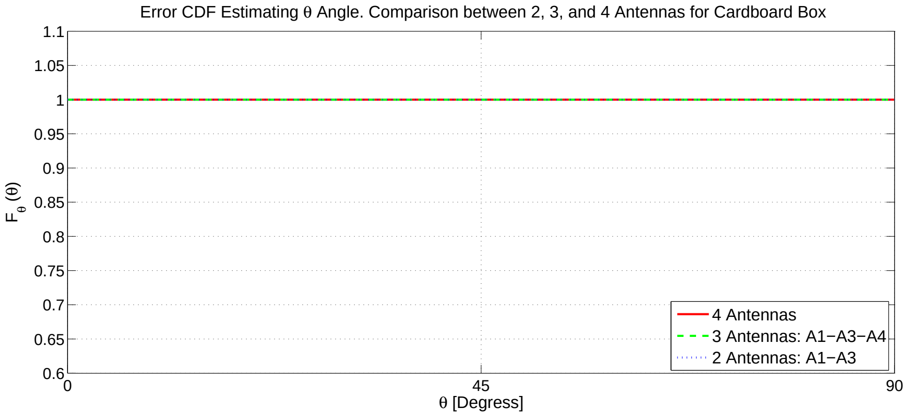

(a) Error CDF for θ using 2, 3 and 4 antennas in the case of the cardboard box.

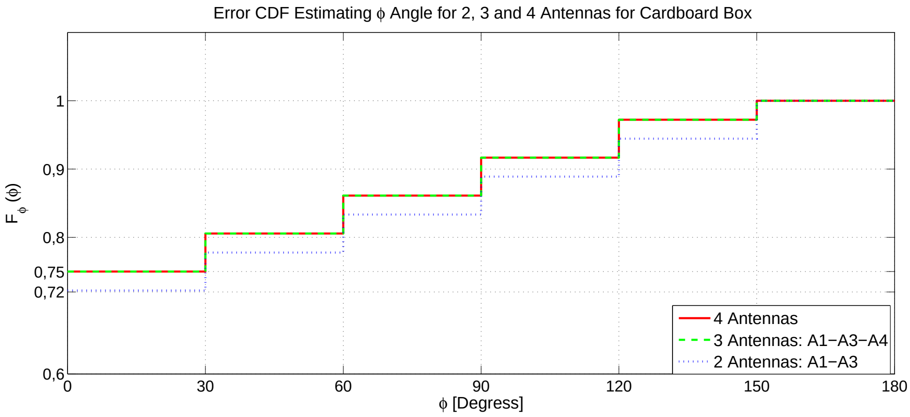

(b) Error CDF for ϕ using 2, 3 and 4 antennas in the case of the cardboard box.

Figure 6.14: Error CDF for θ and ϕ using 2, 3 and 4 antennas in the case of cardboard box.

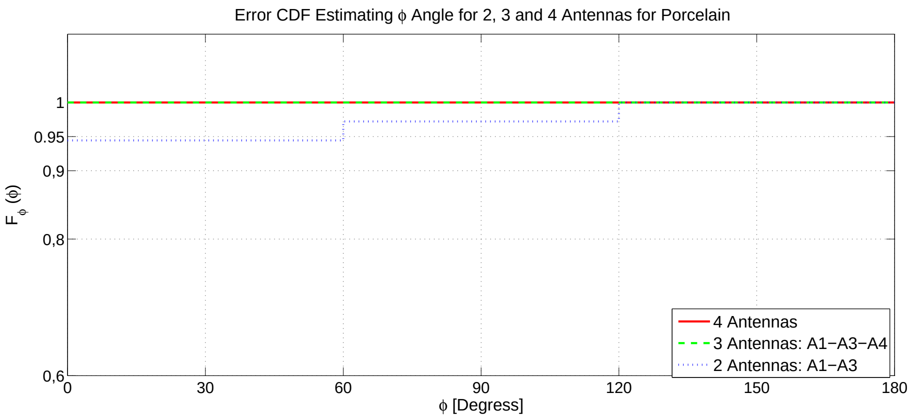

Figure 6.15: Error CDF for ϕ using 2, 3 and 4 antennas in the case of porcelain plate.

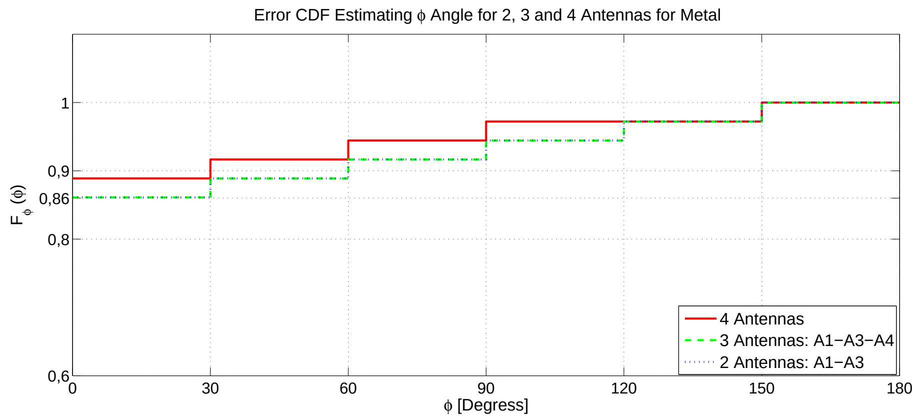

Figure 6.16: Error CDF for ϕ using 2, 3 and 4 antennas in the case of metal plate.

6.3.2 Improving the System by Reducing the Costs Conclusions

Two possibilities are presented in this chapter to reduce the costs of the system: To decrease the time that the Calibration Phase takes and to reduce the number of the antennas needed to estimate the orientation.
The Calibration Phase can be reduced by calculating the calibration data using the PLF and the radiation pattern of the tag instead of measuring the received power for all possible orientations. In this way, it is only needed to measure the power in some points to correct the possible mismatches between the theoretical equations used to make the calculations and the real world. The first step is to calculate the received power for $\theta = 45°$ for all ϕ orientations, then the calibration values for $\theta = 0°$ and $90°$ for all ϕ are calculated and finally, both previous steps are joint together to evaluate the performance of the system. Thus, the amount of measurements are reduced from thirty-six, when it is needed to measure all the points, to twenty-four, when the power values for $\theta = 45°$ are calculated, or to eight estimating the received power for $\theta = 0°$, $45°$ and $90°$.
From the results it can be seen that it is possible to detect θ orientation using both algorithms, Probabilistic and KNN, with a very low error rate at any situations. For ϕ orientation the results are not as good as for the elevation orientation due to the inaccuracy of the radiation pattern of the tag used when the tag is attached to materials and because more values for the azimuth orientation are calculated compared to the θ angle. As a reference and because these are the best ones, the error obtained the 90% of the time estimating ϕ, when the received power values for $\theta = 45°$ are calculated, are shown in Figure 6.17.
In summary, it can be stated that it is possible to estimate θ orientation with very low errors by measuring only in eight orientations in the Calibration Phase.

Once a reduction of the time the system needs to be calibrated has been done, a reduction on its costs is studied by reducing the number of antennas.
For this purpose, an analysis to study if the usage of an antennas subset is viable, is carried out. The main advantage of using a subset of antennas is the expenses reduction when implementing the system because less antennas are needed. This entails a lower complexity for the reader because only four ports are needed.

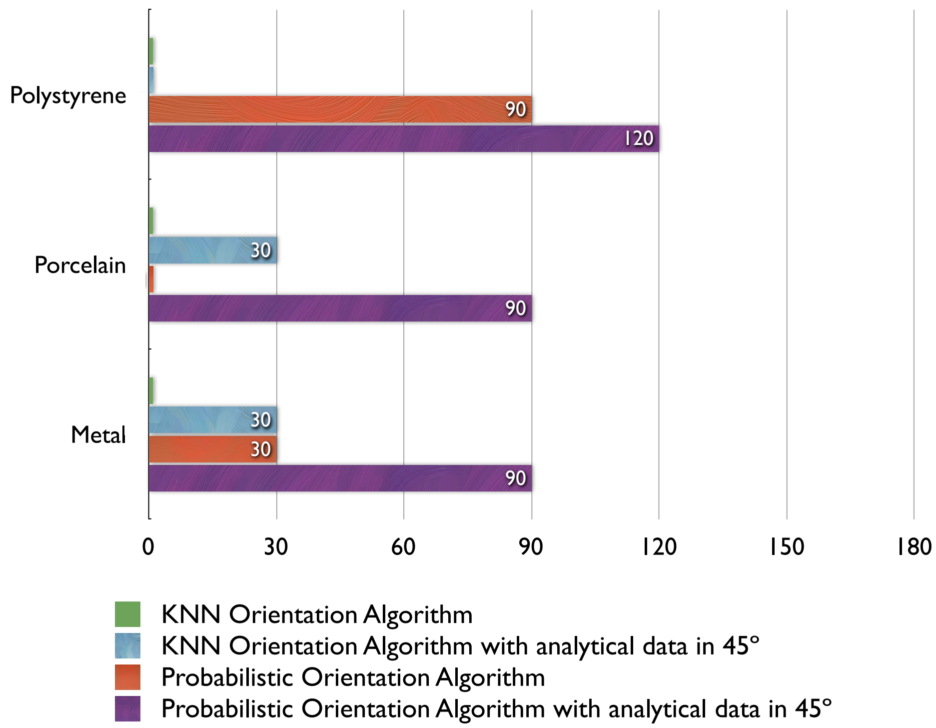

Figure 6.17: 90% of the time values estimating ϕ when the calibration power values are calculated for $\theta = 45°$ for all ϕ.

To evaluate how the results are affected when the number of antennas decreases, it was necessary a previous step where it is checked whether or not matters the subgroup of antennas chosen. In other words: should be the same accuracy achieved when using different number of antennas?.

To answer that, it was taken into account the error made for the case with no object attached (only the box with polystyrene) for all the combinations of different groups of three and two antennas (Figures 6.13 and 6.12). In both cases (three and two antennas) the conclusion is the same: it really does not matter the combination of antennas chosen because the accuracy is very similar.

The next step was to compare the results obtained with four, three and two antennas in order to decide the best choice. This task was carried out in the following cases: polystyrene, polystyrene plus porcelain plate and polystyrene plus metal plate (Figures 6.14, 6.15 and 6.16). As it was expected, the results are better for the case with four antennas but it is not a big improvement respect to the case with only two. This does not means that the other two do not contribute to get better results: using four antennas the uncertainty of the algorithm is lower because the probability of the right estimation becomes higher. However, in this case, the final results do not differ very much when two, three or four antennas are used.

As a conclusion, the usage of four or three antennas does not provide substantially improvements. Therefore, it can be stated that, using only two antennas, the system is able to achieve practically the same accuracy. This means a big improvement of the system because the investment needed to implement it is significantly reduced. Nevertheless, in this project the main goal is to perform a good analysis of the potential of RFID when estimating the orientation of tags and it is not a priority to reduce the number of antennas. Thus, from now on, the system will use four antennas to estimate the orientation of the tags.

So far, the algorithms require to be calibrated before estimating the orientation of the tag. This calibration is made only once in the moment that the system is set up. The same calibration values are used every time is needed to detect the orientation no matter if the environment that surrounds the system is changing. In the following chapter, the algorithms will be calibrated at the same time that the orientation is estimated. In this way the algorithms will be adapted to work within dynamic environments where the surroundings are frequently changing.

Chapter 7

Online Adaptive Calibration Methods

In the Chapter 6 several ideas to decrease the Calibration Phase were proposed. This chapter presents the next step: To remove completely the Offline Calibration Phase by using reference tags. Another goal is to get close to real applications where dynamic environments are usually found. For that purpose the system is tested in different situations, starting with a complex design which fits with the previous experiments but does not provide very good results. Due to this, a simpler design is created and evaluated.

7.1 Removing The Offline Calibration Phase

So far the system has been improved to facilitate the time consuming task of calibrating by reducing the number of positions to measure or even the number of antennas needed. However, in order to have a commercial and implementable system, it is quite important the total elimination of the Offline Calibration Phase. The main motivation for this is to avoid the need of a new Offline Calibration Phase every time the objects, boxes or environment change because it requires time and investment to take the measurements. In this chapter, the Offline Calibration Phase is replaced with an Online Calibration Phase which allows to easily adapt the system to new situations.
This task is going to be carried out by using reference tags. Recall that reference tags are just normal passive tags placed around the target, in known positions or orientations, when the measurements are taken. The results will be more reliable if the reference tags model is the same as the target one. There are many different ways of using these tags such as different positions, orientations or distances from the target. Various proposals will be analyzed in the following sections.

The main idea of using reference tags is to be able to receive the power value from tags with known positions and orientations, at the same time as from the target. In this way, those power values can be compared and the target orientation can easily be estimated.
The shortcomings of reference tags is that they are not affected by the same material as those the actual tags are attached to. That is why the accuracy is expected to be lower than the case with Offline Calibration.

Summarizing, reference tags can provide a new way of calibration (online calibration), which is carried out at the same time as the measurements, and remove the need of previous calibration (offline). However, the results are expected to be a little bit worse than with Offline Calibration because reference tags and the target are affected by different materials.

7.2 Dynamic Environments

In general, real scenarios where applications based on RFID are applied, present a changing environment. People moving around, objects which has been moved or any other movement can cause fluctuations in the wave traveling from the reader to the tag and vice versa and, therefore, in the received power. This constitutes a dynamic environment.

A great advantage of the usage of reference tags is the possibility to adapt the system to dynamic environments. This is due to the fact that the target and the reference tags are affected by the environment at the same time, thus the comparison of the received power values is more reliable.
This does not occur in systems where Offline Calibration is needed. In those systems the measurements are taken in a certain moment in order to make the calibration table which will not change until a new calibration is made. In that case, the receive power from the tag is always compared to the same values without taking into account how the environment has changed.
For the reasons explained, the system will be tested in dynamic environments as well.

7.3 Calibration Box with 36 Tags

In order to use the reference tags, a calibration box which contains them is designed. This box must be placed close to the target so it can be assumed that reference tags and the target are affected by the same environment (although the objects inside the boxes are different).
There are many different options to design the box but, as the main goal of this chapter is to extend and improved the system already implemented, the first design was based on it. The system developed in this project is made to distinguish between 36 different orientations: 12 values of ϕ (every 30°) and 3 values of θ (0°, 45° and 90°). That is why, the box is built to contain 36 reference tags, each of them with a different orientation as can be seen in Figure 7.1.
The main idea is to use the received power from all the reference tags to build a calibration table for all the possible orientations. Then, the algorithms (Probabilistic and KNN) are applied to estimate the target orientation. The principal difference is, as it was said before, that the process now is online. In other words, the calibration table is built simultaneously that the orientation is estimated and there is no need of previous calibration.

7.3.1 Results for Calibration Box of 36 Tags

The experiment was carried out by placing the calibration box around 5 cm over the cardboard box with the target attached. The rest of conditions are the same as in the

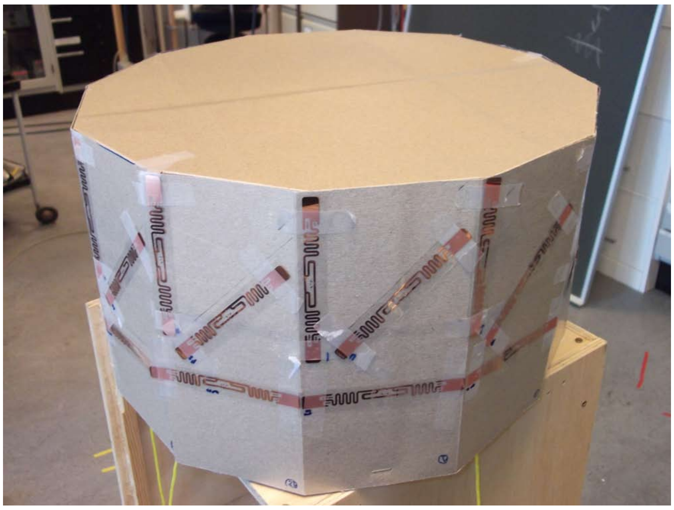

Figure 7.1: Calibration Box with 36 tags

Experiment II explained in Section 5. In Figure 7.2 the results are shown.
Regarding θ, it can be seen that Probabilistic Algorithm estimates it without error the 69% of the time while for KNN Algorithm this percentage decreases to 36%. The 95% of the time both algorithms are estimating the inclination with a maximum error of 45°, thus, the algorithm is able to distinguish between horizontal and vertical positions.
In the case of ϕ, the azimuth is correctly estimated only the 22% and 25% of the time using Probabilistic and KNN Algorithm respectively. Looking at the 90% of the time the errors increases considerably, being the maximum error 150° out of 180° that is considered. Therefore, comparing with the previous experiment, the algorithm accuracy has decreased significantly.

7.3.2 What Is Causing The Results Worsen?

Practically, what makes different this setup from the previous ones is the number of tags. This leads to two possible causes:

- Tag responses are interfering each other: RFID communication is following the Gen2 protocol, which establish the way the tags answer when they are interrogated. The medium access control is known as Q protocol and the basic schema is the following [1]:
  - The reader specifies the number of slots in the inventory round.
  - Tags select a random location to reply within the round.
  - The reader indicates with short commands the beginning of each slot.
  - The tag will reply with a random number in the slot it has chosen.
  - The reader will acknowledge the tag including the random sequence.

  Therefore, if two tags are trying to access to the medium in the same slot and the reader is able to decipher the random number (RN16) sequence at least from one of them, it will send the acknowledge. Both tags will receive the acknowledge (ACK)

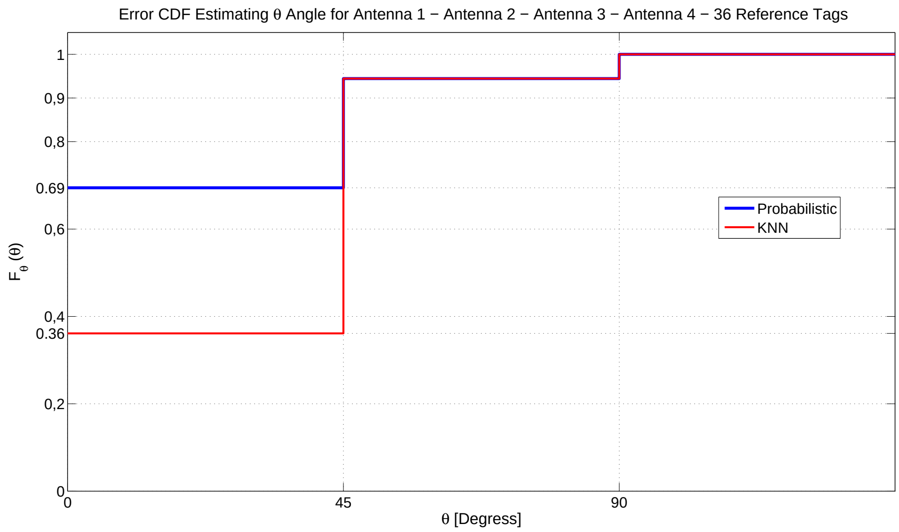

(a) Error CDF for θ using the Calibration Box of 36 tags with Probabilistic and KNN Algorithms

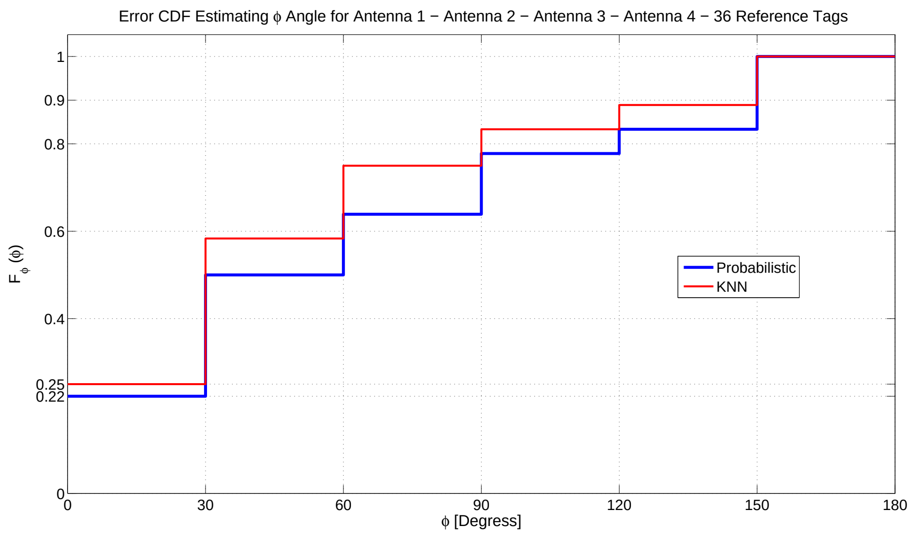

(b) Error CDF for ϕ using the Calibration Box of 36 tags with Probabilistic and KNN Algorithms

Figure 7.2: Error CDF for θ and ϕ using the Calibration Box of 36 tags with Probabilistic and KNN Algorithms

with the embedded random sequence, but only one will send its Electronic Product Code (EPC) (the one which sent the same random sequence). For more information about the protocol, see Appendix B.

This theory discard the possibility of tags interfering each other in most of the cases. However, a experiment to prove it is run: the target is placed close to five tags whose microchips have been previously destroyed in order to avoid them to response to the interrogator. In this way, they are just pieces of metal. Under this conditions, the received power in the reader is still affected. These results fits with the theory which states that several tags interacting with the same reader are responding in different slots of time.

- Tags antennas are interacting with each other: in Figure 7.3 it is shown how is the received power in the reader antennas for 1, 2, 3... until 8 tags. The antennas shown are Antennas 3 and 4. It can be seen that each new tag added to the calibration box modifies the received power in the reader antennas. These modifications change the received power almost 4 dB for some of the orientations when the number of tags goes from 1 to 8 (for instance in Antenna 3 with an azimuth angle of 240° the power is shifted down from -52.3 dB until -56 dB). This is the main cause why the accuracy of the system has decreased.

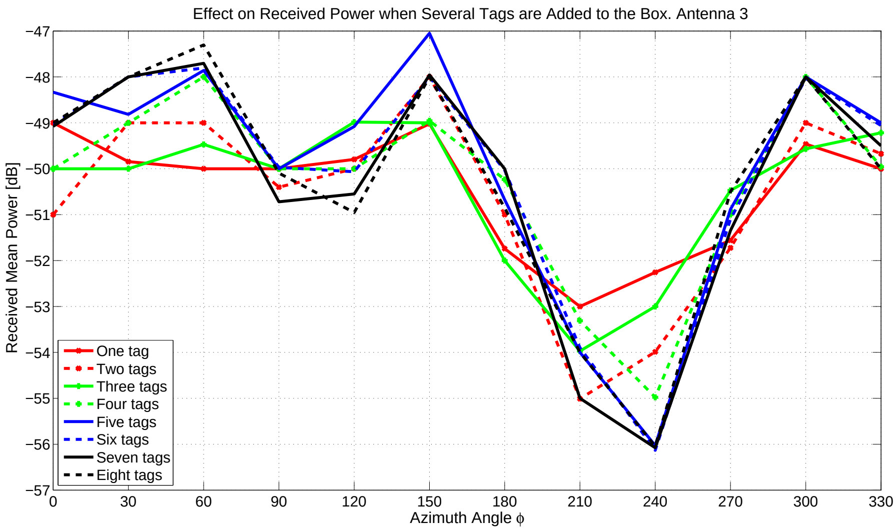

(a) Received Power in Antenna 3 for 1, 2, 3· · · 8 tags

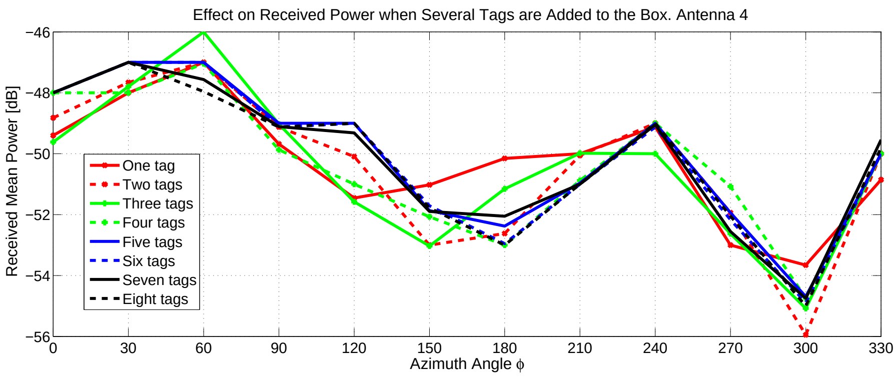

(b) Received Power in Antenna 4 for 1, 2, 3· · · 8 tags

Figure 7.3: Effect of adding new tags the calibration box in the received power in antennas 3 and 4

How the tags are affected by each other is a complex problem to analyze which is not the objective of this project. For this section is only needed to know that for arrays of tags, the scattering can add to or subtract from the incident wave, so the results may behave in an oscillatory fashion with changes in array spacing [1].

Since the calibration box performed with 36 tags does not provide very good results, a simpler calibration box was designed. The next section focuses on the analysis of this new design in static and dynamic environments.

7.4 Simple Calibration Box with 8 Tags

As a result of the previous analysis for the calibration box with 36 tags, the main goal of this section is to avoid a high population of tags in a reduced space, which causes interferences and modifications in the tags responses. For that purpose, a new and simpler design of a calibration box is made. The idea is to use a normal (rectangular or square) cardboard box which will contain 8 tags, placed in groups of two in the four lateral sides of the box. The tags will be arranged in vertical and horizontal orientations as shown in Figure 7.4.

Figure 7.4: Calibration Box with 8 tags (2 per side)

In this way, the number of reference tags decreases. This implies a reduction of the number of orientations that the algorithm will be able to estimate because, in this box, only 8 orientations (2 values of θ and 4 values of ϕ) have a corresponding reference tag associated. This means that θ can be 0° or 90° and ϕ will change between 0°, 90°, 180° and 270°. In other words, only steps of 90° in the inclination and the azimuth are considered.

7.4.1 Results for Static and Dynamic Environments Using the Calibration Box of 8 Tags

The results for the orientation estimation using Probabilistic Algorithm and KNN are presented in this section. The measurements correspond to static and dynamic environment. The latter one was performed by people moving around the reader antennas (between antennas and target or calibration box).

It is important to mention that the same criteria as in the results of Experiment I (Section 4.3) is used: errors equal or bigger than 180° are not considered in order to avoid those

errors caused by the symmetry of the radiation pattern of the tag. Due to this fact, the expected PDF will have one delta in 0° and another one in 90°, which are the possible errors in this experiment. To show only those two values, it is not worthy to plot the CDF figures. That is why, several tables containing the results for θ and ϕ with different materials inside the target box will be shown.
Firstly, the Table 7.1 shows the percentage of time that the algorithms estimate θ and ϕ without error, with the calibration table of eight reference tags in static and dynamic environments with Probabilistic and KNN algorithms. These estimations are done by using Offline Calibration which means that an unique calibration table is created and used to compare the received power from the tag for all the orientations, even in the dynamic environment. Secondly, the Table 7.2 is the result of applying the Online Calibration Phase to the same cases. For that purpose, an Online Calibration which creates a new calibration table (online) each time a measurement is taken, is used. In this way, every time the tag orientation is estimated, the received power from the tag will be compared with the calibration table created in that precise moment. This allows the system to be adapted to any possible modifications in the environment since both, the target and the reference tags, are affected by the same changes.

Material	Environment	Angle	Probabilistic	KNN
Polystyrene - Polystyrene	Static	θ	100%	100%
		ϕ	75%	75%
	Dynamic	θ	100%	100%
		ϕ	75%	62.5%
Polystyrene - Porcelain	Static	θ	100%	100%
		ϕ	62.5%	62.5%
	Dynamic	θ	100%	100%
		ϕ	87.5%	75%
Polystyrene - Metal	Static	θ	75%	75%
		ϕ	62.5%	50%
	Dynamic	θ	100%	100%
		ϕ	87.5%	75%

Table 7.1: Offline Calibration: Percentage of the time in which the orientation angles are estimated without error. Different materials. Static and dynamic environments.

Due to the short availability of the experimental setup used for the measurements, the experiment was performed only once. This means that eight orientations were measured and estimated and, the errors obtained from that, were used to calculate the error CDF. Therefore, it has to be taken into account that the sample space is not big enough to extract definitive conclusions, but they are useful to have a rough idea about how the algorithms are able to estimate the orientation of the tags when a simple calibration box with eight tags is used.

The first part of the tables 7.1 and 7.2 show the results when the target is attached to a cardboard box filled with polystyrene and, as calibration, another cardboard box is used. The second and third part are representing the case of cardboard box with a porcelain plate or metal plate respectively, but using, again, the cardboard box with polystyrene as

Material	Environment	Angle	Probabilistic	KNN
Polystyrene - Polystyrene	Static	θ	100%	100%
		ϕ	75%	75%
	Dynamic	θ	100%	100%
		ϕ	75%	75%
Polystyrene - Porcelain	Static	θ	100%	100%
		ϕ	62.5%	62.5%
	Dynamic	θ	100%	100%
		ϕ	87.5%	75%
Polystyrene - Metal	Static	θ	75%	87.5%
		ϕ	62.5%	62.5%
	Dynamic	θ	100%	100%
		ϕ	87.5%	87.5%

Table 7.2: Online Calibration: Percentage of the time in which the orientation angles are estimated without error. Different materials. Static and dynamic environments.

calibration.

In general, the results are much better than the previous case with thirty-six tags. In addition to this, it can be seen that there is almost no difference between the static and dynamic environments. This could be due to the fact that several hundreds of samples of the received power are measured for each orientation and then, the average of all them is used in the algorithm. By averaging the power values, the dynamic effects in the environment are decreased.

Regarding the comparison between the Tables 7.1 and 7.2 (with Offline and Online Calibration), it possible to see that for Probabilistic Algorithm the results remain the same whereas for KNN Algorithm the accuracy of the system increases (values marked in gray color). The best improvement is achieved for the worst case (polystyrene-metal) where either the inclination and the azimuth are estimated with more accuracy. For instance, θ is correctly estimated the 87.5% of the time in the static environment (75% without adaptive algorithm) and the estimation of ϕ without error increases in 12.5% of the time in both environments.

It can be seen that Probabilistic Algorithm is better than KNN Algorithm in most of the cases. In the worst case, the system is able to estimate θ without error the 75% of the time (polystyrene-metal case) and ϕ the 62.5% of the time (cardboard-porcelain). Moreover, in the simplest case (polystyrene-polystyrene) θ is always perfectly estimated.

A reasonable conclusion could be that the calibration box with eight tags is a good way to adapt our system to dynamic environments and avoid the Offline Calibration Phase obtaining, at the same time, quite acceptable results for the estimation of θ.

Finally, it is important to keep in mind that the sample space is not big enough to have conclusive data and, therefore, to extract reliable conclusions.

7.5 Adaptive Online Calibration Conclusions

This chapter has focused on removing the Offline Calibration Phase by using reference tags. This is supposed to allow the system to be adaptable to real and dynamic environments. The experiments done confirm this expectation.
Firstly, an experiment with a calibration box with thirty-six tags was carried out. Despite the results for the inclination estimation are acceptable (69% of the time without error and a maximum error of 45°), the azimuth is not very well estimated. This is due to the fact that tags antennas are interfering each other and modifying the received power in the reader antennas. This leads the algorithms to fail when estimating the orientation.

In order to avoid those interferences between tags, the next test was made to a calibration box with only eight tags. This implies a limitation: only eight orientations can be estimated (two values of θ and four values of ϕ). The experiments made in static and dynamic environments using Offline and Online Calibration shown pretty good results, above all when no materials are mixed. The inclination θ is very good estimated (100% of the time) in most of the cases in both environments. With regard to ϕ, the system is able to detect it correctly the 62.5% of the time in the worst case using Online Calibration. Although Probabilistic Algorithm is more accurate, the usage of an adaptive calibration improved the results for KNN Algorithm. To sum up, the calibration box with eight tags works properly, above all in the estimation of θ, and allows to avoid the Offline Calibration Phase and to adapt the system to dynamic environments.

Chapter 8

Conclusions

In this chapter a brief summary of the project is presented followed by the final conclusion. Moreover, some ideas are proposed to continue the work done and to improve the developed system.

8.1 Project Summary

The achievement of this project has been to be able to detect the orientation of objects by using a commercial UHF RFID system with passive tags. Nowadays, a "This Side Up" marker is widely used to manually check the orientation of the objects by the workers in a supply chain. This project has the potential of introduce an automatic new application to be able to check the orientation of the objects by using an already deployed RFID system.

As RFID technology is based on radio wave propagation, a channel propagation model was selected within a set of the most relevant ones according to the proposed scenario. The Rayleigh channel model was chosen to be able to use the application in any kind of situations since the potential of an RFID system is that line of sight is not needed to achieve the communication process.

Afterwards, the effects of the received wave polarization and its impact on the orientation of the tag were studied. From this analysis it can be drawn that the best choice was to use dual linear polarized antennas to be able to separate the received signal into vertical and horizontal orthogonal components. From this point, two algorithms were developed to estimate the orientation. One of them is Bayesian theory based which is called Probabilistic Orientation Algorithm, whereas the other one, is based on proximity techniques and called KNN Orientation Algorithm. Both algorithms follow the same procedure which consist on two stages: The first one is to collect the received power values from all the antennas and all the orientations to build a calibration table. This step is called "Calibration Phase". This calibration is made only once in the moment that the system is set up. This concept was called "Offline calibration". Secondly, new power values are collected from the target at the orientation which should be estimated. This is called "Estimation Phase". These new power values are compared with the calibration table according to the method used to detect the orientation. It is worthy to mention that the Probabilistic Algorithm is the optimal procedure in error probability terms since it uses the Bayesian estimator to detect the orientation. Although KNN Algorithm is a sub-optimal procedure, its implementation is quite simple and it can be used as a reference to compare the results.

Before investing time in using commercial devices, both algorithms Probabilistic and KNN, were validated with a simple test which consisted on using a folded meandered dipole as a tag antenna. In order to analyze the results of the test, the symmetric nature of the radiation pattern of the tag should be taken into account. Therefore, the considered errors are shifted from $[0, 360]$ to $[0, 180]$. From the good results obtained in the validation stage, it was clear to proceed to the next step.

Then, the algorithms were evaluated using a commercial RFID system in a variety of situations. As a starting point, the methods were tested in a simple case using a cardboard box filled with polystyrene, in which the radiation pattern of the tag was expected to be as a dipole due to the similarity of the relative permittivity of this material with the air. Next, the algorithms were tested in an intermediate situation using the same box with a porcelain plate inside. Lastly, a metal plate was placed in the box to test the algorithms under hard conditions where a stronger influence on the radiation pattern was expected. The test was run in an office - laboratory environment where the received signal presented a small variance. Theoretically, no answer should have been received from the tag when a total PLF mismatch between the receiver and the tag antenna was present. However, the measurements shown that, for some orientations and due to the reflections, the response from the tag was received. From the results it could be stated that using calibration data which is similar to the target data, the accuracy of both algorithms is very impressive for θ orientation (no errors were made), and quite good for ϕ orientation, despite sometimes it was not possible to activate the tag due to technology limitations.

A new calibration table must be created each time the objects, where the tag is placed, are changed. Thus, the possibility of using the same calibration data for different objects was a desirable option. In this case, a cardboard box filled with polystyrene was used to create the calibration table when the target was attached to a box filled with a porcelain plate or a metal plate inside. It provoked the results worsen: Even though it is possible to correctly estimate θ, the accuracy detecting ϕ orientation will not fulfill the requirements for most of the applications.

In this point, it could be stated that it is possible to estimate θ orientation with no errors using a commercial RFID system and four antennas. As most of the commercial readers have only four ports available (two dual polarized antennas), to use four dual polarized antennas is expensive because it is needed to duplicate the hardware. Consequently, the next step was to analyze how many of these four antennas are sufficient to properly estimate the orientation. As a conclusion, the usage of four or three antennas does not provide substantially improvements. Therefore, using only two antennas the system is able to achieve practically the same accuracy. It means that it is possible to estimate the orientation using only one commercial reader.

Once it was proved that the system is able to work with commercial devices, the next step was to reduce the system expenses in terms of time. That is why the Calibration Phase was reduced by decreasing the number of the angles where the received power is measured. The remaining points of the calibration table were filled by calculating analytically the received power using the Polarization Loss Factor (PLF) and the radiation pattern of the tag. A common erroneous though is that the PLF is affecting to both orientations, azimuth and elevation angle. Actually, only the elevation angle (θ) is causing polarization mismatch and the losses due to the azimuth angle (ϕ) are given by the radiation pattern of the tag.

First of all, the received power values for $\theta = 45°$ were estimated for all ϕ orientations. In this case, it was shown that both orientations are estimated correctly for KNN Algorithm. As it was mentioned in this report, KNN Algorithm is subject to use calibration data similar to the received power from the target. Finally, the power values for $\theta = 0°$, $45°$ and $90°$ were calculated for all ϕ orientations. This step shown that the accuracy of the estimation of θ orientation was slightly decremented for KNN Algorithm but it was possible to detect the angle. The whole procedure of reducing the Calibration Phase proved that even though the performance of the system is decreased, it is possible to detect θ orientation reducing the measuring points up to eight positions.
Since the Calibration Phase should be done each time the objects inside the box where the tag is attached or the environment which surrounds the system are changed, the final step was to study the possibility of making the system working under dynamic conditions. Thus, the Offline Calibration concept was removed: Instead of calibrating the system when it was set up, it was calibrated at the same time the orientation was estimated using reference tags. This new concept was called “Online calibration”. In this way, the system was expected to be more robust against dynamic effects.

A calibration box with several reference tags was created and placed close to the box where the target was attached. As a result, all powers from the reference box and the target were received at the same time and compared to estimate the orientation. This procedure was carried out for two different cases: Using thirty-six and eight reference tags attached to the calibration box.

The results for the thirty-six reference tags box were not as good as it was expected due to the tags antenna were interfering each other. Thus, the next step was to decrease the number of reference tags to avoid this effect. The simplest case was to use only eight reference tags attached to the calibration box. Consequently, only eight orientations could be estimated. To prove the robustness of the system, this last case was made under static and dynamic environments and for different materials. With the eight reference tags, θ was detected with no errors in most of the cases. Furthermore, KNN Algorithm increased its accuracy using online calibration.

8.2 Conclusion

From the work done to carry out this project it can be extracted, as a conclusion, some points which define the strengths, the weakness and the general overview of the system.

There are some good points and strengths of the system that it is important to mention:

- θ orientation is estimated in most of the cases with a low error rate.
- It is possible to reduce the calibration points up to eight by estimating the received power for some orientations, especially for $\theta = 45°$ for all ϕ orientations.
- The system can be implemented using only one commercial RFID reader and two dual linear polarized antennas. In this way, the expenses when the system is implemented are reduced.
- The orientation is properly estimated when the calibration data is similar to the target data and when the calibration is performed with similar objects to the target box filling. Furthermore, θ orientation can be well estimated even when calibration box and target box are filled with different objects.
- The system is working properly even under dynamic conditions when θ is estimated.

However, not everything was as good as it was expected because some ideas did not work as well as others. For example some of them are listed:

- It is not possible to estimate ϕ orientation with an accuracy as good as for θ orientation. ϕ is very sensitive to any changes introduced in the system like changing the objects and environment or estimating the received power. The fact that the system could be employed to estimate this angle will depend of the requirements and specifications of the application.
- For some cases the system is not able to detect a change of 180° in the orientation for azimuth and elevation planes.
- The online calibration did not throw the results that it was expected. It was needed a reduction in the number of the orientations to be estimated due to the tag antennas interference.

Despite of these previous weakness of the system, it can be assured that it has been partially solved the problem of estimating the orientation of an object due to θ can be estimated without any problem, but not ϕ. From our point of view, not to be able to estimate ϕ properly is not necessarily a problem because, in a lot of applications, the inclination is the important orientation to be estimated.

8.3 Future Work

For future work it will be interesting to investigate the following aspects:

- During this report the errors have been limited to 180° due to the symmetric nature of the tags radiation pattern. This limitation should be removed before the developed algorithms are used in real scenarios.
  For example, when the reader antennas are close enough to the target to vary the gain due to difference in height (30 cm Figure 8.1) between the tag in position A and B, it will cause a change in the received power allowing the algorithm to estimate the orientation. Notice that if the tag is placed in the middle of one of the box sides, the received power will remain the same.

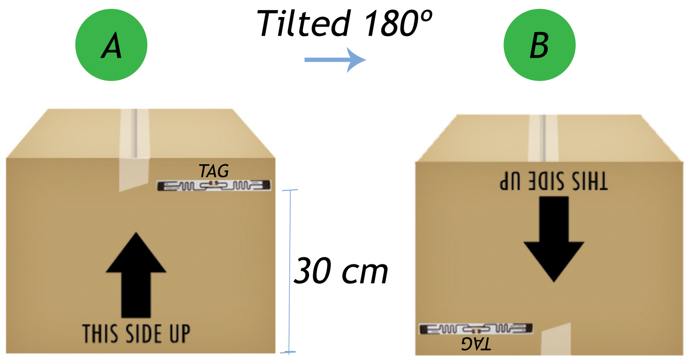

Figure 8.1: An example of how to place the tag in order to distinguish positions which differ in 180°.

- The usage of two or more tags attached to the target is an interesting area of research. As it was mentioned in the report, several tag orientations will cause a total PLF or gain mismatch, thus the tag will not be activated in those orientations, causing errors in the estimation of the orientation. If several tags are added in orthogonal planes, this uncertainty could be decreased, because at least one of the tags will be read by the reader. In Figure 8.2 it is proposed a way to assure that at least one of the tag in the target will be read no matter the orientation. In the proposed example, if the box is facing one of the antennas, the vertical component will read Tag 1, while the horizontal component of the antenna will read Tag 2. However, if only Tag 1 is considered, the algorithm will have no information from the horizontal components.

Figure 8.2: Three tags are placed in the box to assure that all the antennas will activate at least one of the tags.

- To analyze the performance of both algorithms when the distance between the target and the antennas is not fixed. For example, when several boxes orientation that are piled have to be estimated, the distance of each target with respect to the antennas will be different from the calibration data. In addition to this, when the number of targets raise, it will be necessary to decrease the time interval used to estimate the orientation. As it was explained in Section 5.1 (page 31), the accuracy is not expected to be severely affected.

- The Online Calibration Phase shown great potential to adapt to dynamic environment, and therefore it will be desirable to study a possible solution to the nearby tags problem, which have a strong impact in the results.

- In Section 6.2.1 (page 48), it was presented a method to analytically calculate the received power of $\theta = 45°$. It will be interesting to apply the same method to the Simple Box with 8 tags, to increase the possible values for θ from the set $\{0°,90°\}$ to $\{0°,45°,90°\}$, without adding extra tags.

Appendix A

What Is Radio Frequency Identification?

Radio Frequency Identification (RFID) is a technology that uses communication via electromagnetic waves to exchange data between a terminal and an object. The principle goal of RFID it is to transmit the unique identity of an object, a person or an animal.

RFID technology emerged because of the need to transmit electrical energy from a power source to an electrical load without interconnecting wires. Wireless transmission is useful in cases where interconnecting wires is inconvenient, hazardous, or impossible. In these situations the efficiency is the most important parameter: it is necessary that the most part of the sent energy reaches the receiver to make the system economical. [25]

RFID is not a new technology. It has existed for a long time but they needed the integrated circuit technology improve their capacity and decrease their price in order to be inexpensive, small and simple. These days, the main application of RFID is supply chain management so tags need to be robust, economical, small and readable from a few meters.

Why is it important?

Imagine a task like to make the inventory of your store. Using the typical barcode readers you can spend all the day. With RFID tags and only one reader it is a task of minutes.
Other visual implementation may be a market food where the queues are avoided because when you want to pay, you only have to cross one arch with the RFID readers and instantly all the items are read.

Figure A.1: RFID adhesive tag [26]

A.1 RFID Technology

RFID systems usually consist of a reader and transponders or tags. Both readers and tags have the capacity of transmitting and receiving information, so they include integrated antennas to establish communication.

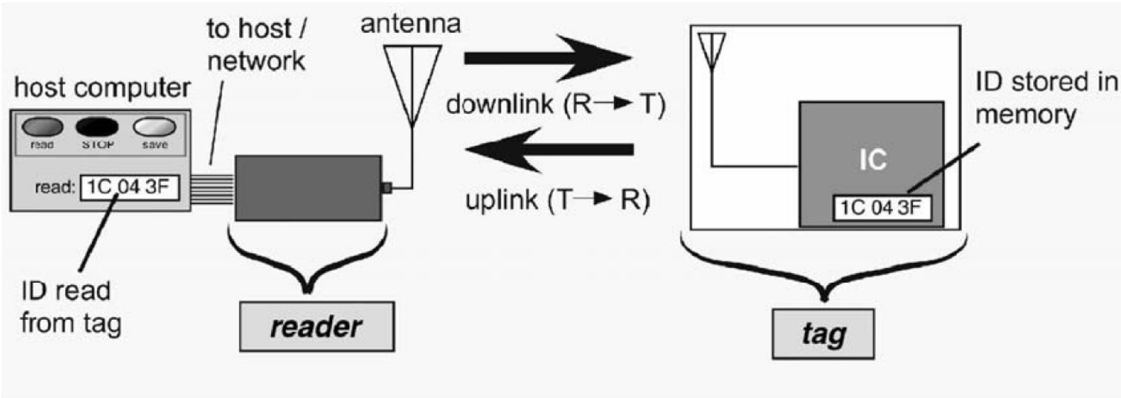

Figure A.2: Overview of an RFID system [1]

To have a better understanding of an RFID system, the concept and different kind of tags and readers is explained.

A.1.1 Tags

Tags consist basically of a microchip with memory to carry data which is attached to an antenna. They send information to a reader when they are activated. Most tags have at least one integrated circuit (IC) containing the tag ID and the logic needed to navigate the protocol that guides discussions between the tag and reader. It is possible to differentiate between three main types of tags:

Passive Tags

Passive tags have no battery so they get power from the reader to work. The tag antenna current is induced by the electromagnetic wave that comes from the reader. Passive tags have limited range of broadcasting; they need the reader antenna to be close.

Semi-Passive Tags

The communication is the same as with passive tags but the power is got from an external battery. These tags are used to increase the read range.

Active Tags

The power needed to run microchips and to transmit signals to the reader comes from an internal battery which should be replaced periodically. These tags provide the largest read range.

A.1.2 Readers

Readers are devices that read the contents of RFID tags in the vicinity. A reader may contain an user interface of its own but, more often, they are connected to a network or a particular host computer which interacts with the user. In this way, it is possible to control the reader and store and display the resulting data. In passive systems, they transmit power to the tags that makes enabling them to reflect the signal. There are two different kinds of readers:

- Read only: they only read data from the tags.
- Read and write: these devices are able to read and write information on tags.

Figure A.3: Example of a commercial reader [27]

Appendix B

EPCglobal Class 1 Generation 2 (Gen2) Basics Related to the Project

This appendix summarizes some relevant parts of the EPCglobal Class 1 Generation 2, so called Gen 2 for this project. The basic aspects presented cover the physical and mac layer of the protocol. In other words, it is explained the elementary communication parameters in the RFID setup used in the experiments.

B.1 Gen 2 Protocol Basics

The basics of the RFID technology are explained in Appendix A (page 81). This section provides a more technical view of the protocol.

The Gen 2 protocol is a reader-talk-first protocol, in which the transmitted reader symbols are amplitude modulated (PIE). Two layers can be differentiated: Physical Layer and Mac Layer. It can be also noted two parts into the communication the Downlink (Reader to Tag, R=>T) and the Uplink (Tag to Reader, T=>R). In Europe the regulations specify that the range for RFID is from 865 to 868 MHz and an Effective Radiated Power (ERP) of 2 W.

B.1.1 Gen 2 Physical Layer

As mentioned in the RFID basics, the passive tags have not battery, that is why the Reader must transmit a Constant Wave (CW) so the tag by harvesting the energy of this RF signal will be able to respond to the Reader [18].
The communication between the Reader and the tag (Downlink) is amplitude modulated in which a binary '0' is differentiate from a '1' with the time between zero amplitude pulse. This is known as pulse-interval-encoded (PIE). The reader will define a Tari value (the time duration for a 0) and the binary '1' will have a minimum duration of 1.5 Tari and a maximum duration of 2 Tari, as can be seen in Figure B.1 [1].

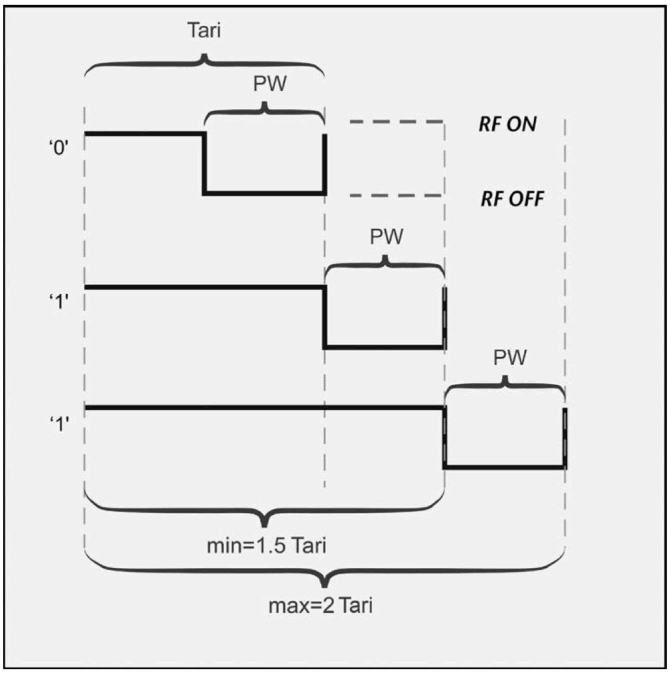

Figure B.1: Binary '1' and Binary '0' send by the Reader in Gen 2 [1]

From Figure B.1 it can be seen that a '0' differs from a '1' by the duration of the RF ON, both digits are finished always by a zero amplitude with a certain duration: Pulse Width (PW). The tag will interpret as '1' all the symbols which shape and duration are like the figure. Standard values of the Tari are 6.25, 12.5 and 25 microseconds.

The protocol specify three different operating modes for readers: single interrogator, multiple interrogator and dense interrogator. From now on, it will be only considered the single interrogator mode because the extra complexity of the other two modes is not justify according to the project goals.
The uplink -Tag to Reader- communication is as follows: The tag will convert the RF signal of the Reader into direct-current (DC) to get the energy needed to operate. From this RF signal the information will be extracted and the response will be modulated on the backscatter signal.

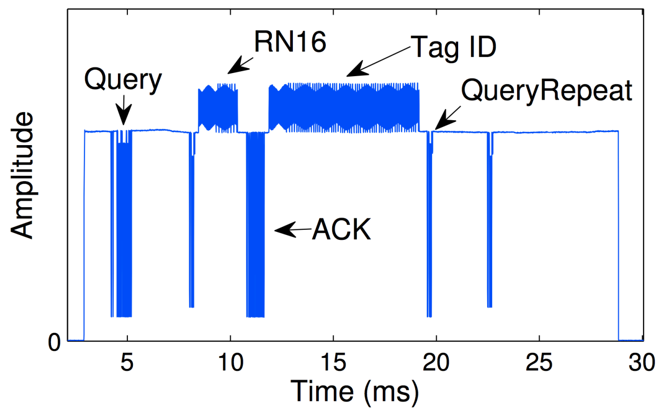

Figure B.2: Example of UHF RFID Gen 2 Communitacion in Baseband [28]

The Gen 2 protocol provides several types of modulation (this modulation is chose by the Reader), the default modulation is FM0, the other option is to use Miller-modulated subcarrier (MMS). Depending on the modulation and the carrier cycles per bit, the uplink data rate will change between 40 to 650 KHz.

A full view of the Downlink and Uplink communication can be seen in Figure B.3. The downlink communication are: the query command, ACK (acknowledgement) and the Query Repeat, while RN16 and Tag ID are the uplink messages. In order to get a better understanding of the full communication the Gen 2 Mac Layer is introduced.

B.1.2 Gen 2 Mac Layer

Gen 2 is a packetized protocol, where the reader selects most of the parameters of the communication. Because the tags are not able to listen to other tags in the area, they will randomly choose a slot in which they will responds. The tag with slot equal to '0' will be the only one who replies to the Reader. Afterwards, the Reader will send a command (QueryRep) to decrease the slot number. The tags that already replied to the tag will stay in silence.
The idea of slots can be understood as a number in the queue, where you are only allow to speak if you ticket number is zero. Each time one tag speaks the Reader will tell you to decrease your ticket number (slot), if at this moment your number is '0' you are able to respond. In this way the tags collision are significantly reduced.

Complex inventory commands or the tag modifications command that the Gen 2 protocol defines will be discard, focusing only in the basics instructions to get the tags responses. These basics commands are [18]:

Select: Usually is the first command used by the readers. The basic idea is to select a subset of the tags for the inventory.

Query: the query command starts a new inventory round. Its length is 22 bits, where the first 4 are always '1000'. This command is very important because its defines most of the parameters of the uplink communication.

- DR(Tag To Reader Calibration -TRcal-): sets the uplink(from the tag to the Reader) frequency.
- M(cycles per symbol): sets the uplink data rate and modulation.
- TRext: by setting this bit to '1' all tag transmissions are preceded by a pilot tone of 12 binary 0 symbols.
- Sel: chooses a subgroup of tags from the entire population which respond to the Query command.
- Session: chooses a session for the inventory round.
- Target: selects whether Tags whose inventoried flag is A or B participate in the inventory round.
- Q: indicates the number of slots in the inventory round.

RN16: the tag responds with a 16 bits random sequence. That the Reader has to acknowledge the tag containing the RN16.

ACK: the reader will acknowledge the tag to confirm it has been read.

PC+EPC+CRC: the tag responds to the ACK command from the reader with a sequence of PC (Protocol-Control word) word either StoredPC or PacketPC plus the EPC that contains a code the object to which the tag is related. Finally a CRC (cyclic redundancy check) is sent to allow the Reader verify the sequence PC+EPC received. Note that the EPC is what we need to properly identify the reference tag from the target.

QueryRep: when a tag receives this command it will decrement its slot counter and if slot=0 after the subtraction, it will backscatter an RN16 to the Reader.

QueryAdj: adjusts Q (slot counter) in the tags.

Figure B.3 puts on view all these commands:

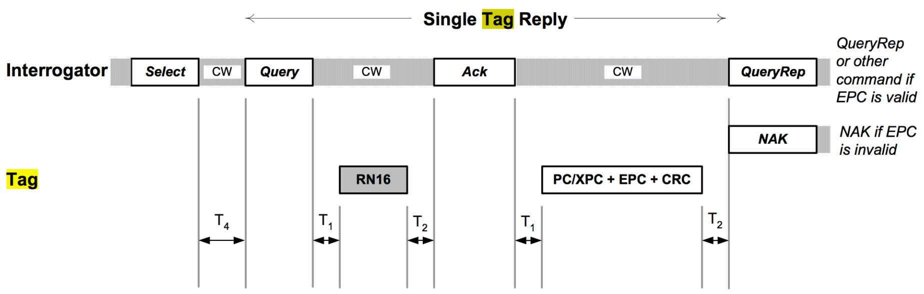

Figure B.3: Example of UHF RFID Gen 2 Commands Sequence [18]

Appendix C

Hardware Used in the Project

This appendix gives an overview about the hardware that have been used to perform the experiments and the practical work of this project.

Many of these experiments, specially the last ones, deal with minimum two tags at the same time: The target tag and at least one reference tag. Thus, somehow, the hardware and the software used should be able to distinguish the tags. The equipment should have the capability of extracting the Radio Signal Strength Indicator (RSSI) which gives the received power and the tag ID to be able to identify which tag is responding.

To carry out this task, three different proposed hardware setup are explained in this section. The first setup is to use an USRP device to develop an RFID reader. with the desirable capabilities. The second one is to use a spectrum analyzer to sample the signal and MATLAB to extract and decode the response of the tag and the third one is to use a commercial reader. These three hardware setups have been carried out through the project development.

C.1 Using an USRP Device

The Universal Software Radio Peripheral (USRP) is a family of hardware manufactured by Ettus Research which could be programmed to implement any kind of software radio. The USRP hardware is open source and, normally, it is programmed by using the GNU Radio Software which allows to get a complete open software radio system. However, it is possible to make it working with LabView and MATLAB/Simulink [29].

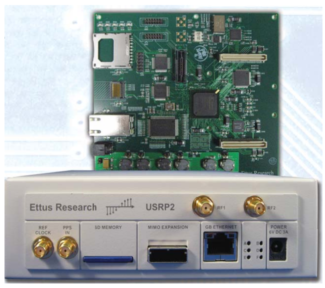

Figure C.1: USRP2 Device [29]

The hardware consists of a set of A/D and D/A converters, downconverters, upconverters, RF receiver and transmitter boards, FPGAs and interfaces to connect it to a computer. Two versions of the hardware can be found: USRP1 and USRP2 than can be chosen

according to the applications requirements.
In the beginning, the main idea was to use the USRP to develop a complete UHF RFID reader with the capability of extracting the RSSI value from the answer of the tag, as well as being able to decode the answer of the tag to extract the tag ID (EPC) in order to identify which tag is responding to the reader interrogation in case of more than one tag is being used.

For this proposal, an already developed project "Gen2 RFID Tools" can be used. This project consits of two components: A Gen2 monitoring system that decodes all Gen2 traffic across the Gen2 band [28] and a Gen2 RFID reader [30]. USRP2 version was used to implement these softwares.

Despite all the documentation that can be found on The Internet, to make the software running on the USRP device was not an easy task. However, the Gen2 monitoring system was implemented on USRP2 and it was able to successfully extract all the parameters needed for the project through the entire RFID band 865 - 868 MHz. The only parameters to be adjusted are the center frequency, 866.5 MHz for this case, and the sampling frequency. This last one factor should be carefully selected not only to sample the signal properly, but also to make the computer which controls the device be able to process the big amount of information generated by the USRP. In practical, the information obtained with a sampling frequency of 3 Mega samples per second (Ms/s) can be processed by normal computers.

Due to the fact that the USRP2 only have by default one port to transmit and one port to receive, it is only possible to connect one antenna and an amount up to four dual polarized antennas were used in this project. In the worse case, a total number of eight USRP2 devices were needed (four for vertical antennas and four for horizontal antennas) and that amount of USRP2 was not available.

C.2 Using a Spectrum Analyzer and MATLAB

The second idea was to use a spectrum analyzer to sample the signals that are involved in an RFID communication. Although the spectrum analyzer does not have enough ports to connect all the antennas, using an automatic switch, it was possible to sample the signals coming to all the antennas. It is just a matter of fitting the switching speed and the sampling frequency of the spectrum analyzer in order to get the information from all the antennas.

Once all the data was collected, it should have been processed to get the signal strength value and the tag ID. To this end, the Gen2 RFID Tools project was translated and implemented in MATLAB. Thus, just with the samples obtained from the spectrum analyzer, MATLAB was able to work as a reader and it was able to provide all the required parameters.

C.3 Final Hardware Used in the Project

Afterwards, a new commercial reader was available for this project. This new commercial reader is able to provide the RSSI and the tag ID for all the tags that are involved in the communication. To use this reader instead of the MATLAB implementation is easy and more comfortable in order to make the experiments, so finally, the option of using this reader was accepted.

References

[1] Daniel M. Dobkin. *The RF in RFID: Passive UHF RFID in Practice.* Elsevier Science, 2007.

[2] H. Hashemi. The indoor radio propagation channel. *Proceedings of the IEEE*, 81(7):943 –968, jul 1993.

[3] A. Lazaro, D. Girbau, and D. Salinas. Radio link budgets for uhf rfid on multipath environments. *Antennas and Propagation, IEEE Transactions on*, 57(4):1241 –1251, april 2009.

[4] Andreas F. Molisch. *Wireless Communications.* John Wiley & Sons, Inc., 2005.

[5] Curt A. Levis, Joel T. Johnson, and Fernando L. Teixeira. *Radiowave Propagation. Physics and Applications.* John Wiley & Sons, Inc., 2010.

[6] Gordon L. Stuber. *Principles of Mobile Communication.* Kluver Academic Publishers, 2001.

[7] *Antennas, Propagation and Diversity Course Class Slides*, 2010. 8th Semester of Mobile Communications Master. Aalborg University.

[8] *CyberLab*, Accessed February 2011.
http://en.wikipedia.org/wiki/Antenna_(radio).

[9] *CyberLab*, Accessed February 2011.
http://en.wikipedia.org/wiki/Elliptical_polarization.

[10] John S. Seybold. *Introduction to RF Propagation.* John Wiley & Sons, Inc., 2005.

[11] *Antenna Polarization Considerations in Wireless Communications System.* Cushcraft Corporation. 48 Perimeter Road. Manchester, NH 03103.

[12] Rasmus Krigslund, Petar Popovski, Gert F. Pedersen, and Kristian Bank. Potential of rfid systems to detect object orientation. Aalborg University. Department of Electronic Systems.

[13] T. Cover and P. Hart. Nearest neighbor pattern classification. *Information Theory, IEEE Transactions on*, 13(1):21 – 27, jan 1967.

[14] Duda Richard O. and Hart Peter E. *Pattern Classification.* John Wiley & Sons, Inc., 2001.

[15] Alberto Leon Garcia. *Probability and Random Processes for Electrical Engineering. Second Edition.* Addison-Wesley Publishing Company, 1994.

[16] *Impinj Speedway Revolution RFID Reader*, Accessed April 2011.
www.impinj.com/Speedway_Revolution_Reader.aspx.

[17] *ALN-9640 Squiggle Inlay Datasheet.* Alien Technology.

[18] *Class 1 Generation 2 UHF Air Interface Protocol Standard "Gen 2"*, Accessed February 2011.
http://www.gs1.org/gsmp/kc/epcglobal/uhfc1g2.

[19] *LLRP Toolkit Homepage*, Accessed February 2011.
http://www.llrp.org/.

[20] *Arduino Boards Homepage*, Accessed April 2011.
http://arduino.cc/en/Main/Hardware.

[21] *Dielectric Constants of Materials. Clipper Controls*, Accessed May 2011.
https://www.clippercontrols.com/pages/dielectric-constant-values.

[22] Constantne A. Balanis. *Antenna Theory.* John Wiley & Sons, Inc., 1997.

[23] *Antenna Radiation Fields in the Sinusoidal Steady State*, Accessed April 2011.
http://web.mit.edu/6.013_book/www/chapter12/12.4.html.

[24] Fang-Yao Kuo, Che-Yang Chiang, Heng-Tung Hsu, Ting-Jui Huang, and Rung-Sheng Sung. A new approach for radiation pattern measurement of rfid tag antenna under chip-loaded condition using friis equation. In *Microwave Conference Proceedings (APMC), 2010 Asia-Pacific*, pages 2184 –2187, dec. 2010.

[25] *Transcore*, Accessed January 2011.
http://www.transcore.com/.

[26] *CyberLab*, Accessed January 2011.
http://www2.cpttm.org.mo/cyberlab.

[27] *ADC Solutions*, Accessed January 2011.
www.adcnordic.com.

[28] Michael Buettner and David Wetherall. A gen 2 rfid monitor based on the usrp. *ACM SIGCOMM Computer Communication Review*, 40(3), july 2010.

[29] *USRP1 and USRP2 Datasheets.* Ettus Research.

[30] Michael Buettner and David Wetherall. A software radio-based uhf rfid reader for phy/mac experimentation. In *RFID (RFID), 2011 IEEE International Conference on*, pages 134 –141, april 2011.

List of Figures

List of Tables

Abbreviation List

ACK	Acknowledgement
BER	Bit Error Rate
CDF	Cumulative Density Function
CRC	Cyclic Redundancy Code
CW	Constant Wave
DC	Direct Current
EPC	Electronic Product Code
ERP	Effective Radiated Power
FPGA	Field-Programmable Gate Array
GEN2	EPCglobal Class 1 Generation 2 Protocol
ID	Identification
KNN	K-Nearest Neighbor
LLRP	Low-Level Reader Protocol
LOS	Line Of Sight
MPCs	Multipath Components
NLOS	No Line Of Sight
PC	Protocol Control Word
PDF	Probability Density Function
PIE	Pulse-Interval-Enconded
PLF	Polarization Loss Factor
PW	Pulse Width
RF	Radio Frequency
RFID	Radio Frequency Identification
RN16	16 bits Random Number
ROSPEC	Reader Operation Specification
RSSI	Radio Signal Strength Indicator
SNR	Signal to Noise Ratio
UHF	Ultra High Frequency
USRP	Universal Software Radio Peripheral
XML	eXtended Markup Language

Symbol List

c	Speed of Light
x	Set of received power for a measurement or category
α	Angle between the incident wave polarization and the receiver antenna
β	Category
$\circ$	Degrees
δ	Dirac delta function
$\frac{d}{dp}$	Differenciate with respect to the power
μ	Mean value
$\overline{P_{Rx}}$	Mean received power
π	Pi
σ^2	Variance
σ	Standard deviation
θ, ϕ	Spherical coordinates / Orientation components
A	Peak of the line of sight component
d_A	Absolute distance
d_E	Euclidean distance
$d\{\}$	Distance function
dB	Decibel
dBi	Decibel isotropic
dBm	Decibel in miliwatts
e	Error
$F()$	Cumulative Density Function
$f()$	Probability Density Function
F	Polarization Loss Factor
G_{Reader}	Reader antenna gain
G_{Tag}	Tag antenna gain
i,j	Indexes
Io	Modified Bessel Function of the first kind and zero order
K	Ricean Factor

KHz	KiloHertz
L_{Path}	Path Loss
$max\{\}$	Maximum
MHz	MegaHertz
$min\{\}$	Minimum
$mod()$	Module
Ms/s	Megasamples per second
N	Number of samples
P_i	Incident Power
P_r	Power coupled into the receiver antenna
$P_{RxReader}$	Received power at the reader antenna
P_{RxTag}	Received power at the tag antenna
$P_{TxReader}$	Reader transmitted power
p	Received power
$pdf()$	Probability Density Function
r	Envelope of the signal
R	Rayleigh random variable
T_b	Tag backscattered coefficient
T	Trainning set
V	Volts
W	Watts
x'_n	Nearest Neighbor
X	Gaussian random variable
y_i	Received power at antenna i